



Ville Koivusaari

## **Investigation of Direct Driven Hydraulics Implementation to Differential Cylinder Driven Systems**

Thesis submitted as partial fulfilment of the requirements for degree of Master in Science (Technology).

Espoo 23.11.2020

Supervisor: Professor Matti Pietola  
Advisor: Jyrki Kajaste, D.Sc. (Tech.)



---

**Author** Ville Koivusaari

---

**Title of thesis** Investigation of Direct Driven Hydraulics Implementation to Differential Cylinder Driven Systems.

---

**Master programme** Mechanical engineering

**Code** ENG25

---

**Thesis supervisor** Professor Matti Pietola

---

**Thesis advisor(s)** Jyrki Kajaste, D.Sc. (Tech.)

---

**Date** 23.11.2020

**Number of pages** 4 + 92

**Language** English

---

## **Abstract**

In this thesis, the requirements and implementations of a pump-controlled differential hydraulic cylinder circuit have been investigated. The type of hydraulic system is direct driven hydraulics (DDH), which is one subcategory of electro-hydrostatic actuators (EHA). The aim is to propose a circuit capable of meeting the basic functionality of load-lifting industrial applications and operating with better energy efficiency than a traditional valve-controlled hydraulic system. The research has focused on finding out which valves and control methods are required to create an energy-efficient system so that the system maintains sufficient driving stiffness in all load situations. Also, the circuit must be able to regenerate both the kinetic and potential energy of the load. Different valve types have been investigated such as: asymmetrical flow compensation valves, load-holding valves, and safety valves. In addition, the filtering of the DDH system has been studied, and various solutions are evaluated.

The simulation model of the DDH system is created with MATLAB / Simulink software. The simulation results have been used to analyse the circuit's performance to ensure the best energy efficiency and system functionality. In addition, various efficiencies as well as energy consumption, have been calculated for the system from the simulation results, and research objectives for future experimental work have been defined. The different efficiencies determined from the results were: the system's total efficiency, the regeneration efficiency, and the system's total efficiency during the reuse of regenerated energy. For future experimental tests of the proposed circuit, a test system was designed, which uses Beckhoff's measurement and control system.

Actively controlled proportional flow control valves have been selected to compensate the flow rate of the proposed DDH circuit, which opens with control logic identifying the operating quadrant. The load holding system consists of pilot-operated check valves that are opened with an actively controlled pilot pressure line. The system's highest efficiency, with energy reuse and a load of 1145 kg, was calculated to be 85.4%, resulting in the regeneration efficiency of 58.4%. Research has shown that the proposed circuit is potentially capable of operating in a high-performance load-lifting application, energy efficiently, and safely. Thus, the construction of a test system has begun to obtain measurement results. Both to validate the results of this study and to improve the simulation model's accuracy.

---

**Keywords** pump-controlled cylinder, electro-hydrostatic actuator, EHA, direct drive hydraulics, DDH, differential cylinder, energy efficiency, energy regeneration.

---

---

**Tekijä** Ville Koivusaari

---

**Työn nimi** Investigation of Direct Driven Hydraulics Implementation to Differential Cylinder Driven Systems.

---

**Maisteriohjelma** Mechanical engineering

**Koodi** ENG25

---

**Työn valvoja** Professori Matti Pietola

---

**Työn ohjaaja(t)** Jyrki Kajaste, D.Sc. (Tech.)

---

**Päivämäärä** 23.11.2020

**Sivumäärä** 4 + 92

**Kieli** Englanti

---

## Tiivistelmä

Tässä diplomityössä on tutkittu pumppuohjatun differentiaali hydraulisylinteripiirin vaatimuksia ja toteutustapoja. Hydraulijärjestelmän tyyppi on suoravetoinen hydraulikka (DDH), joka on yksi sähköhydrostaattinen toimilaitteiden (EHA) alaluokka. Tarkoituksena on esittää piiri, joka pystyy täyttämään kuormaa nostavien teollisuus sovellusten perusvaatimukset ja toimimaan paremmalla energiatehokkuudella kuin perinteinen venttiiliohjattu hydraulikkajärjestelmä. Tutkimuksessa on keskitytty selvittämään mitä venttiilejä ja ohjausmenetelmiä vaaditaan energiatehokkaan järjestelmän luomiseksi, siten että järjestelmä säilyttää riittävän ajojäykkyyden kaikissa kuormitusilanteissa. Lisäksi piiriin on kyettävä talteen ottamaan sekä kuorman kineettistä että potentiaalista energiaa. Tutkittavana on ollut erilaiset venttiilityypit kuten: epäsymmetrisen virtauksen kompensointiventtiilit, kuormanhallintaventtiilit ja varoventtiilit. Lisäksi on tutkittu DDH-järjestelmän suodattusta ja arvioitu erilaisia ratkaisuja.

DDH-järjestelmän simulointimalli luodaan MATLAB / Simulink-ohjelmistolla. Simulaation tuloksia on käytetty piirin suorituskyvyn analysointiin, parhaan energiatehokkuuden ja järjestelmän toiminnallisuuden takaamiseksi. Lisäksi simulaatiotuloksista on laskettu järjestelmälle eri hyötysuhteet sekä energiankulutus, ja on määritetty tutkimustavoitteet tulevaisuuden kokeelliselle työlle. Tuloksista määritettyjä eri hyötysuhteita olivat: järjestelmän kokonaishyötysuhde, talteenottohyötysuhde ja kokonaishyötysuhde talteen otetun energian uudelleenkäytön aikana. Ehdotetun piirin tulevia kokeellisia testejä varten on suunniteltu testijärjestelmä, joka käyttää Beckhoff:in mittaus- ja ohjausjärjestelmää.

Ehdotettu DDH-piiriin tilavuusvirran kompensointiin on valittu aktiivisesti ohjatut proportionaaliset virtauksen säätöventtiilit, jotka avautuvat toimintakvartaalin tunnistavalla ohjauslogiikalla. Piiriin kuormanhallintajärjestelmä koostuu ohjattavista vastaventtiileistä, joita avautuvat aktiivisesti ohjatun ohjauspainelinjan avulla. Järjestelmän suurimman hyötysuhteen, energian uudelleenkäytöllä ja kuormituksella 1145 kg laskettiin olevan 85,4%, jolloin talteenottohyötysuhde oli 58,4%. Tutkimus on osoittanut, että ehdotettu piiri pystyy potentiaalisesti toimimaan korkeaa suorituskykyä vaativissa kuormaa nostavassa sovelluksessa, energia tehokkaasti ja turvallisesti. Täten testijärjestelmän rakentaminen on aloitettu mittauksien hankkimiseksi. Sekä tämän tutkimuksen tulosten varmentamiseksi ja simulointimallin tarkkuuden parantamiseksi.

---

**Avainsanat** pumppuohjattu sylinteri, sähköhydrostaattinen toimilaite, EHA, suoraveto-hydraulikka, DDH, differentiaali sylinteri, hyötysuhde, energia talteenotto.

---

## Acknowledgements

*This thesis was part of the EL-Zon project's research of direct driven hydraulics. I got introduced to this subject during the mechatronic project course and continued working in the EL-Zon team since. The first research device I build was a symmetrical cylinder driven low-cost DDH system, and this thesis is a continuation of that work. The work has been very challenging and at the same time an enriching experience, during which my professional skills have had the opportunity to develop.*

*I want to give thanks to, my advisors, Jyrki Kajaste, Olof Calonius for support during the DDH circuit and simulation model development process. Especially to Jyrki for all the teaching and knowledge you have given me during my studies. My supervisor, professor Matti Pietola who provided the opportunity to be part of this project. Antti Sinkkonen for technical support and the rest of Aalto's talented people who made this work possible. I want to give a special thanks to my co-worker Mehrdad Khodayari who did magnificent work with the test bench designing process.*

*This research was enabled by the financial support of Tekes, the Finnish Funding Agency for Technology and Innovation, (project EL-Zon) and internal funding at the Department of Mechanical Engineering at Aalto University.*

Espoo 23.11.2020



Ville Koivusaari

## Table of contents

Abstract	
Acknowledgements	
Table of contents	1
Nomenclature	2
Abbreviations and Acronyms	5
1 Introduction	6
1.1 Direct driven hydraulics	7
1.2 Problem statement and thesis aims	8
1.3 Outline of the thesis	9
2 State of the art EHA	10
3 DDH system investigation	14
3.1 Hydraulic system	14
3.1.1 Hydraulic power	16
3.1.2 Reservoir	17
3.1.3 Flow compensation components	18
3.1.4 Safety components	25
3.1.5 Hydraulic fluid management	29
3.1.6 Hydraulic components	34
3.2 Electrical system	36
3.2.1 Electrical power	36
3.2.2 Sensors	38
3.2.3 Control system	39
3.3 Load system and test bench	41
4 Simulation model	45
4.1 Volume model	46
4.2 Pump model	46
4.2.1 Pump flow	47
4.2.2 Pump torque	47
4.3 Flow resistors	48
4.3.1 Check valve and PRV models	48
4.3.2 Pilot Operated Check Valve model	50
4.3.3 Proportional valve model	51
4.3.4 Load holding system	52
4.4 Cylinder model	53
4.4.1 Cylinder's seal friction force	54
4.4.2 Cylinder's end force	56
4.5 Load model	57
4.6 Motor and valve control system	58
4.7 Simulation model	59
5 Results and discussion	60
5.1 System performance analysis	61
5.2 Energy efficiency analysis	68
6 Conclusion	74
6.1 Future work	75
List of Annexes	85
A. Simulink model	85

## Nomenclature

$A_0$	[m <sup>2</sup> ]	Area of the orifice
$A_A$	[m <sup>2</sup> ]	Piston A-side area
$A_B$	[m <sup>2</sup> ]	Piston B-side area
$A_{dynamic}$	[m <sup>2</sup> ]	Dynamic response of the valve's poppet opening.
$A_{leak}$	[m <sup>2</sup> ]	Closed valve leakage area
$A_{max}$	[m <sup>2</sup> ]	Fully open valve passage area
$b_{end}$	[-]	Cylinder end damping coefficient
$b_v$	[-]	Viscous friction coefficient
$C_f$	[-]	Coulomb friction coefficient
$C_{s,ext}$	[-]	External laminar flow loss coefficient
$C_{s,int}$	[-]	Internal laminar flow loss coefficient
$C_v$	[N/(m/s)]	Viscous friction coefficient
$C_q$	[-]	Discharge coefficient
$d_{adj}$	[-]	Adjustment constant
$E_{DDH}$	[J]	DDH system energy
$E_{lift}$	[J]	Actuator lifting energy
$E_{lower}$	[J]	Actuator lowering energy
$E_{Reg}$	[J]	DDH system regenerated energy
$F_c$	[N]	Actuator force
$F_{cf}$	[N]	Coulomb friction force
$F_{end}$	[N]	Cylinder end force
$F_{load}$	[N]	Load force
$F_{max}$	[N]	Force when valve is fully opened
$F_{POCV}$	[N]	Poppet force
$F_{pilot}$	[N]	Pilot piston force
$F_s$	[N]	Static friction force
$F_{seal}$	[N]	Cylinder seal force
$F_{spring}$	[N]	POCV's spring force
$K_0$	[-]	Leakage at valve's closed position
$K_{100}$	[-]	Valve flow capacity at valve's fully open position
$K_{end}$	[N/m]	Spring constant of cylinder
$K_f$	[GPa]	Bulk modulus
$k_3$	[-]	Pilot piston's piston area ratio
$k_4$	[-]	Pilot piston's rod area ratio
$K_L$	[-]	Internal laminar leakage coefficient
$k_L$	[-]	Linear constant
$k_{poppet}$	[-]	Poppet area ratio
$k_{R,cs}$	[-]	Spring constant of the cylinder seal
$m$	[kg]	Load mass
$n$	[r/s]	Pump rotational velocity
$p_1$	[Pa]	Valve chamber 1 pressure
$p_2$	[Pa]	Valve chamber 2 pressure
$p_A$	[Pa]	A-side pressure
$p_B$	[Pa]	B-side pressure
$P_{c.lift}$	[W]	Actuator lifting power

$P_{c.lower}$	[W]	Actuator lowering power
$p_{crack}$	[Pa]	Cracking pressure of valve
$P_{hydraulic}$	[W]	Hydraulic power
$p_{max}$	[Pa]	Pressure needed to fully open the valve
$P_{e.motor}$	[W]	Mechanical power
$P_{e.motor.reg}$	[W]	Regenerated power
$p_{system}$	[Pa]	Maximum system pressure
$p_x$	[Pa]	Pilot pressure
$p_Y$	[Pa]	Drainage pressure
$q_v$	[m <sup>3</sup> /s]	The flow trough the orifice
$q_{v,A}$	[m <sup>3</sup> /s]	Cylinder A chamber flow
$q_{v,B}$	[m <sup>3</sup> /s]	Cylinder B chamber flow
$q_{v.leakage}$	[m <sup>3</sup> /s]	Internal leakage flow of cylinder
$q_{v,L,nominal}$	[m <sup>3</sup> /s]	Nominal leakage flow rate of the valve
$q_{v,L,pump}$	[m <sup>3</sup> /s]	Pump's leakage
$q_{v,nominal}$	[m <sup>3</sup> /s]	Nominal flow rate of the valve
$q_{v,pump}$	[m <sup>3</sup> /s]	Pump's flow rate
$q_{v.in}$	[m <sup>3</sup> /s]	Flow rate going into hose
$q_{v.out}$	[m <sup>3</sup> /s]	Flow rate leaving hose
$T_c$	[Nm]	Constant torque loss
$T_p$	[Nm]	Pump torque
$T_{L,pump}$	[Nm]	Pump torque losses
$U_c$	[-]	Control signal
$U_{c,max}$	[-]	Maximum control signal
$U_{c,min}$	[-]	Minimum control signal
$v$	[m/s]	Actuator velocity
$v_{\mu}^{min}$	[m <sup>2</sup> /s]	The speed when friction reaches its minimum value.
$V_A$	[m <sup>3</sup> ]	A chamber volume
$V_{A,0}$	[m <sup>3</sup> ]	A chamber death volume
$V_B$	[m <sup>3</sup> ]	B chamber volume
$V_{B,0}$	[m <sup>3</sup> ]	B chamber death volume
$V_{hose}$	[m <sup>3</sup> ]	Hose volume
$V_i$	[m <sup>3</sup> /r]	Pump displacement
$V_{ref}$	[m <sup>3</sup> /r]	Pump's reference displacement
$x$	[m]	Piston position
$x_{def}$	[m]	Approximation of the seal deformation
$x_{max}$	[m]	Cylinder stroke
$z_{cs}$	[m]	Bend of the cylinder seal
$z_{cs}^{max}$	[m]	Maximum bend of the cylinder seal
$\alpha$	[-]	Cylinder piston area ratio
$\epsilon$	[-]	Pump angle setting
$\nu$	[m <sup>2</sup> /s]	Fluid kinematic viscosity
$\rho$	[kg/ m <sup>3</sup> ]	Oil density
$\tau$	[-]	Time constant of the valve dynamic
$\Delta p$	[Pa]	Pressure difference over the orifice
$\Delta p_{AB}$	[Pa]	Pressure difference between pump's inlet and outlet chambers
$\Delta p_{AT}$	[Pa]	Pressure difference between pump's A chamber and tank
$\Delta p_{BT}$	[Pa]	Pressure difference between pump's B chamber and tank

$\Delta p_{nominal}$	[Pa]	Nominal pressure difference of the valve
$\Delta p_{L,nominal}$	[Pa]	Nominal pressure difference of leakage is measurement
$\zeta_{d,cs}$	[-]	Damping constant of the cylinder seal
$\omega$	[rad/s]	Pump angular velocity
$\eta_{servo}$	[-]	Servo system efficiency
$\eta_{DDH}$	[-]	DDH system efficiency
$\eta_{Reg}$	[-]	DDH system regeneration efficiency
$\eta_{DDH.w.reuse}$	[-]	DDH system efficiency with energy reuse



## Abbreviations and Acronyms

BLDC	Brushless direct current
CAD	Computer assisted design
CBV	Counterbalance valve
CV	Check valve
DDH	Direct driven hydraulics
EHA	Electro-hydrostatic actuator
EtherCAT	Ethernet for Control Automation Technology
EMA	Electro-mechanical actuator
EV	Electric valve
PC	Personal computer
PLC	Programmable logic controller
POCV	Pilot operated check valve
PRV	Pressure relief valve
PWM	Pulse-width modulation
SHA	Servo-Hydraulic actuator

# 1 Introduction

Today's industry's general trend is to improve energy efficiency and reduce the machine's operating costs, increasing the interest in finding novel solutions for conventional hydraulically powered systems. The traditional way of controlling the hydraulic actuator is to utilize directional valves that directs the desired flow rate into the actuator. These systems are classified as valve-controlled systems, and they utilize one or several constantly rotating pumps that maintain system pressure level [1]. When the hydraulic pump is a fixed displacement pump, the system pressure is controlled and limited with a pressure relief valve (PRV) [2]. While the system is in a standby state, the motor runs continuously, and the pump's pressure is led to the tank through PRV or alternatively through open or tandem center directional valve spool. Generally, the valve-controlled systems have low energy efficiency because of the throttling losses at control valves. In mobile hydraulic systems, load-sensing or pressure compensation technologies have been used to mitigate these losses, where pump displacement can be adjusted to meet the required hydraulic power [3][4]. However, even with a typical load-sensing system, the control valve's throttling losses can consume 35% of the input energy received from the power unit [5]. These factors lead to high engine power requirements and generation of large amounts of heat during operation [6].

One solution to solve the valve-controlled system's disadvantages in linear actuator applications is to use the electro-mechanical actuator (EMA), which utilizes a ball screw actuator controlled by a gearbox and electric motor, as shown in Figure 1. These units have better energy efficiency and controllability than most conventional hydraulic system. EMA is a compact unit where all components are connected to the actuator's surface. This offers a high power-to-weight ratio, straightforward plug and play installation, and low maintenance costs due to a smaller amount of power transmission components required. Despite the useful features, these systems have disadvantages that limit their usage in industrial applications. Such as limited durability due to the wear of screw and gears, decreased load capabilities, inadequate overload protection, and overheating in some operation situations can be mentioned above all [7].

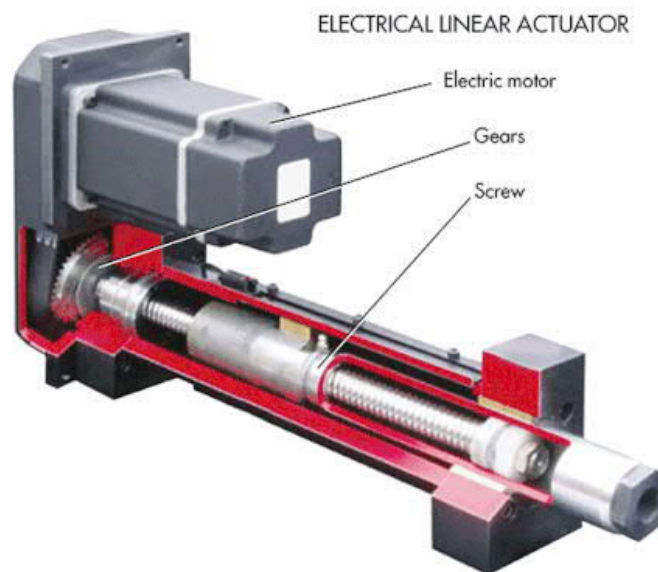


Figure 1 Electro-mechanical actuator [7].

The hydraulic alternative for EMA is to use pump-controlled hydraulic cylinders. The hydraulic pump runs only when movement is required, and the direction of the actuator's movement is controlled by changing the pump's rotation direction. Therefore, these closed-loop pump-controlled systems do not need a directional valve for controlling the flow direction. This allows more energy-efficient operation than traditional valve-controlled systems because throttling losses at flow control valves are lower. This type of hydraulic system architecture is typical in hydrostatic transmissions shown in Figure 2 where hydraulic power is generated with a variable displacement pump and charge pump circuit [8]. Additionally, one benefit of pump-controlled cylinders is when system's all actuators have separated power units like EMA has. Therefore, all required valves can be located close to the actuator. This makes the hydraulic system more compact, which increases the serviceability of the system and reduces the risk of failure or leakage in hydraulic power transmission lines. Furthermore, compactness can reduce the system's overall weight, which increases the possible payload of the machinery and overall efficiency [1]. These advantages have led to many studies considering the possibilities of the pump-controlled cylinder systems.

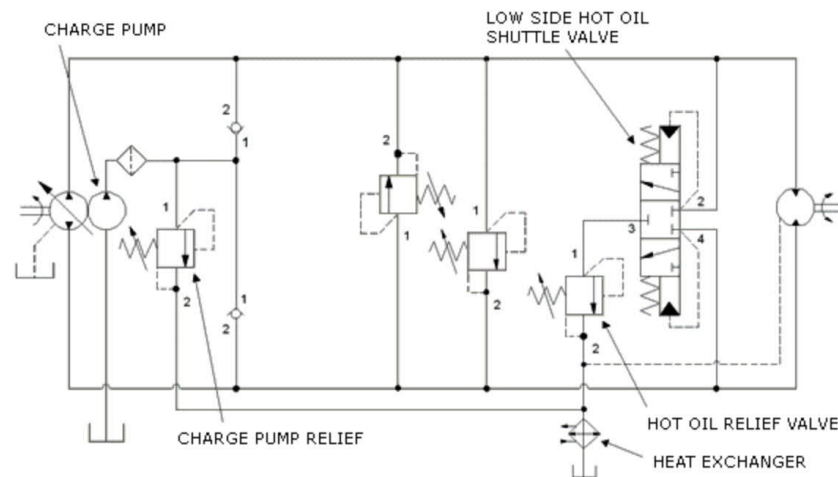
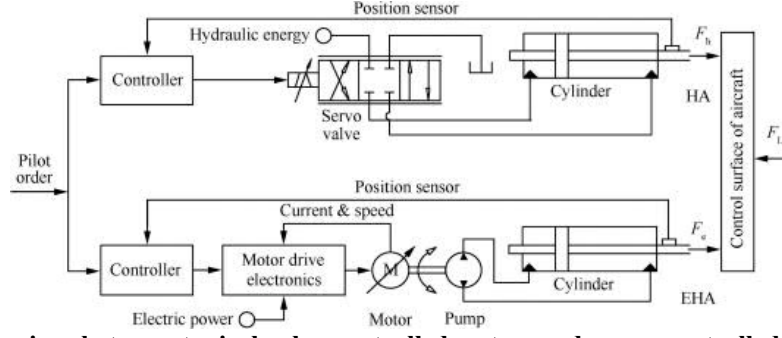


Figure 2 Typical hydrostatic transmission [8].

### 1.1 Direct driven hydraulics

Closed loop pump-controlled systems are commonly called electro-hydrostatic actuators (EHA). This technology has been available since the 1980s and it has been commonly used especially in the aerospace industry from the beginning of the 1990s [6]. These systems used in aerospace industry usually include a single symmetrical cylinder which is directly controlled with a hydraulic pump that is driven by an electrical motor. For example, the electrical motor's rotation speed can be controlled with a position feedback loop [10], as Figure 3 shows. Each EHA unit controls a separate aircraft control surface, which allows the hydraulic pump to be utilized only when required. This allows the aircraft's hydraulic circuit to be divided into more compact and lighter units. In addition to that, because the cylinder's both chambers are connected to the pump's pressure lines, the kinetic and potential energy regeneration is possible [6].



**Figure 3 Comparison between typical valve-controlled system and pump-controlled system [10].**

Although this technology has been common in the aerospace industry, also other industry sector have taken a step towards utilizing EHA systems in applications like wind turbine's pitch control [11], injection moulding machines [12], sheet metal bending machines [13], and wire clamping machines [14]. Most EHA systems utilize a symmetrical cylinder because it has the same piston areas in both cylinder chambers. This allows a simpler system and control design. However, these cylinders require more space than differential cylinders and cannot produce high force output due to the cap end side's lower surface area. That is why these cylinders are not suitable for some industrial applications, and more than 80% of cylinders used in industrial applications are differential [6]. In this thesis, a differential cylinder is used that utilizes direct-driven hydraulics (DDH) system architecture, which is one subcategory of EHA. This system category usually uses one or several fixed displacement pumps, which speed is controlled with an electrical motor. Essential for DDH systems is that the control takes place mainly by controlling the electrical motor's rotational speed. However, some control features can also be implemented, for example with valves or driving a variable displacement pump in a fixed displacement mode that allows multiple pump displacement options [15].

## 1.2 Problem statement and thesis aims

The main research goal of this thesis is to ensure the basic functionality of the differential cylinder based DDH system that is aimed to operate in load-lifting industrial applications. The thesis investigates problems that currently available differential pump-controlled cylinders have and how those can be possibly resolved in the future. Based on this investigation, the thesis proposes a circuit that can encounter the following problems with the best performance reliability.

The most significant problem which this type of systems face is the asymmetric flow out of cylinder chambers. This is caused by a difference between cap side piston side area  $A_A$  and rod side piston area  $A_B$  shown in Figure 4. This difference is defined as cylinder piston area ratio  $\alpha$ .

$$\alpha = \frac{A_A}{A_B} \quad (1.1)$$

If the asymmetric flow compensation is not done properly, the system could suffer from problems like inaccuracy in position control, insufficient drive stiffness, reduced energy efficiency, and pressure oscillations [6]. To ensure the system remains high and reliable performance, different flow compensation circuits needs to be evaluated.



**Figure 4 Differential cylinder's piston areas.**

Additionally, many industrial applications require safety features like load holding capabilities if the system is de-energized or overrunning loads are acting on the actuator. Implementation of the load-holding system can cause undesirable system behaviour [16] or decrease the energy efficiency of the DDH system [17]. Because there is not any universal solution available in the industry for closed loop hydraulic systems the possible solutions need to be evaluated.

Industrial applications also require high reliability and long service life, and fluid management has a significant part in ensuring long-lasting reliable performance. This is managed by placing the filter into the system to remove any contamination in a hydraulic fluid that forms during the system's service life. Many DDH systems existing are lacking suitable filtering solutions and therefore different solutions needs to be investigated. In addition to that, the air in hydraulic fluid is a significant issue with the DDH system, affecting performance on both component and system performance [18]. Therefore, thesis aims investigate these fluid management problems and propose solutions which can be later tested in the test system.

High energy efficiency is one main goal of the EHA systems, and the ability to regenerate energy is one crucial part of this. This can be difficult in some load scenarios, and many EHA systems cannot regenerate potential energy when load is lowered [19]. Therefore, the system is required to be able to regenerate energy kinetic and potential energy of load mass when it is possible.

In addition, the design of the proposed system must favour commercially available components to ensure easy and cost-effective implementation in industrial applications. The system needs to perform in applications that require high dynamics operation with good energy efficiency. Therefore, all components must also provide high performance for the system.

In order to achieve these basic functionalities, a MATLAB/Simulink model is built. The model describes the system's behaviour mathematically and includes all physical features needed to analyse its performance and energy efficiency. The simulation model must be accurate enough to be able to compare its results with the measurement data of the proposed DDH circuit. The aim of the simulation model is to clarify the system's operation and define research objectives for experimental work. In addition to that, the thesis includes the design of the testing system, which needs to be able to measure the circuit's physical behaviours. Therefore, the system needs to include all the necessary sensors to measure the performance of the circuit. The measurement data is used to validate the results of this study and improve the simulation model's accuracy.

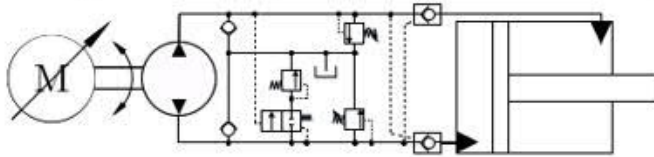
### **1.3 Outline of the thesis**

The rest of thesis is divided into five chapters. Chapter 2 describes and reviews current state of the art differential cylinder EHA systems. Chapter 3 describes required components of the DDH based system and design of required test system. Chapter 4 describes the simulation process. Chapter 5 presents and discusses the results of simulation model. Chapter 6 provides a conclusion and future research goals for experimental work.

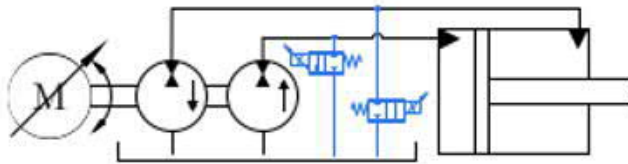
## 2 State of the art EHA

Recently, many researches have been aimed to develop an EHA system which overcomes differential cylinder's asymmetric chamber flow rate problem. These systems can be classified depending on the number and type of prime movers and pumps. S. Ketelsen and his research team provide classification and description of state of the art systems [20] which is shown in Figure 5. The first three systems can be classified as DDH systems. However, this thesis's prime focus is to investigate the systems that fall into the 1st category of this classification. Main components of that type of system are explained more detailed in next chapter.

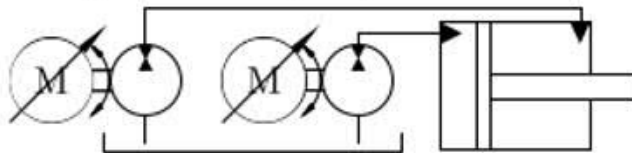
1. Single variable speed prime mover and single fixed displacement pump.



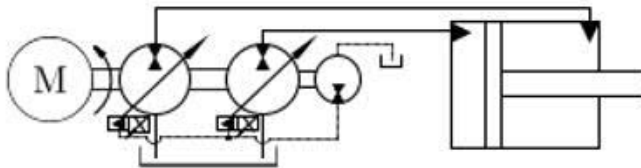
2. Single variable speed prime mover and multiple fixed displacement pumps.



3. Multiple variable speed prime movers and multiple fixed displacement pumps.



4. Single constant speed prime mover and multiple variable-displacement pumps.



5. Single constant speed prime mover and single variable-displacement pumps.

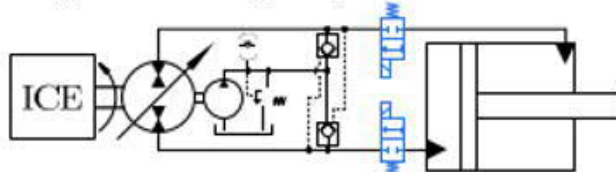


Figure 5 Classification of pump-controlled differential cylinder systems and example circuits [20].

The following section will present a brief introduction to these classes and explain systems' key features. Additionally, this section will give an understanding: how these classes are different from each other and what are major problems with these classes that need to be solved with future research.

Class 1 consists of a system with only one fixed displacement pump, and the speed control is implemented with a variable prime mover, which is commonly an electrical motor in these systems. The type of system requires flow compensation valves because of the cylinder's asymmetric flow rate. The compensation valves can be either passive or active type and they are discussed in more detail in this thesis's chapter 3.1.3. In addition to these, there is one different approach to asymmetric flow control than is not included in 3.1.3 chapter which is called asymmetric pump that is invented [21] and patented [22]. The system is based on customised fixed axial piston pump that has three ports. This is accomplished by modifying the pump's valve plate to have an additional groove for the tank line. Therefore, the pump can be connected simultaneously to both cylinder's chamber line and tank line. In this way, the valve plate's design can be reworked to match the cylinder's piston area ratio, which means that no additional flow compensation components are needed. However, this creates a problem, when the valve plate design relates to a specific piston area ratio and therefore one pump can only be used with a certain cylinder size. The asymmetric pump's functionality is similar to the next class's system, which has two fixed pumps connected together with a shaft.

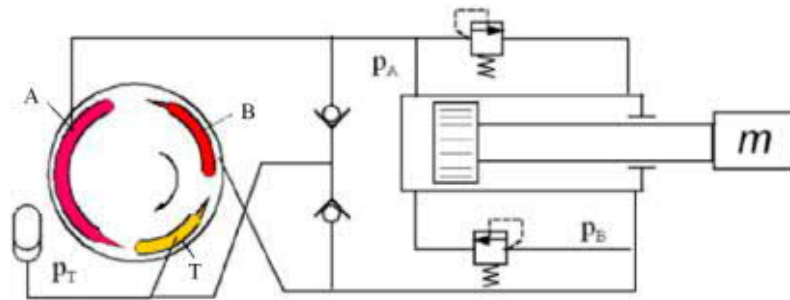


Figure 6 Asymmetric pump's modified valve plate illustration [23].

Class 2 consists of a system that has one variable prime mover and two fixed pumps connected with a shaft. The system handles the asymmetric flow compensation using two pumps with different displacements, each connected to a different cylinder chamber. The ratios of these displacements need to be close to the cylinder's piston area ratio to create the proper flow compensation for the cylinder chambers. This approach makes the hydraulic circuit simpler. However, achieving the correct ratio with two pumps and their nominal displacements, has been found to be complicated and this is commonly called as sizing error. In some situations, leakage in pumps will result in uneven flow compensation, resulting in pump failure. One research has suggested that adding a pressure accumulator to A chamber side can solve this problem, and this is tested to be a suitable solution [24]. However, in some situations, placing a pressure accumulator can negatively affect systems driving stiffness. Other research has suggested an alternative solution for this type of system that uses anti-cavitation valves and PRV instead of pressure accumulator to prevent sizing error caused by pump leakage [25]. Additionally, this system included two proportional valves that connect the cylinder chambers to the tank with control logic, which is designed to compensate for excessive pressure. With these valves, the system was reported to be feasible for handling cavitation and excessive pressure problems. However, the circuit requires more hydraulic components than the pressure accumulator solution.

Class 3 is like the previous class, but instead of connecting two fixed pumps with the shaft, each pump has a separate variable prime mover. This approach solves the previously mentioned sizing error to some extent. While this circuit is driving the cylinder in



one direction, one of the pumps is working as a prime mover, and one is working as a generator. In this way, the system is regenerating energy back to the battery or electric grid. However, this approach makes the system's overall cost relatively high compared to the system with only one prime mover. Also, this system requires a more complex controlling system that, for example, class 2 does.

Class 4 has a similar structure to class 2, but it has variable pumps as a flow controlling device and constant speed prime mover. Because constant speed prime movers are often used in mobile machinery, this solution is aimed at this industrial sector. The solution also overcomes the sizing error between two pumps, but this will need a complex controlling system. Additionally, variable displacement pumps are rather expensive components and will need a change pump for displacement controlling purposes, which, together with the controlling system, makes this solution expensive.

Class 5 consists of one constant prime mover and one variable displacement pump, making this class also suitable for the conventional mobile industry. This type of system requires the same type of flow compensation valves, as class 1 does. Additionally, this type of system often needs a charge pump, which is required to control the variable pump's displacement in low-pressure conditions and to increase driving stiffness. This additional pump makes the system more complex and adds the overall cost of this type of system. The system can also utilize hydraulic transformers as flow compensation devices. However, the solutions based on commercially available components have been a rather bulky and complex system because they need two rotating machines. This makes this solution hard to implement into a system that is intended to be compact [20]. However, in the new design of transformers by INNAS based on so called floating cups, the variable transformer is only one rotating unit which has three flow ports [26][27]. This could make the transformer solution feasible for industrial use in the future.

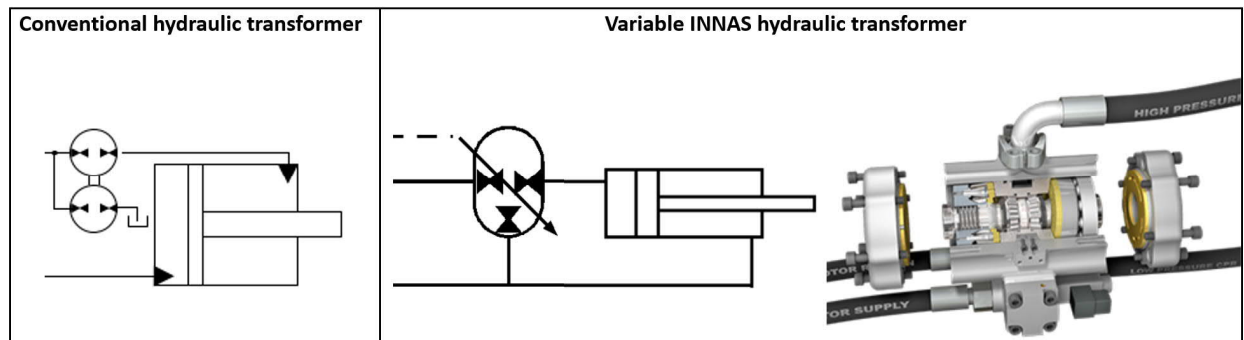


**Figure 7** Conventional hydraulic transformer [20], schematic of variable INNAS hydraulic transformer [26], and the picture of the current design of variable INNAS hydraulic transformer [27].

Research has been done related to variable asymmetric pumps [23] that can potentially solve flow compensation problems for class 5 in the future. However, this solution also requires a charge pump that controls the displacement angle, as shown in Figure 8.



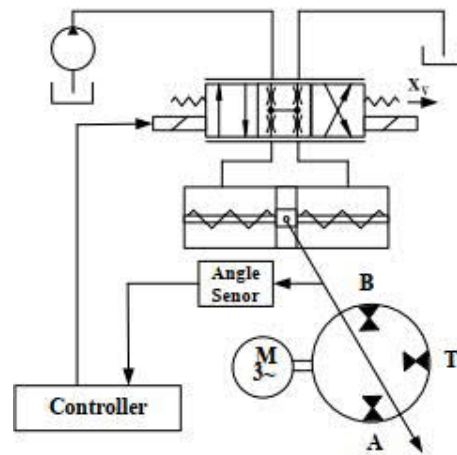


Figure 8 variable asymmetric pump's valve plate angle control [23].

All previously mentioned systems have been achieved better energy efficiency than a similar conventional valve-controlled hydraulic system. However, all of these have not fully solved this asymmetric flow compensation problem without pressure oscillations, or they are ineffective solutions for real-life industrial applications. Some of the key features related to functionality that are still missing and need to be improved in the EHA systems. The main problems to be solved and imperfections to be corrected are to improve compactness of the system, scalability of the system, cost effectiveness of the system's components, and drive stiffness. Additionally, many of these systems miss some safety functions implemented by load holding valves and fluid management systems like filtering required in some industrial applications [20]. Therefore, all these approaches need more research and development. In this thesis, class 1 is selected and investigated in more detail because it is presumably a cost-effective circuit due to the requirement of only one fixed displacement pump and one electrical motor. It can also achieve high energy efficiency levels and good driving stiffness with commercially available components. Additionally, all valves and other components can be easily mounted on hydraulic cylinders' surface, allowing a compact system structure for the circuit.

### 3 DDH system investigation

As previously mentioned, the system which is investigated and designed in this thesis is based on the DDH architecture, that is according to the previous classification 1<sup>st</sup> category of the EHA system. This type of system consists of several component categories that give the system desirable functionality. These categories are

- Electrical power components, that convert the electrical power to mechanical power.
- Hydraulic power components, that convert the mechanical power to hydraulic power.
- Reservoir, that stores hydraulic oil.
- Flow compensation components, that provide compensation to the cylinder's asymmetric flow rate.
- Safety components, that provide safety features for the hydraulic circuit.

All these component categories and their common connection order is shown in Figure 9. The chapter's structure is based on this category classification, where the hydraulic system is investigated as a separate section, and the electrical system is explained after that part. Electrical system section includes electrical power components investigation in chapter 3.2.1. Additionally, this chapter involves the test system design and explains the functionality of it.

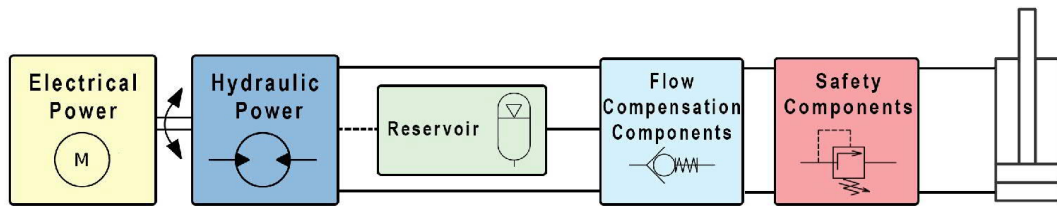
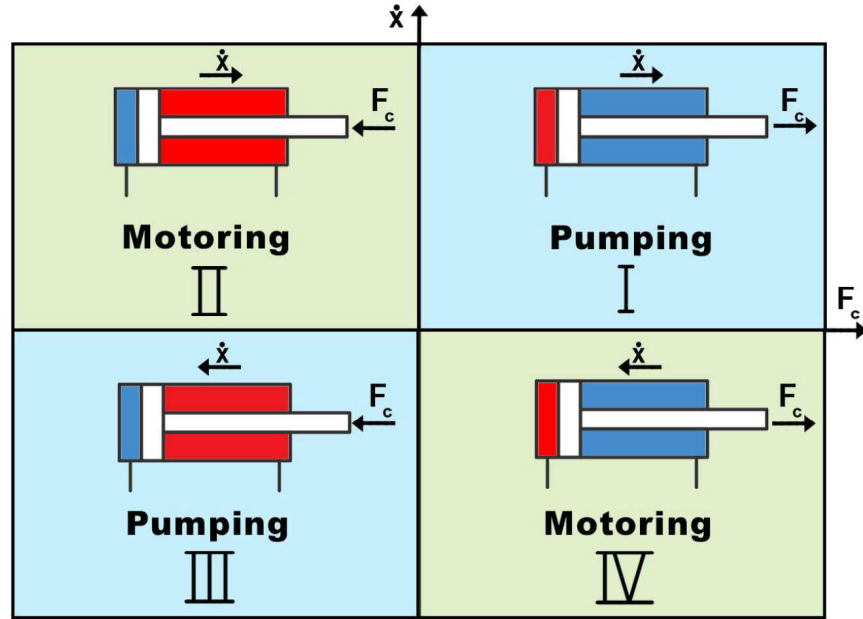


Figure 9 Component categories of the DDH system.

#### 3.1 Hydraulic system

One of the main goals the DDH systems have is to increase the system's overall efficiency and the achieve ability to regenerate energy, which otherwise would turn into heat. This is accomplished by selecting hydraulic components with respect to hydraulic quadrant division. When considering the energy balance of the hydraulic system moving a load with the actuator, the operation can be defined as four operation quadrant division. These divisions are defined by the direction of velocity and actuator force [28] presented in Figure 10. This division shows that when the system is acting in pumping mode (quadrant I and III), the system needs to consume energy to provide the desired velocity and actuator force to move the load. However, during motoring mode (quadrant II and IV), the system does not usually consume energy, and there is a possibility to regenerate the moving load's potential and kinetic energy. Many previous EHA designs are based on older quadrant division, where force used for quadrant definition was external load force rather than hydraulic actuator force created by the hydraulic pressure difference over cylinder piston surfaces [29]. Recent studies have shown that this presentation does not accurately describe the hydraulic cylinder's operation, which is suggested to be the reason why previous attempts to create an oscillation free system have failed [28].



**Figure 10 Quadratic division of hydraulic cylinder system.**

Following equations give a definition to quadratic division according to the first law of thermodynamic [28].

When considering the cylinders force balance according to Newton's second law.

$$p_A A_A - p_B A_B - F_{seal} - F_{load} = m \dot{v} \quad (3.1)$$

Where  $p_A$  is piston side pressure,  $p_B$  is rod side pressure,  $F_{seal}$  is piston's seal friction force,  $F_{load}$  is force of load and  $m$  is load's mass.

The actuator force,  $F_c$  is obtained from equation 3.1.

$$F_c = m \dot{v} + F_{seal} + F_{load} = p_A A_A - p_B A_B \quad (3.2)$$

Energy balance of the cylinder when using equation 3.2 and equation  $q_v = A v$  we get:

$$\begin{cases} p_A q_{v,A} - p_B q_{v,B} - F_c v = 0; & \text{resistive load (Q1)} \\ p_A q_{v,A} - p_B q_{v,B} + F_c v = 0; & \text{assistive load (Q2)} \end{cases} \quad (3.3)$$

$$\begin{cases} -p_A q_{v,A} + p_B q_{v,B} - F_c v = 0; & \text{resistive load (Q3)} \\ -p_A q_{v,A} + p_B q_{v,B} + F_c v = 0; & \text{assistive load (Q4)} \end{cases}$$

When equation 1.1 is used, the following equations can be obtained:

$$\begin{cases} F_c v = + (p_A \alpha - p_B) q_{v,B}; & \text{resistive load (Q1)} \\ F_c v = - (p_A \alpha - p_B) q_{v,B}; & \text{assistive load (Q2)} \end{cases} \quad (3.4)$$

$$\begin{cases} F_c v = - (p_A \alpha - p_B) q_{v,B}; & \text{resistive load (Q3)} \\ F_c v = + (p_A \alpha - p_B) q_{v,B}; & \text{assistive load (Q4)} \end{cases}$$

Equation 3.4 shows that the hydraulic system operates in pumping mode when  $F_c > 0$  and  $v > 0$  (Q1), and when  $F_c < 0$  and  $v < 0$  (Q3). The system operates motoring mode when  $F_c < 0$  and  $v > 0$  (Q2), and when  $F_c > 0$  and  $v < 0$  (Q4) [28]. So, we can observe quadrant as a net balance of hydraulic power through actuator, where  $(p_A \alpha - p_B) q_B > 0$  as in (Q1, Q3) and  $(p_A \alpha - p_B) q_B < 0$  as in (Q2, Q4) [19]. These equations can be used in the control systems to determine the quadrant in which the actuator is currently operating.

### 3.1.1 Hydraulic power

In a conventional system, the hydraulic pump operates only in one direction, and the prime mover's speed is constant. Additionally, pressure in the pump's suction side is low, and case pressure should be lower than the maximum permissible pressure of a shaft seal especially with gear pumps. Often, hydraulic pumps and motors in conventional systems also need to have an external or internal drain line where fluid accumulated inside the case due to internal leakage is led to the tank to relieve pressure behind the shaft seal [30] as shown in Figure 11.

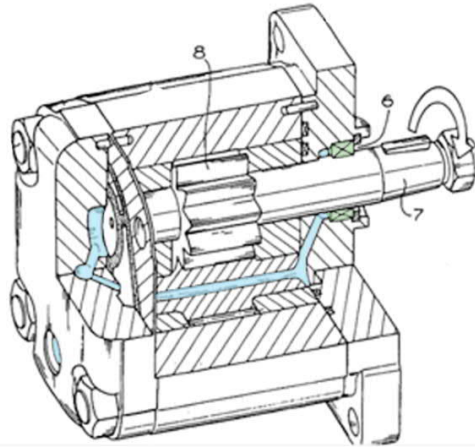
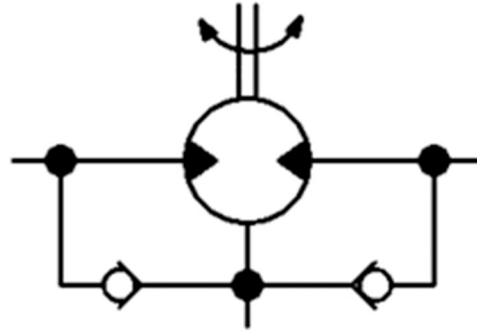


Figure 11 Hydraulic motor's drain line (blue color) and shaft seal (green color) [31].

However, in the DDH systems pump is required to operate in a bi-directional way with various rotation speed because of which the pressures can be high on both pump's connection lines. Therefore, in some situations, the case pressure can be increased too high, resulting in a failure of a shaft seal. To ensure that that case pressure is maintained within pressure level permissible to shaft seal, two check valves are added to the system in as Figure 12 shows. These valves always connect case pressure to the lowest port pressure [30]. However, this alone is not enough for the DDH system, where the pressure accumulator elevates the tank pressure. Therefore, the hydraulic motor's shaft seal needs to be selected to be a high-pressure seal that can withstand high-pressure levels, which usually vary from one to six bar with commercially available seals. However, research has been done on new types of shaft seals that can withstand even higher pressures. For example, Marzocchi Pompe company has invented the shaft seal that is reported to withstand 30 bar constant pressure [32]. Therefore, in the future, this technology can make a hydraulic pump even more reliable when implemented in the DDH systems. Additionally, the system's driving stiffness can be improved because of the possibility of using higher pressure accumulator pressure levels.



**Figure 12 Hydraulic motor external drain line's check valves [33].**

When designing a DDH system with modern pumps, one factor must be considered that limits the slow speeds of the DDH system. This is the lowest rotational speed limitation of the hydraulic pump. If the pump is operated under this speed limit, it can set the pump at a risk for failure because hydrodynamic bearings do not provide assure adequate lubrication for the pump's rotating components [34]. With commercially available pumps, limits for rotational pumps are usually between 50 - 700 RPM. However, there has been research related to this subject which is aimed at developing a piston pump that can operate at a low rotation speed. This piston pump developed by INNAS is based on floating cup principle with both fixed and variable displacement models that can function even at 1 RPM [35]. The pump is available commercially from Bucher hydraulics [36], however it not used for the proposed DDH circuit. Therefore, when the actuator needs to operate at lower speeds, an extra circuit is needed to be added to recycle excess flow coming from the pump. For example, this can be an actively controlled bleed loop connected to pump's suction and pressure lines that is activated during low rotational speed operation [37]. In this way, the pump can operate at the minimum speed, and the unwanted flow rate is directed back to the pump's suction side.

The selected pump for this DDH system is Vivoil X1M/3.2 external drained reversible hydraulic motor, which is suitable for all requirements mentioned earlier with the exception of low rotational speed requirement. These motors are external gear type pumps where two identical gears rotating against each other, create a liquid flow from the suction port to the outlet port [38]. The motor's shaft seal is defined to withstand 6 bar drain line pressures, and it can produce a maximum of 300 bar outlet pressure. This motor's rotation speeds vary from the minimum of 700 RPM to the maximum of 6000 RPM [39].

### 3.1.2 Reservoir

In the DDH system, a hydraulic accumulator acts like a conventional vented oil tank but also maintains the system's elevated tank pressure. This allows a more compact design with better system performance. With open loop hydraulic circuit, the tank size is advised to be a 1.5 - 2 maximum flow rate requirement of the pump per minute [40]. The larger volume ensures that the air bubbles generated during return flow can be deaerated passively before the oil gets back to the pump's suction line [41]. This volume requirement is smaller with a closed loop system where only the compensated flow needs to be stored in the reservoir, and most of the hydraulic fluid for the pump's suction side comes from the cylinder chamber.

Accumulator's primary purpose is to store hydraulic oil from asymmetric flow compensation directed to the tank line. The accumulator stores oil when the cylinder retracts and provides oil when the cylinder extends. The minimum accumulator size is determined by the compensation need of the hydraulic cylinder's chamber volume difference when the actuator's rod is fully extended. However, the pressure accumulator needs also to keep the tank pressure at a constant level, which can fluctuate because of temperature change or leakage in a closed loop system. The temperature change can elevate pressure levels because the pressure change is inversely proportional to the volume change, and increasing temperatures will expand the gas volume and raise the pressure level [42]. Therefore, to reduce the changes in accumulator pressure level the gas volume has to be large enough which needs to be taken into account in designing phase. Additionally, a closed loop system can have small leakages, causing a decrease in the amount of hydraulic fluid, which causes deterioration of driving stiffness. Therefore, the pressure accumulator needs to have space for additional oil, which can be added during assembly. The extra fluid can be released to the system in case of small leakage provided better operation reliability. Additionally, the extra is beneficial for cooling purposes where extra fluid provides enough time for heat to exchange from the fluid before it is directed back to the circuit. Furthermore, the accumulator is used to increase the system's driving stiffness by having an elevated minimum pressure level. Stiffness is better at higher pressure levels because hydraulic fluid's effective bulk modulus is affected by the air bubbles it contains especially at low pressure levels. When higher pressure is applied the volume of air bubbles decrease making the effective bulk modulus higher and increasing the hydraulic stiffness. [43].

An appropriate accumulator needs to be compact in size being still able to store enough fluid to ensure the system's functionality. It is also beneficial if it has small response time. Therefore, weight or spring-loaded accumulators are not suitable for DDH systems because the structure and size of these accumulator types is not favorable for compact circuit design. The type of accumulator which is more suited for this use is the nitrogen gas-charged accumulator models. These fall into three different categories, which are bladder, diaphragm, and piston accumulators. The piston accumulator has a slower response time than the other two types. It also must be operated frequently to avoid piston seal leakages which could affect the pressure levels. Therefore, bladder or diaphragm is a better option for the DDH system, but these also have differences that affect accumulator type choice. The bladder accumulator can have greater oil quantities than the diaphragm, but it has limitations in a mounting position [44]. The bladder accumulator is recommended to mount in a vertical position because otherwise, uneven bladder wear or fluid trapped inside the accumulator can cause deterioration in functionality or mechanical failure [45]. Therefore, the diaphragm accumulator was selected to be used in this DDH system because it allows a more versatile mounting position and system orientation.

### 3.1.3 Flow compensation components

Asymmetrical flow compensation is the most crucial part of the DDH system component configuration when considering its stiffness and controllability. Undesired instabilities can occur if compensation is inefficient or timing is incorrect. Additionally, the oscillations may occur as mode shift oscillations, which happens when systems change the operation quadrant. This phenomenon happens because the actuator velocity is a discontinuous function of the operating quadrant. If the operation mode constantly changes while the actuator moves, it will cause uneven flow compensation, which increases or decreases the actuator's velocity by a factor of  $\alpha$ , causing instabilities in the system [46]. This occurs



for example when actuator is moving a light load with a high velocity. When the speed is increased the hydraulic cylinder's friction force  $F_{seal}$  becomes higher than load force  $F_{load}$ . This will make the flow compensation valve to switch operating position which may lead to uneven flow compensation and operation quadrant changes between pumping and motoring modes [46]. The phenomenon occurs until actuator velocity is lowered enough that the oscillations are damped. Region where this phenomenon happens is identified as a critical zone [17] shown in Figure 13.

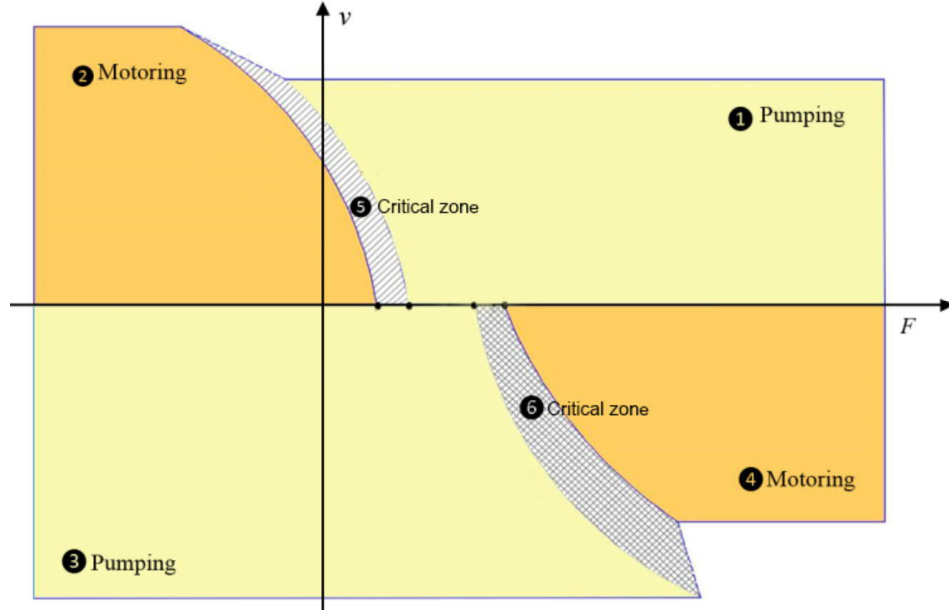


**Figure 13 Operation quadrants division with a critical zone of pilot-operated check valve operated system [17].**

The shape of critical zones is affected by Coulomb friction, viscous friction, flow compensation valve cracking pressure and transmission line losses [17]. These critical zones change the definition of the quadratic division shown Figure 10 where mode change happens and make it more complex to encounter with system configuration. Moreover, the zone border's locations are challenging to define because those depend on the magnitude of friction forces and other energy losses, which are difficult to model [19].

When designing flow compensation, one crucial factor is to ensure that circuit retains its driving stiffness in every operation quadrant. This means that the cylinder chamber against load force -often called control volume, needs to maintain enough backpressure that the load can be controlled safely and accurately with electrical motor by using position tracking. If the wrong flow compensation valve opens the control volume to the reservoir the control stiffness is lost, and the load is uncontrollable until the valve closes, or the load or actuator force's direction changes. This can cause unwanted oscillations and operation safety problems if this is not considered in designing.

To solve the problems of asymmetric flow compensation and pressure oscillations many studies have been presented with different valve configurations. A lot of these configurations are categorized as passive valve compensated systems that benefit from having low electrical control requirement. This type of system commonly utilizes an inverse shuttle valve [47], pilot-operated check valves (POCV) [48], or passively operated directional control valves [49] which are shown in Figure 14. These valves use pilot line pressures for opening according to control logic, which makes this system much more reliable in harsh conditions than electrically operated valves but will have limitations creating complicated controlling logics.

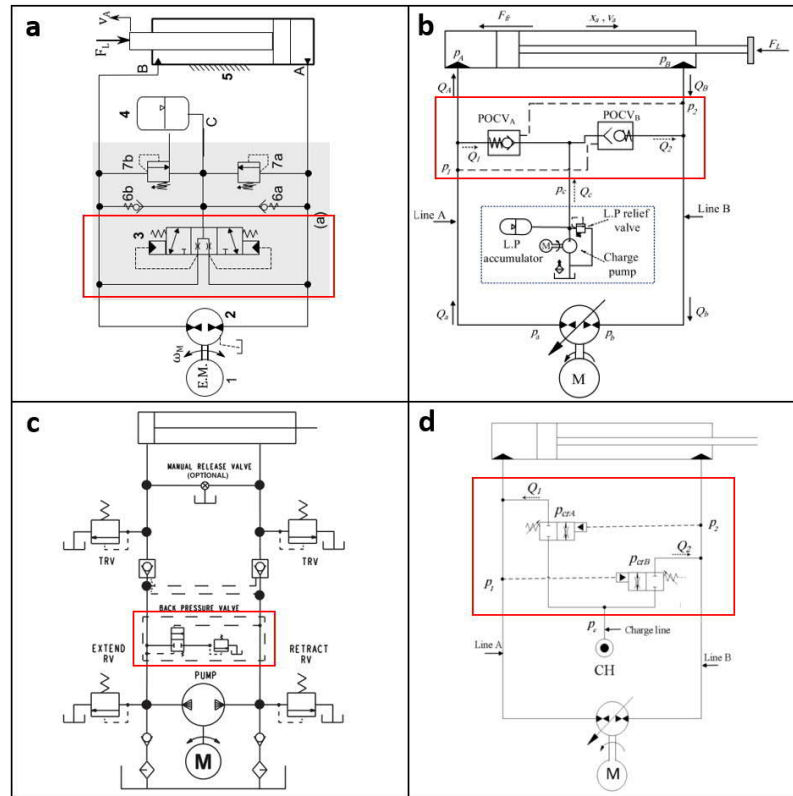


**Figure 14** Examples of flow compensation components. **A:** Inverse underlapped shuttle valve [47], **B:** POCVs and charge pump circuit [50], **C:** Passively operated directional control valves and pressure relief valve [49], and **D:** Limited throttling valves [50].

In the case of the inverse shuttle valve, the hydraulic circuit remains very simple compared to other solutions. This valve is actuated with two pilot line pressures from both pressure lines, which are acting against the spring force. The shuttle valve connects the low-pressure side to the tank or pressure accumulator where the compensated flow is directed from asymmetrical cylinder. Otherwise, this valve stays in the center position, in which the flow paths to the tank are closed. However, researches have reported that the closed center shuttle valve based systems suffers from mode oscillations [47][50]. To mitigate the oscillation issue, the valve spool design, which has an underlapped center position shown in Figure 14 a, was introduced to allow small leakage [47]. This was intended to dampen pressure oscillations while the system operates within a critical zone. However, this was reported to work only with lower speeds and loads. Therefore, applications of this type of circuit are limited [50].

Another common flow compensation method is to use two POCVs (Figure 14 b). This system operates in a way that pilot lines of these POCVs are connected to the opposite side of the circuit. Operation principles are very similar compared to the shuttle valve. However, POCVs are reported to have better operation performance at higher loads and velocities than shuttle valves. Although, in lower load and velocity operations, these circuits also suffer from mode oscillations, making them impractical for some applications [50]. This happens because if two POCVs are closed or opened simultaneously, it will affect the controllability. When both POCVs are closed, this creates a situation where the pump will have an unequal flow rate entering the suction side and leaving the pressure side, making a sudden variation on the load's velocity, and generates pressure transient in the cylinder's chambers. Furthermore, in the case where both POCVs are open, the control volume is connected to the tank, which results in loss of load's control in cases of actuator velocity changes [19].



The circuit which uses throttling valves has been investigated as a solution for both load controlling and mode shift oscillation issue. This system architecture uses passively operated directional control valves and pressure relief valves (Figure 14 c) [49], or limited throttling valve (Figure 14 d) [50], or counterbalance valve (Figure 15) [51].

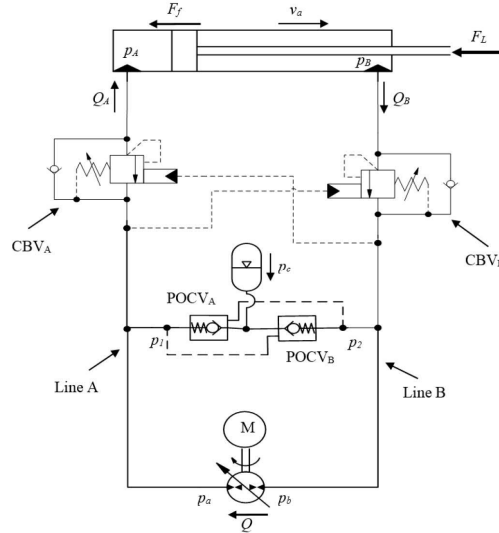


Figure 15 Counterbalance-valve-based circuit [51].

These circuits are reported to increase the driving stiffness and diminish the mode oscillations. However, because all these systems are based on the throttling type of valve solutions, DDH system's energy efficiency is decreased. Additionally, it is reported that these circuits have limitations with energy regeneration during motoring modes. For example, the passively operated directional control valve and pressure relief valve Figure 14 c, cannot regenerate any energy because it is all consumed for maintaining the back-pressure [19]. The counterbalance valve circuit Figure 15 was reported to regenerate energy during Q2 only when the rod side counter valve is opened directly by the B chamber's pressure [19]. However, a novel design of a limited throttling valve could solve this mode shifting problem, which was previously shown in Figure 14 d. It is designed to combine good features of the shuttle valve and POCVs, creating a valve that uses throttling at low load conditions and opens fully when load condition starts to be higher. This is accomplished with the careful design and dimensioning of the pilot area, cracking pressure, and spring stiffness [50]. However, the valve's design needs to be precise to ensure optimal performance and is not yet commercially available.

Another approach has been to use a hydraulic logic valves, which can passively compensate the flow during correct quadrants. This type of valve has been designed for variable displacement pump systems, which directs the charge pump pressure to correct flow compensation valves pilot inlet. Therefore, this circuit cannot be implemented directly to the passively controlled DDH system because it requires an additional charge pump. However, the same signal processing logic can be implemented into actively controlled flow compensation valves shown in Figure 16. In the control system at first the memory valve V connects the charging pressure to C valves based on the assumption that quadrant division is based on cylinder force. So, the memory valve compares pressure  $\alpha p_A$  to pressure  $p_B$  where pressure  $p_A$  is amplified with pressure amplifier I which is designed based on piston area ratio  $\alpha$ . Based on this operation the flow compensation valves' V pilot line can be activated and valves  $V_A$  and  $V_B$  opened if pressures  $p_A$  or  $p_B$  exceed the C valves' cracking pressures.

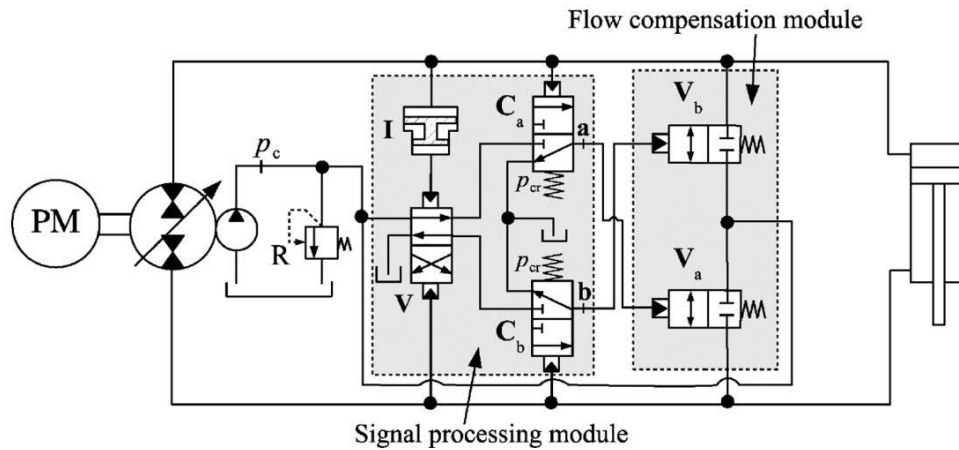
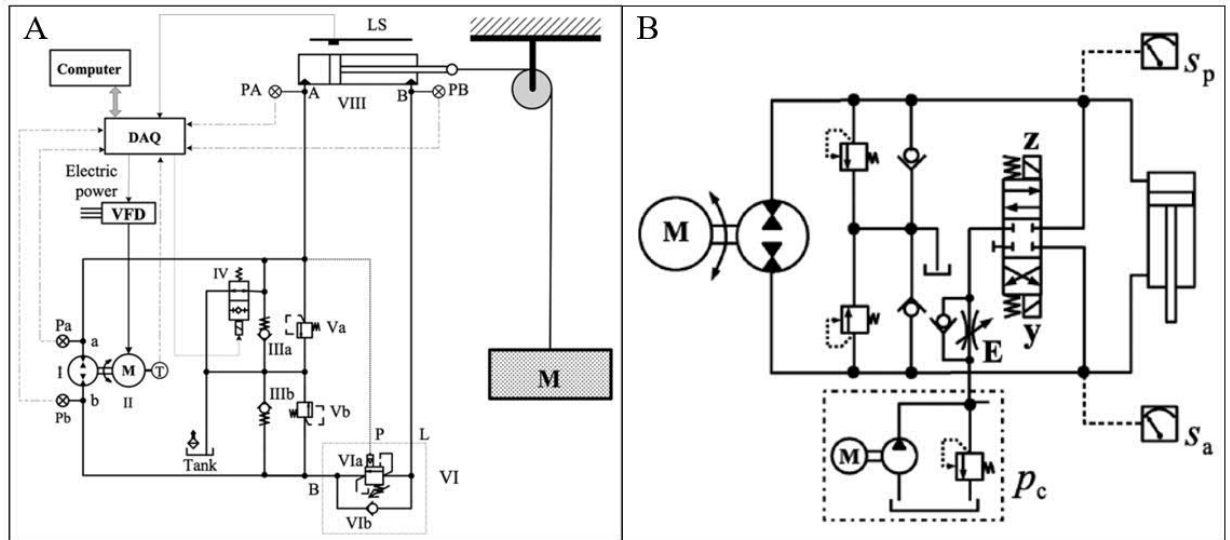


Figure 16 Using logic valves for processing flow compensation valve's pilot pressures [28].

Because passive valves require a lot of designing effort or complex logic circuits for having the most optimal performance, it can make the manufacturing process very expensive and complicated. Therefore, it is more favorable to have actively controlled valves where the system controller analyses sensor data and opens valves according to that. This makes circuit design simpler and gives more flexibility for system compatibility to cylinders of different sizes. Also, most of the modern systems start to be more digitalized. The hydraulic systems already have sensors that can measure chamber pressures and direction of movement, so therefore the implementation of active flow compensation is possible for these systems.

The most straightforward system that utilizes actively operated valves is the one which has a flow compensating valve on A chamber side controlling the valve's opening according to the direction of the cylinder piston. The valve opens to the tank when the cylinder starts retraction and compensates for the uneven flow from A chamber. This approach has been studied in the system, which utilized an actively controlled 2/2 ON/OFF valve IV and a counterbalance valve VI shown in Figure 17 a. Circuit's performance was tested, and it showed excellent performance in motion tracking, and the system was more energy-efficient than the similar valve-controlled system. However, this system was only tested with operation quadrants Q2 and Q3, and its operation is limited only to these quadrants [52]. If the system is operated on Q4, the controlling stiffness is deteriorated because A chamber is always connected to the tank when the cylinder retracts. Also, the system's functionality was based on the throttling counterbalance valve, which decreases the system's possible efficiency. Therefore, it is advisable to have a different approach to system design if the system is desired to operate in all load situations and achieve maximum energy efficiency. As previously presented hydraulic logic circuit can be used to determine the correct operation quadrant, and flow compensation can be done according to that information. This has been researched by using a system, which actively controls 4/3 closed center directional control valve and by using pressure sensor data from cylinder chambers shown in Figure 17 b. The circuit compensates the flow rate by connecting the A-side to the tank circuit during Q2 and Q3, and B side to tank circuit during Q1 and Q4. In this way, the system can compensate for the flow rate without the control volume being connected to the tank under any load conditions.



**Figure 17 A: Actively controlled flow compensation: single ON/OFF valve [52] and B: 4/3 closed center directional control valve [28].**

To achieve more control over opening timing the 4/3 flow compensating valve can be divided into two 2/2 directional control valves where one is connecting the A chamber and the other the B chamber to the tank shown in Figure 18. In this way, valves can be controlled individually, giving more possibilities for future controlling system improvements. For example, theoretical research has been done to predict when mode oscillations happen and how to dampen those by opening valves at the right moment. This is accomplished by running a virtual system parallel to the actual one when the system is operating. This virtual system is used to estimate the hydraulic force used for controlling the actual system's valve opening timing [53]. However, this theory is not fully finished, and the virtual model contains many simplifications and assumptions that may affect its accuracy but still is a promising approach that can be utilized when using actively controlled flow compensation valves.

Therefore, two 2/2 proportional flow control valves were selected to be used as flow compensation valves, giving more control over valve opening timing and providing a more versatile system configuration. Flow compensation is also combined with anti-cavitation valves, which provide passive flow compensation from the pressure accumulator. The functionality during different operation quadrant is shown in Figure 18.

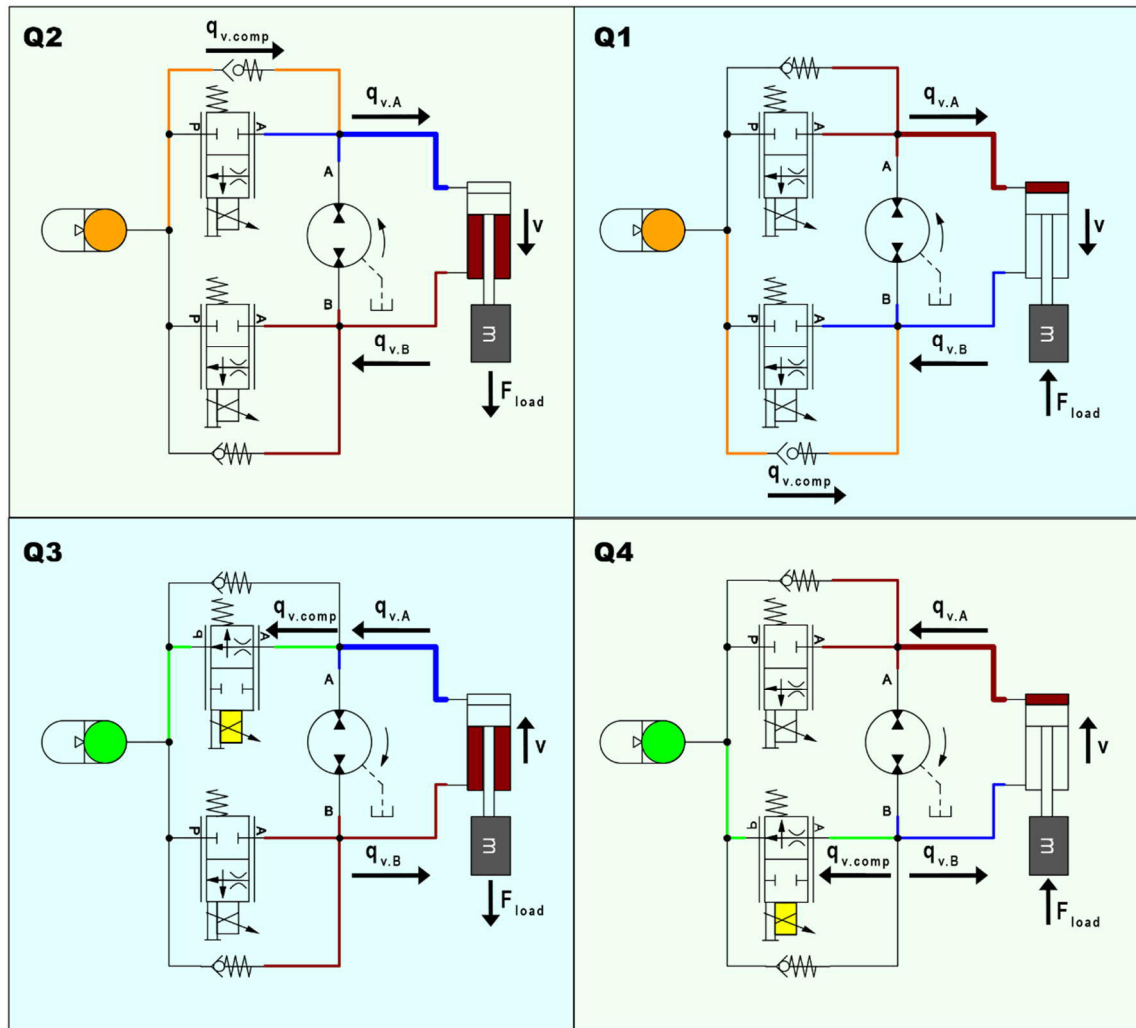


**Figure 18 Flow compensation in all operation quadrants.**

The pictures in Figure 18 presents flow rates with colors where red color represents control volume, which governs the motion of mass and maintains its drive stiffness. Therefore, this volume can never be connected to the pressure accumulator. Additionally, the red line represents the elevated pressure level caused by an external load. The blue color represents the flow rate, which is compensated to provide the correct amount of fluid to another cylinder chamber. This flow rate is also related to the system's low-pressure side, in which pressure levels remain close to tank pressure. When the system operates in Q1 and Q2, the compensated flow rate comes from the pressure accumulator represented as orange color. This flow can be passively compensated because the low-pressure side can open the check valve (CV). The flow is added to the flow rate coming from the chamber B during Q1 and flow rate flowing into chamber A during Q2. When the system operates in Q3 and Q4 it needs to be actively compensated by activating 2/2 directional valve's solenoid according to the operation quadrant in which the system operates. The solenoid energization is indicated with the yellow color. A side solenoid is activated during Q3, and B side is activated during Q4. The compensated flow rate is directed into the pressure accumulator, where the fluid is stored until the system starts to operate again in Q1 or Q2. The pump needs to produce different amounts of flow rate depending on the direction of the load. During the Q1/Q4 flow rate  $q_{v,A}$  is fed through the pump and during the Q2/Q3 with  $q_{v,B}$  flow rate. This affects the rotational speed requirements where Q1/Q4 need a higher rotational speed than Q2/Q3 needs to achieve the same actuator velocity.

### 3.1.4 Safety components

All hydraulic systems require safety components that ensure proper functionality and safe use during and after an operation. These types of components are often referred as pressure sensing and controlling components [2]. Two primary types of this category of valves are PRVs and load holding valves, which need to be included in the DDH system's hydraulic circuit. However, these valves affect the controllability and energy efficiency of the EHA systems, and that is why they need to be selected and configured precisely. Some load-holding valves will especially affect DDH systems' performance in the fourth quadrant [16] [19].

The primary purpose of relief valves is to limit system pressure and reduce excessive pressure generated in the system, usually due to external forces or component failure. If this excessive pressure is not limited, the system pressure will exceed the maximum design limits of a hydraulic component in the circuit, which leads to leakage in gaskets or complete mechanical failure of that hydraulic component. Therefore, the PRV is a mandatory component in the DDH-system to protect components from unwanted failure. In these systems, the relief valve is required to be connected to both of the main pressure lines because the flow path is bi-directional. This is often solved with two PRV valves which are connected to the tank. However, when DDH-systems intend to be a compact system, another more space-efficient solution is to use the CV logic circuit, which selects the highest pressure and connects that to the PRV valve, as Figure 19 shows.

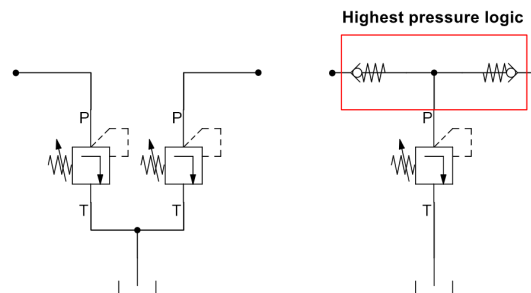


**Figure 19** Two PRV valves connected to both main pressure lines on left and one PRV with CV logic circuit on right.

The load holding valve's primary purpose is to sense load pressure changes in a hydraulic actuator and provide load holding, control, and safety capabilities. For example, some industrial applications, such as boom-operated cranes, require load holding where the hydraulic system needs to be able to reliably hold load stationary over specific periods of time and provide smooth load lowering performance. Additionally, many systems require safety features in case of a hose failure or power shutdown, and load holding valves are often used for this [54]. Therefore, when conventional hydraulic systems are replaced with DDH type of systems, they need to include these functionalities.

One common solution is to use a counterbalance valve (CBV), which is one variation of a pilot-operated relief valve [55]. The valve has excellent holding and control capabilities, which are achieved by having a check valve for forward flow direction and relief valve for regulating reverse flow from the actuator to the tank. This valve type will ensure that the actuator's load side will sustain backpressure while the actuator is moving. Backpressure is created by limiting the relief valve's opening according to the pilot lines pressures [58] as Figure 20 shows.

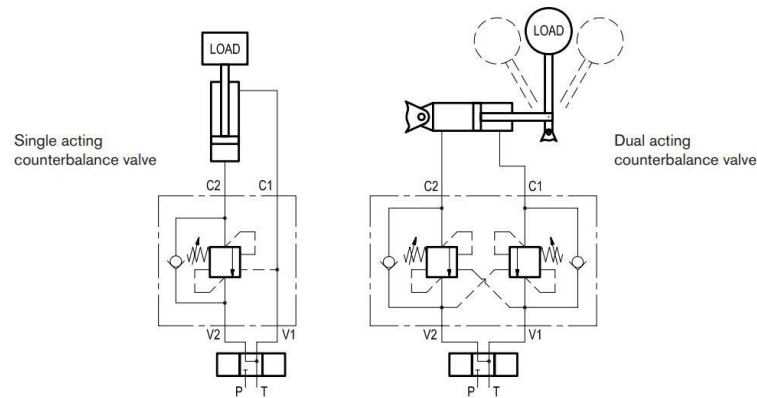


**Figure 20 Single acting CBV configuration for actuator motion in one direction of freedom and dual acting CBV for actuator movement in multiple deriction of freedom [58].**

Several studies have been done of implementing CBVs into EHA systems [17] [56] [57]. These have shown high controllability and better energy efficiency than a similar valve-controlled conventional system. However, this high performance requires precise CBV flow rate, cracking pressure, and pilot ratio selection [17]. Additionally, these researches have shown that when EHA systems are using CBVs in load holding function, it cannot regenerate energy during motoring modes [17] [19]. Research has also shown that the circuit consumes 12% more energy than the circuit without the throttling type of valves [17]. Therefore, these types of circuits are not the most optimal solution for energy-efficient hydraulic circuits.

Another common solution for the load holding solution is to use POCVs which are sensing the pilot pressure to open the valve from the opposite pressure line as Figure 21 shows. Additionally, this configuration has been already introduced in commercial servo-hydraulic actuator (SHA) product by Bosch Rexroth AG [59]. Although this load valve arrangement is functional in some loading scenarios, research indicates that this type of circuit will cause unwanted system behavior while encountering overrunning load [16]. Overrunning load creates a pressure drop in another cylinder chamber, which will affect the pilot pressure that is holding POCV's pilot piston in an open position. This will cause POCV to close momentarily and will generate a pressure transient in the cylinder chamber pressures. Transient affects actuator's motion tracking and produces temporary safety risk.

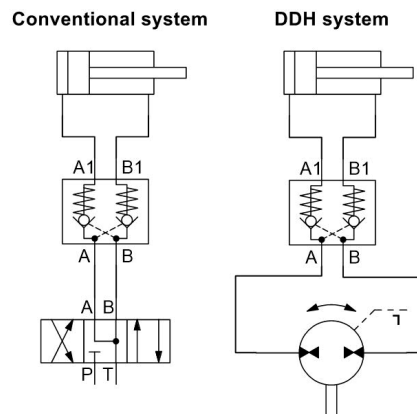


**Figure 21 Conventional way of POCV circuit configuration and same configuration in DDH system.**

Different types of pilot line arrangement have been proposed, which diminish some of the unwanted oscillation behaviors of POCVs [16]. This circuit shown in Figure 22 will provide more control over pilot pressure, which will affect how POCVs open. The circuit has a 3/2 electrical directional control valve, which connects in the de-energized position the POCVs pilot lines to the pressure accumulator. This provides a passive load holding functionality while the system is on idle mode or in case of power shutdown. Because of the pilot line's low flow rate need, the high response time directional valves can also be utilized to control the pilot pressure which often allows only small flow rate levels. When the system starts its work cycle, the directional valve is energized, and the highest chamber pressure is selected from the CV logic circuit which is connected to POCV's pilot chamber. The logic circuit ensures that even in an overrunning load scenario, the pilot pressure is connected to dominant actuator pressure, and both POCVs stay open while the actuator is moving.

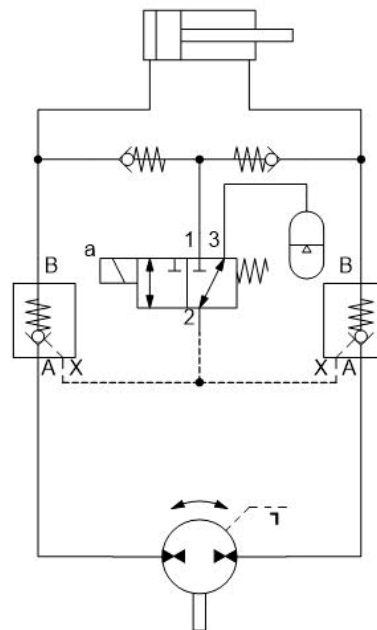


**Figure 22 POCV load holding circuit.**

Another aspect that needs to be considered while choosing the POCV valve for DDH applications is to ensure that poppet of POCV is completely opened when the actuator is activated. Otherwise, if the poppet is not entirely opened, it does not affect the actuator position but will cause a higher pressure drop across the valve, resulting in lower overall energy efficiency [16]. Valve opening can be ensured by selecting POCV, which has an external drainage pilot port shown Figure 23 b.

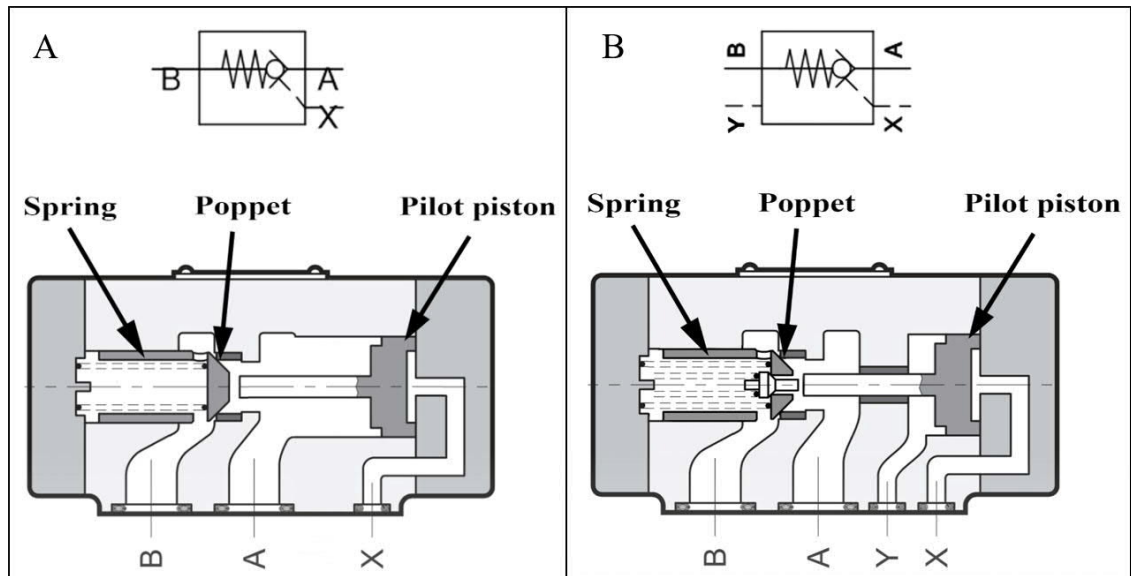


**Figure 23 A: Common POCV chambers arrangement example and B: Diplomatic VP-P/P-MU POCV with drainage pilot port and pre-opening valve [60].**

Commonly used POCVs have a pilot piston that shares a chamber with A-line, which creates back pressure to the pilot piston's rod side area shown in Figure 23 a. Therefore, pilot pressure needs to overcome spring force, B line pressure, and backpressure of A-line. In some scenarios, the back pressure can cause POCV's poppet not to be entirely lift of the seat [60]. This causes more throttling losses at POCV's orifice, making the valve less energy efficient. However, with an external drained valve, the A-line and the pilot piston have separate sealed chambers shown in Figure 23 b. This is often called Y inlet, which can be connected to any pressure line. In the case of the DDH system, this could be the tank pressure, which contains steady and low-pressure level. Since tank pressure is stable, this will ensure that the POCV stays fully open reliably. Some high-end POCVs also have a pre-opening function, which reduces pressure oscillations when the valve is opened. Commonly, this is done with a small poppet or ball which is placed inside of the main poppet shown in Figure 23 b. The pre-opening poppet and pilot piston have high area ratio differences, which allows the poppet to open even with low piloting pressures [60].

Another possibility for load-holding function is to use an activity-controlled 2/2 bi-directional poppet valve as a load-holding valve shown in Figure 24. The valve allows active control over the valve's opening, so it encounters problems that POCV had on opening the valve with pilot pressure. This type of circuit has been used in the DDH research unit, which lifts loaded carriers in a vertical direction [15]. The solution makes the circuit simpler and requires less space than the previously proposed circuit.



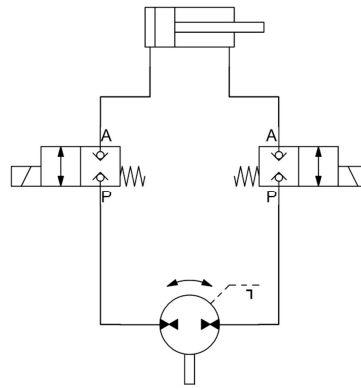


**Figure 24 Actively controlled 2/2 bi-directional poppet valves as load holding system.**

However, these 2/2 valves have a couple of drawbacks, which makes this solution unsuitable for some applications. When POCV is an almost leakage-free valve, the 2/2 poppet valve has some leakage while it is in close position. This is typically around 0.33-0.7 cc/min [62][63], where POCV typically has ~0-0.13 cc/min [64][65][66]. This means that when the system uses a cylinder with  $\varnothing 50$  mm piston and 600 mm stroke, it will lower from top position to down position in 1.2-2.5 days with a 2/2 poppet valve solution. The POCV system can hold load over two and half times longer period. This lowering time can be a limiting factor for some applications. Also, these valves have a longer response time than the POCV system, which is usually 50 ms or higher. Even though this can be enhanced with solenoid boosting, it can be too slow for some applications and better response time is easier to achieve with the POCVs system. Additionally, with a high flow rate (over 50 L/min), typically 2/2 poppet valves have a higher pressure drop than high-end POCVs. Therefore, if high flow rate and energy efficiency are required, POCV could be a more suitable solution.

### 3.1.5 Hydraulic fluid management

One crucial factor in ensuring reliable long-term functionality is to keep hydraulic oil quality high through the operation time. In a conventional system, contaminations in oil are handled with several oil filters. Filters are nearly always placed into system's return line and frequently also to pump's pressure line. These filters ensure that the oil which is flowing into different hydraulic components maintains the acceptable contamination level, which is often given by the manufacturer with ISO 4406 or SAE AS 4059 rating.

In many EHA-systems that have been researched filtration is not included in the system. This is true especially in architectures with sealed tanks. There has been a discussion on whether these systems can be left without filtering elements because they are sealed from external contaminations. One study showed that after a close hydraulic system had operated 960 hours with standard ISO VG 46 hydraulic oil, the self-contamination had resulted in high particle load. This showed that if the DDH system runs with standard hydraulic oil, it requires a filtering system if systems is wanted to be reliable in long term [66]. This is especially important when the system has spool operated directional or proportional valves included in the circuit. These are more sensitive to high particle levels than standard flow control valves, and their performance may be deteriorated if the particle load in the system becomes too large. Therefore, addition of filtering system to the actively controlled DDH system is critical factor if system reliability is wanted to maintain at a safe level.

Because the fluid can flow both directions inside the DDH system's pressure lines, the pressure filter cannot be placed into the lines without extra valves. The hydraulic oil filter is designed to function only in one direction. Usually the fluid goes into the filter element from the outer surface and cleaned oil flows out of the element through the hollow center. Therefore, it is essential to ensure that oil is flowing in the right direction, for example, with check valves. The most common way is to place one CV in front of the filter's outlet line to ensure that the oil is not returning the wrong way to the filter under any circumstances. However, if this type of configuration is placed into a pressure line where the flow rate is bi-directional, this will lead to system malfunction where fluid cannot return from the actuator. Therefore, the DDH system needs to have a CV configuration, which directs the flow rate in the correct direction through the filter or allows it to pass through the CV. These filters are often called bi-directional filters and reverse flow filters, commonly used in hydrostatic transmission systems.

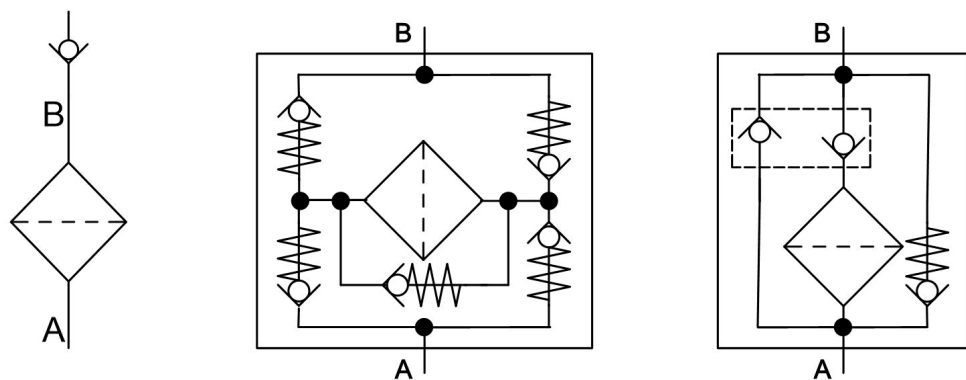


**Figure 25** Different filter CV configurations, left: front of the outlet, middle: bi-directional flow control, and right: reverse flow control.

One oil line which needs to be filtrated is the pump's case drain line. This line will contain a small number of particles, which can cause failure in the system in some situations. Because of this fluid line's low flow rate and pressure level, a small size filter can be used with CV blocking the flow from the accumulator back to the pump's case, as shown in Figure 26. The pump's case drain needs to maintain the pressure level behind the shaft seal lower than the seal's maximum designed pressure level. If the filter creates back pressure the pressure level of the drain line will increase. This can lead to a seal's failure, which results in mechanical failure of the pump [67]. Therefore, the case drain filter system setup and dimensioning needs to be considered when designing the DDH circuit if the tank pressure is close to maximum seal pressure.

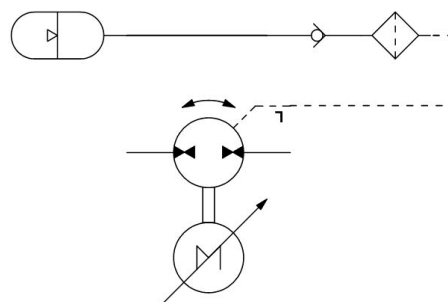


**Figure 26** Pump case drain filtering.

Best filtering results would be achieved if pressure filters are placed on both pressure lines of the DDH circuit. This could, however, result in deterioration of controlling stiffness which happens because the filter element acts as small oil reservoir where fluid flows through it. Because the fluid is compressible, the filter element will act as a spring caused by the hydraulic fluid's limited bulk modulus. Therefore, if a bi-directional filter is placed in the control volume line, it could cause motion tracking deterioration. The reverse flow filter could also create just the same effect, but this will be only in one direction because it allows fluid flow freely to another direction, and good driving stiffness can be maintained. Therefore, it is a good alternative if loading cases are known, and the load acts in only one direction. However, this solution will filter the oil only in one direction and in this way affect the overall oil cleanness. In addition, these filters need to withstand high-pressure levels and flow rates and, for this reason, need to be pressure filter type. Thus, those are usually quite large-sized and expensive components for the DDH system which is intended to be compact and reasonably priced. Additionally, there is limited supply in the commercial market for pressure filters designed to function in closed loop systems.

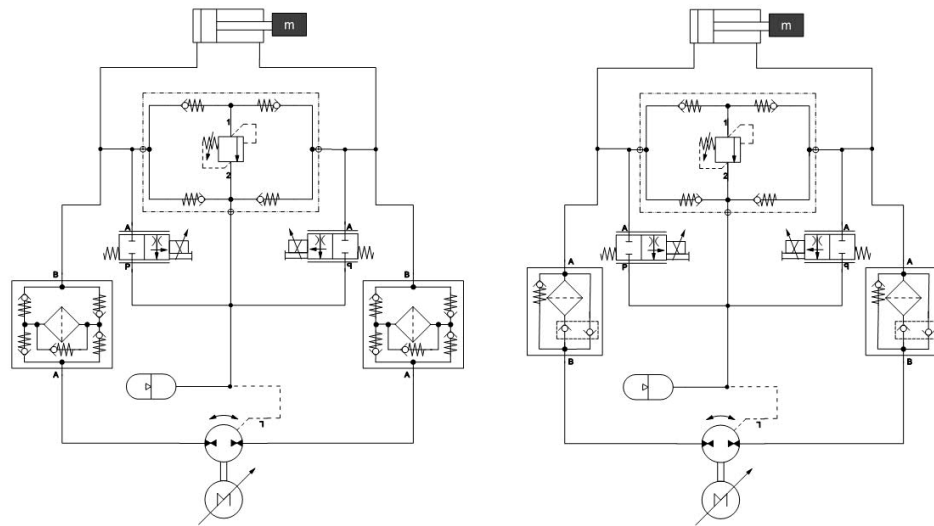


**Figure 27** Examples of possible pressure filters for a DDH system.

Therefore, another solution for the system's filtering is to place the filter in the line, which is always connected to the tank, acting as a return filter. In this way, the controlling stiffness can be maintained at the desired level. The solution will also allow the usage of lower pressure level filters, which will reduce the size and price of these components. The return filter can be placed after the flow compensation valves, and in this way, the oil flowing to the pressure accumulator will be maintained clean. This type of circuit was built for one EHA system that was tested using one CV and one POCV valve [16] shown in Figure 28. The circuit filters the compensated oil when the system is operating at Q4. However, this circuit has one problem since the filtering circuit is designed to function only during one quadrant, the filtering performance is therefore minimal. The system could operate in a way that this Q4 would be rarely operated causing that the oil could stay unfiltered in some load scenarios. Therefore, it is beneficial to connect both flows compensation valves to the return filter so the oil will be filtered during the Q4 and additionally during Q3 as shown in Figure 28 right side.

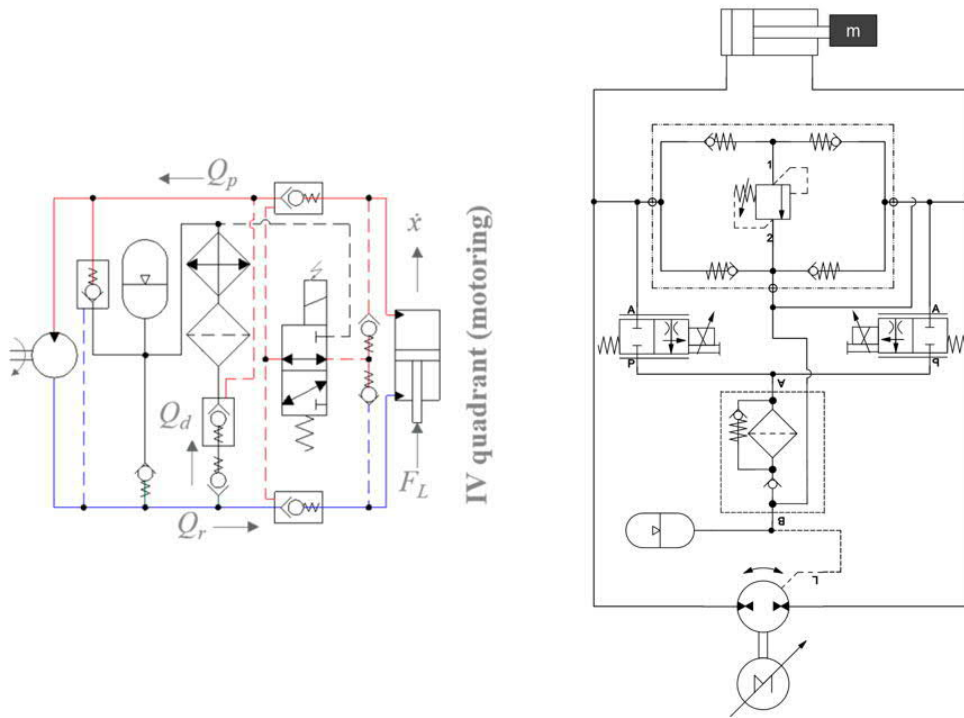


**Figure 28 Left: DDH system return filter circuit. The researched circuit that works at Q4 [16] and right: the proposed circuit, which works at Q3 and Q4.**

One possible solution for the oil filtration problem would be to design a separate filtration system for recycling oil through the filter using a small hydraulic pump. This could happen while the system is idling or while the system is running. The benefit of this kind of system would be that it could work in a way that the drive stiffness is not compromised while the system is operating. This system could also be used as cooling purposes if the rising oil temperature is a problem while the system is running. However, this type of circuit will make the system's space requirement higher, increase the system's overall cost, and decrease the energy efficiency.

In addition to oil cleanness, another problem that the DDH systems face is the air in the system, which will get dissolved into hydraulic fluid or get trapped into the system as air pockets or bubbles, for example during the circuit's assembling phase. If the system does not have any air bleeding solutions, this will increase system's cavitations, oscillations, response lag, power loss and foaming which all decrease system's controllability. The air in the oil directly affects the fluid's bulk modulus, which will decrease proportionally to air quantity which is absorbed in the fluid [68]. Therefore, it is essential to get the most air out of the system before it starts its operation. The cavitation can especially lead to other system problems later on if fluids have high air quantity and the system continues operating. When a local pressure drop occurs due to increasing velocity, the micro-bubbles form when pressure falls under the solubility threshold for air in the fluid. As pressure increases, these bubbles start to be compressed and implode under pressure creating small a shock waves. When this phenomenon happens close to the system surfaces, it can cause surface erosion, and it will also cause thermal-oxidative stresses to hydraulic oil, which can shorten the system's operation life [69]. This can lead to mechanical failure, especially in the DDH system's hydraulic pumps gears.

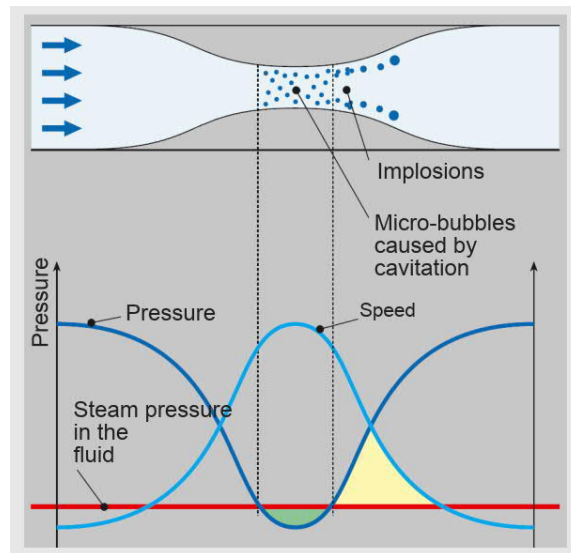


Figure 29 Cavitation in hydraulic oil [69].

According to Henry's Law, the fluid's solubility is proportional to the fluid's pressure, and even in atmospheric pressure 10% of oil can be air [69]. Therefore, the air needs to be dissolved from the liquid while the system is closed to 0 bar pressure or even when it is in a vacuum. Because the DDH system is a closed loop system which does not have a tank with a breather valve, deaeration needs to be completed in the system's assembly phase. Additionally, this process needs to be performed while the pressure accumulator is disconnected from the hydraulic circuit or nitrogen gas chamber is unpressurized. The cheapest solution is to have cylinders with air bleeding screws as Figure 30 shows. However, this solution is a laborious process where air bleeding screws need to be on the system's highest point. When the piston is driven to one end, a small amount of air can be released at once, and then oil needs to be added to the system to replace the air.

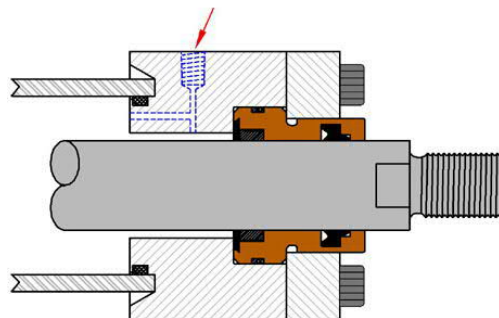
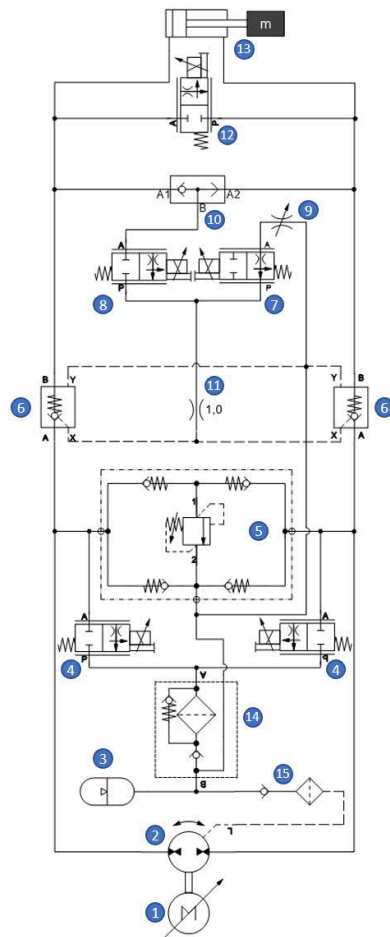


Figure 30 Air bleeding screw at a cylinder head [70].

Therefore, a more suitable solution would be a separate system that is connected to the DDH circuit when it is deaerated while assembling or maintaining the system. This system could have a small hydraulic pump and tank with a breather to recycle hydraulic fluid. In this way, the air has time to dissolve from the oil while it is in a separate tank, and new oil could be fed to the system through the pump.

### 3.1.6 Hydraulic components

The proposed DDH circuit was designed based on investigations of DDH systems presented in the previous chapters. The circuit is seen in Figure 31 where the component list is also included. The maximum work pressure of this hydraulic circuit is set to be 210 bar.



Number	Description	Component
1	Servo motor	Beckhoff AM8052-0L20-0000
2	Hydraulic pump/motor	Vivoil XV-1m/3.2
3	Accumulator	Min. 2l
4	2/2 Proportional Flow Control Valve	Parker DF102C6
5	Dual cross over relief, pilot operated with anti-cavitation check valves	Bosch Rexroth A-VAA-CC-150
6	LHV (POCV)	Sun Hydraulic CVCVXCN
7	2/2 Proportional Flow Control Valve	Parker DF102N6
8	2/2 Proportional Flow Control Valve	Parker DF102C6
9	Needle valve	Bosch Rexroth RDF-7
10	Shuttle valve	Bosch Rexroth VFC 05.99.05.00-Y
11	Needle valve	Bosch Rexroth RDF-7
12	2/2 Proportional Flow Control Valve	Parker DF102C6
13	Hydraulic cylinder	50x30x600
14	Main filter block	OMTI CS AN, 10 $\mu$ m
15	Motor drain line filter	In-line FL 140, 25 $\mu$ m

**Figure 31** Proposed DDH circuit's scheme and component list.

The following circuit presented in Figure 31 is using Beckhoff's servo motor which is discussed more detailed in chapter 3.2.1 and Vivoil gear pump-motor as a power source. This will provide fast and accurate control for the DDH system. The flow compensation is created with two Parker's DF102 proportional flow control valves (4), which are opened during the third and fourth quadrant. This allows more control over valve opening timing, and even throttling during critical situations is possible. These quadrants are identified using acceleration and chamber pressure data, which is processed in Beckhoff PC's control algorithm. For the circuit's pressure relief and anti-cavitation operations, Bosch Rexroth's A-VAA-CC-150 valve (5) is used, which provides a compact valve block design. The anti-cavitation valves will also function part of the flow compensating system as Figure 18 previously showed. Customized divider manifold is designed under the A-VAA-CC-150 valve, where connections for A, B, and tank line's fittings and sensors are placed. For the load holding solution, POCVs with external drainage port (6) from Sun Hydraulics brand are used. However, one of these valves can be in the future research changed to the high-end Duplomatic model shown in Figure 23 to compare these valves' performance. The pilot signal is taken from cylinder chambers through the shuttle valve



(10), which is providing dominant actuator pressure. This pressure is then led through a proportional valve (8), which controls the timing of pilot pressure activation. This line is closed when the system is in idle mode, and pilot pressure is connected to tank pressure through a proportional valve (7). This circuit is similar to one present in Figure 22. However, the 3/2 directional valve is replaced with two proportional valves to acquire more pilot pressure control for research purposes. Needle valve (9) is placed between the proportional valve and tank line to ensure that leakage through the proportional valve during idle mode is minimum. Needle valve (11) however, is placed before POCV pilot lines to provide a smoother pilot signal. The proportional valve (12) is placed between cylinder chambers to provide the possibility to move the cylinder at a slower speed. That is because the Vivoil pump's minimum rotational speed is 700 RPM. When the cylinder is intended to run with slower speeds, this proportional valve is opened slightly. Additionally, another purpose of the valve is to be a possible pressure oscillation damper mechanism. The performance of this function can be tested and its effect on system's overall performance.

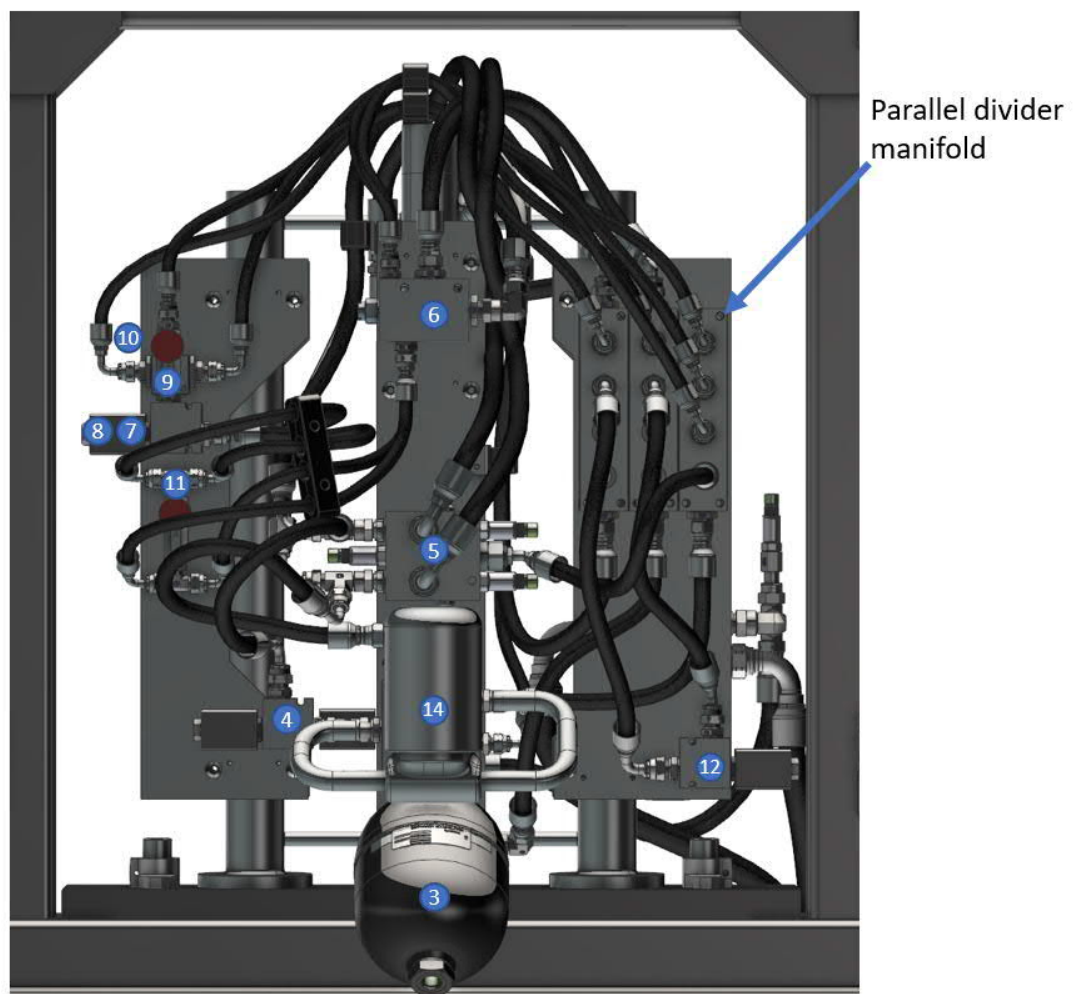


**Figure 32 Computer assisted design (CAD) model of proposed DDH-system.**

Hydraulic components are connected using hoses, giving the system more modularity for future changes, such as switching one of the Sun Hydraulic's POCV to Duplomatic VP3-P/P-MU. Hose sizes used are  $\frac{1}{2}$  inch hose for pump connection,  $\frac{3}{4}$  inch hose for pressure lines, and  $\frac{1}{4}$  inch for pilot lines. Three parallel divider manifolds are included in the circuit

to increase the test circuit's modularity and to make the deaeration process easier. Deaeration components such as deaeration screws or connectors for a separate oil recirculation circuit can be easily connected on top of these manifolds.

The servo motor and hydraulic pump are connected with KTR Rotex flexible couplings, which are covered with aluminum casing. These are placed on another side of the DDH cylinder. The elastomer coupling provides torsional vibration and shock dampening, making high dynamic operations more efficient for the DDH system. The motor and pump are attached to separate connecting plates which are bolted to the mounting plate. This arrangement provides stiff and secure installation for the motor and pumps connection.

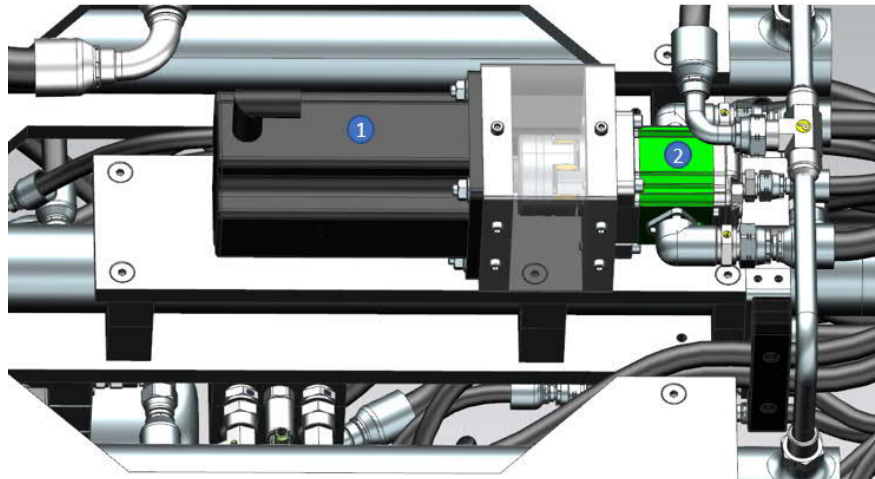


Figure 33 CAD model of motor connection.

## 3.2 Electrical system

The test bench's electric system is based on Beckhoff's programmable logic controller (PLC) system. DDH-system's control, position tracking, and data acquisition are made with Beckhoff embedded-PC CX5130-0155 with a 40 Gb CFast flash memory card for data storage. Data communication is implemented with Ethernet for Control Automation Technology (EtherCAT) system, which provides a fast and accurate platform for this purpose [71]. This technology gives the possibility to run a real-time Simulink model for the controlling purposes used in future research. The following chapter will provide information on different electrical components utilized in this test system.

### 3.2.1 Electrical power

Mechanical power for the DDH system comes from electrical motors that convert electrical power to mechanical power and provide energy regeneration properties. EHA systems have been mainly based on either brushless DC (BLDC) motors [56], AC three phase motors [15][17], or servo motors [16]. All of these have shown good performance in EHA systems in specific loading scenarios or work cycles. Generally, DDH systems need precise speed and torque control under load, which affects the specific application's motor choice. Additionally, the pump displacement will also have an influence on motor choice because different motors are limited to rotating at certain speed. Figure 34 shows the general features and advantages of different types of small-size motors, which will give a better understanding of the different influences of electrical motor choice for a specific application.



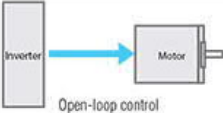
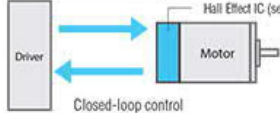
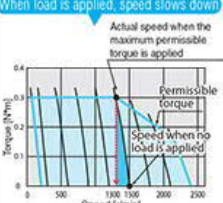
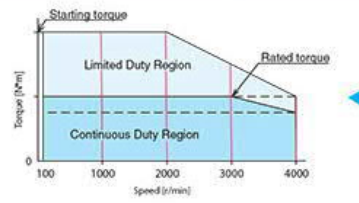
	Inverter + Three Phase Motor	Brushless Motor	Servo Motor
Composition / Structure / System	Three-phase induction motor + General-purpose inverter	Sensor mounted to magnet motor (SPM type) + Dedicated driver	Encoder is mounted to magnet motor (SPM type/ IPM type)
	The same as the servo motor except that Hall Effect IC (sensor)	Encoder detects rotor position, more accurately than sensor.	
	 Open-loop control	 Closed-loop control	
Control Function	Speed control with accuracy not required	Speed control (Torque control is partly possible)	Speed control, position control, torque control
Rotation Speed (speed ratio)	100–2400 r/min (1:24)	80–4000 r/min (1:50)	Up to 5500 r/min
Torque			
Price for Reference: Motor (w/ gear) + Driver	200 W ~ \$374 Comparatively inexpensive	200 W ~ \$441 Less expensive than servo motor	200 W ~ \$1,500 Comparatively expensive to other control motors (Different depending on the accuracy and output of encoder)
Motor Exterior	Induction motor	The same mounting as induction motor. Length (depth on the size of motor) is very short.	Mounting is small for its output. Length (depth on the size of motor) is very long.
Efficiency / Energy Saving Performance	Efficiency of induction motors is not high.	High efficiency thanks to permanent magnet motor	
Speed Regulation (load)*	-3 ~ -15%	±0.2 ~ ±0.5%	±0.01%
Responsiveness	Low	High	High
Overrun	Yes, Large variations	Yes, Large variations	Performs highly accurate positioning
Suitable Operations	<ul style="list-style-type: none"> <li>The main use is for operation at a fixed speed.</li> <li>When speed needs to be changed quickly</li> </ul>	<ul style="list-style-type: none"> <li>When speed changes, torque and speed are kept stable.</li> <li>Multi-speed operation</li> </ul>	<ul style="list-style-type: none"> <li>Highly-responsive and high-precision positioning, speed control, and torque control</li> <li>Multi-speed operation</li> </ul>

Figure 34 Comparison of small industrial motors done by Oriental motor CO, LTD [72].

For a small-scale system, a more favorable solution is to use either a BLDC motor or servo motor over the AC three phase motors. These motor types have generally higher energy efficiency than AC motors, making the system's overall energy efficiency better if they are applied in the system [73]. Also, BLDC and servo motors have better speed regulation and higher maximum speeds than AC motors, which is beneficial in the DDH circuit. Additionally, when the load is applied to the AC three phase motor, the motor speed slows down, resulting in the inefficient performance of the DDH system. However, in some industrial application which require high power output AC motor could be a better solution because servo and BLDC motors have lower power limitations [73]. If BLDC and servo motors are compared, both of these can function in the DDH application well. However, the main difference between these two is the accuracy of the speed regulation and torque control. The servo motor has better rotor position tracking because it is equipped with an integrated encoder. BLDC motor has usually only integrated hall sensors, which results in more inaccurate position tracking than with the encoder. Additionally, some smaller BLDC motors are provided in a sensorless version, which has been tested to be inappropriate for the DDH system used in the previous test system design [74]. Therefore, rotor position tracking is a required feature for the DDH. Also, the DC motor does not have accurate torque control, which is also a requirement for the DDH system. Moreover, servo motors can more easily have a faster response time and higher energy efficiency, which will be needed if the application requires high dynamics and performance. However, the expenses of a servo-driven system and space requirements are much higher than BLDC's. That is why BLDC motor with sensors could be a good alternative for a low budget DDH system which does not require very precise motion accuracy.

Because the proposed DDH circuit is actively flow compensation and indented to be high performing system the selected motor type is an AC servo motor. This allows precise and fast control of the motor, which has a significant role in designing a control system which with its high dynamics is also capable of dampening pressure oscillations in the system. The selected motor is Beckhoff's AM8052-0L20, which has 8.2 Nm standstill torque and peak torque 35 Nm with 11.3 A current. Rated torque is 5.4 Nm at a nominal rotation speed 7300 RPM, where the rated power output is 4.13 kW. The voltage level for this system is 400-480 V, which gives the possibility to achieve higher efficiency levels. Controlling is realized with Beckhoff's PLC PC. The motor is capable of 20 - 30 ms response times, which makes this suited motor choice for high-performance research application [75].

Additionally, the servo motor has an external brake resistor where regenerated energy is dissipated into heat. This arrangement is made because test facilities have limitations for feeding electricity back to the main electricity grid, and a battery storage system is not implemented in this test system. Otherwise, this energy could be transferred straight back to the grid, which could compensate for the DDH system's electricity expenses. Another possibility would be using a battery system where the regenerated energy could be stored and later used to accelerate the servo motor in order to move the load. The brake resistor is connected to the servo drive's DC link with cables. This estimate for regenerated energy is calculated by using voltage and current data provided from the servo drive.

### 3.2.2 Sensors

All sensors and their locations in the test system are shown in Figure 35. Sensors are read with Beckhoff's EtherCAT connection through PLC PC (1). Sensors that are used for controlling purposes are servo drive (2), linear position sensor (10), cylinder chamber pressure sensors (4), and acceleration sensor (8). Servo drive includes the motor's current, torque, and rotation speed sensors used for servo motor control. The DDH cylinder has an inner MTS's magnetostrictive linear position sensor (10), which provides position data for the controlling system and limits the movements close to the cylinder ends. Also, cylinder chamber pressure sensors and acceleration sensors provide data for controlling flow compensation valves. Some of these sensors have also a role in the safety functions of this system. These include oil temperature sensors for tank (3) and cylinder chambers (7) that limit the system's operation when oil temperature approaches a specific hydraulic oil's maximum operating temperature. The second sensor for safety functions is the linear position sensor, which prevents the cylinder's piston from colliding with the chamber's ends. The system has two additional pressure sensors used for analysing DDH system's performance; these are tank (5) and load holding circuit's pilot pressure sensors (6). Also, the actuator force is measured with HBM load shell (9), which is placed between the cylinder and loading plates. This instrument is used for calculating the potential energy required to complete the specific lifting cycle.

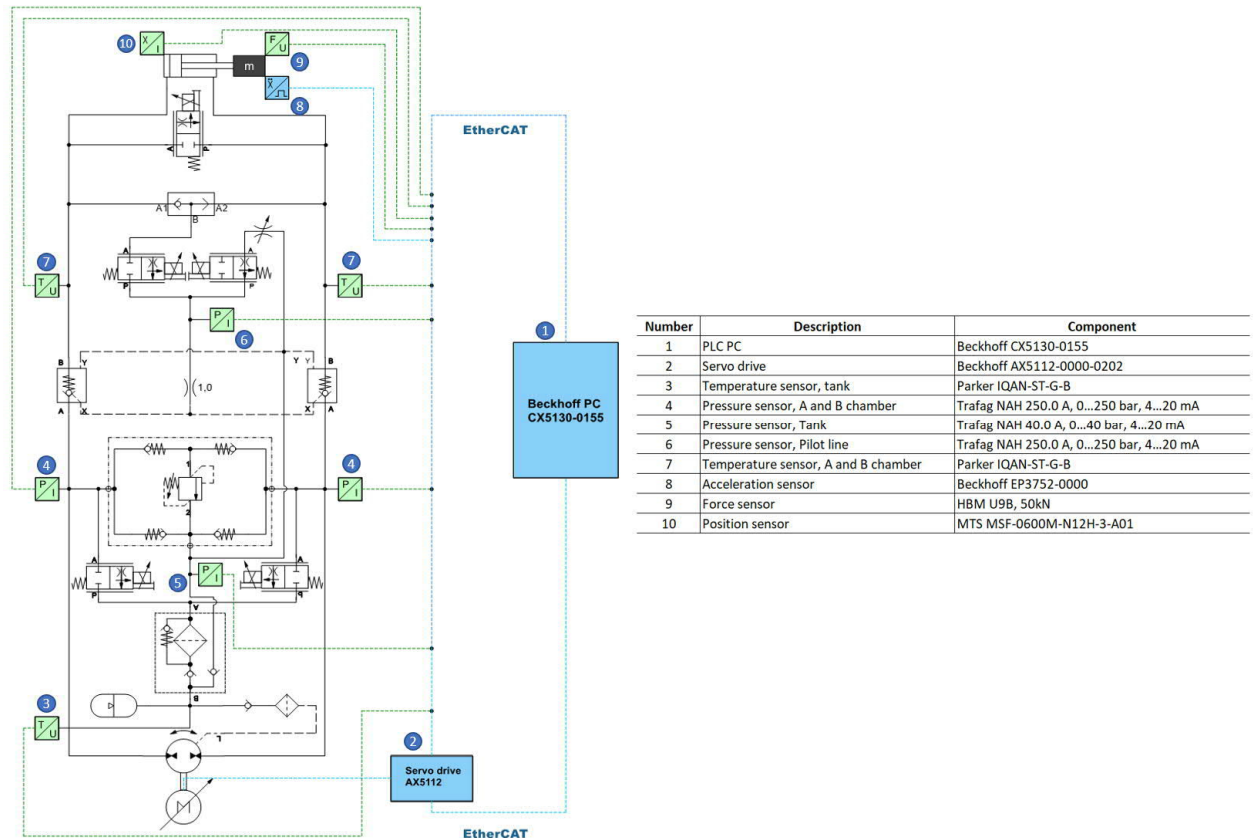


**Figure 35** Test bench's data acquisition system, green dash line means analog signal and blue dash line means digital EtherCAT signal.

Sensors have a different type of output signals, which are gathered using Beckhoff EtherCAT connection. Temperature sensors and force sensors have voltage output while pressure sensors and linear position sensors have current output; these are system's analog sensors. The system has also a couple of digital sensors that are directly connected to EtherCAT. These are acceleration sensors and sensors included in servo drive. Data from analog sensors is read through Beckhoff's 4-channel analog input terminals, which can read voltage signals  $\pm 10$  V and current signals  $\pm 20$  mA. This terminal digitalizes all inputs signals with a 16-bit resolution [76]. All sensor data is recorded with the PLC PC, and this data is used to analyse the system's performance and energy efficiency. Additionally, the data is used in comparison with the simulation model's results, and to refine system parameter values to achieve a more accurate model.

### 3.2.3 Control system

The control system of the DDH circuit is shown in Figure 36. The user can select either manual or cyclic driving mode in which the system can be driven. The manual driving option allows the cylinder to be controlled with a keyboard and mouse, which will determine the servo motor's rotational speed and direction. This will be mainly used when the system is calibrated and for air bleeding of the hydraulic circuit, but also manual driving tests can be conducted. Although, most tests will be executed in the cyclic driving mode, which gives better repeatability. For the DDH cylinder an applicable work cycle can be designed, which it will execute while data is recorded from sensors. This work cycle's parameters are the cycle's number, which is counted from cylinder position data and velocity speed profile given to the motor controller. The work cycle can be adjusted to

achieve reliable results related to flow compensation performance and fluid management properties. Motor control will use PI control to adjust the motor's speed to respond to the speed profile. The servo motor speed command will be affected by the torque, rotational speed, motor position, and current data gathered from servo drive. The safety controlling system will be implemented to monitor oil temperature, cylinder position, servo motor and brake resistor temperature, as well as the safety switch, which can be used in case of emergency. This safety control will stop the ongoing work cycle until the system is safe to use again, and it will give a corresponding error message.

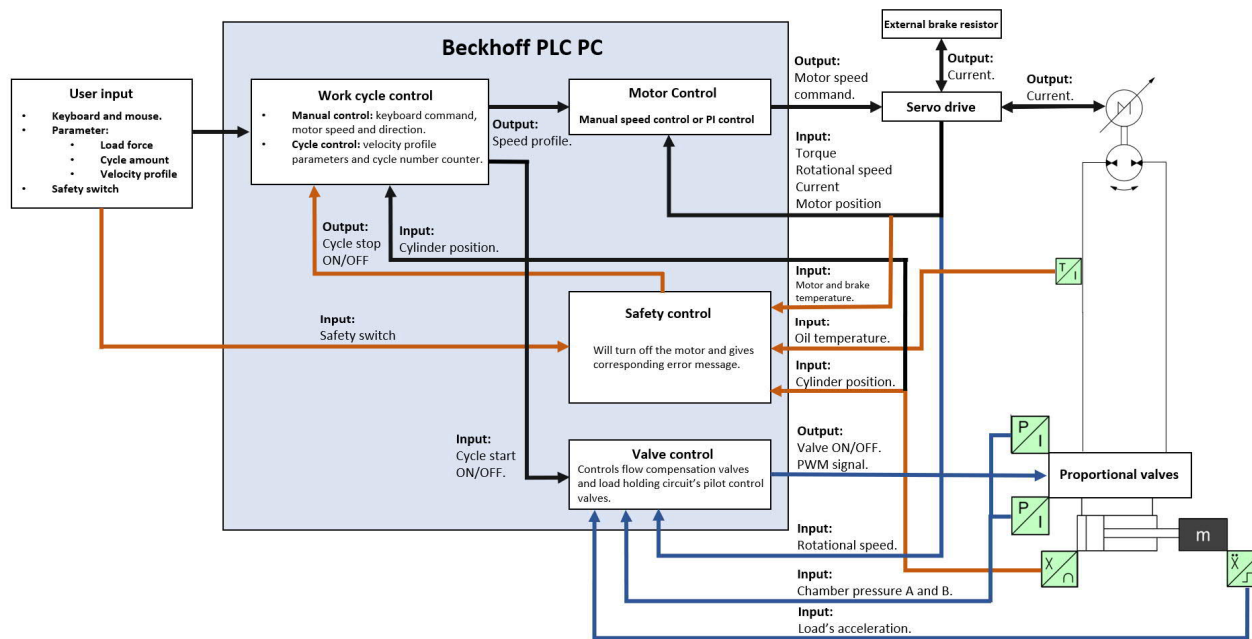


**Figure 36** The DDH cylinder's simplified control logic with input and output data.

Valve control's simplified process control is shown in Figure 37. This system will control the flow compensation valves, pilot pressure control valves, and flow rate regulating proportional valve between cylinder chambers. When the motor starts, the work cycle will give the cycle start parameter command to valve control, which will energize pilot pressure control valves. The timing can be adjusted in a way that the valves can be opened slightly before starting the motor, which can reduce pressure oscillations when the system is started. The flow compensation valve's opening will be based on the direction the actuator force and the cylinder's movement direction. When the cylinder is retracting, the asymmetric flow from A chamber needs to be compensated. Therefore, the control logic will compare the direction of actuator velocity, as the value has minus sign, it will give true value for the next logic section. Then the direction of cylinder's force is derived using equation 3.4, where chamber A pressure times cylinder's piston area ratio is compared to B chamber pressure. When B side pressure is higher, comparison sends a false value to the next logic section to inform about the force direction which is related to quadrants Q2 and Q3. On the other hand, when the result of this comparison is true, the logic circuit knows that system is functioning in Q1 or Q4. After these comparisons, the logic circuit can identify in which operation quadrant it is currently working. B side flow compensation valve is activated when pressure comparison is false, and velocity variables are true, and A side is activated when pressure and velocity are true. The motor's flow rate regulating valve will activate when the hydraulic pump's rotational speed falls under lowest rotational speed limit, and the flow rate needs to be adjusted.

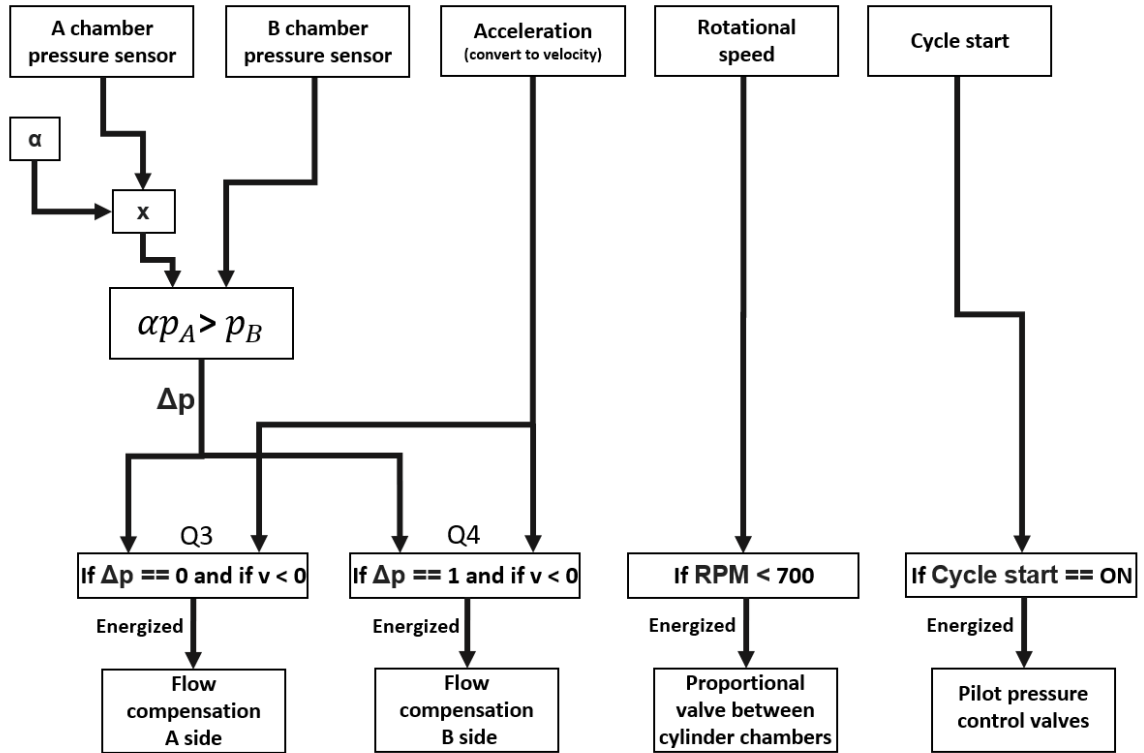


Figure 37 Simplified valve control process flow.

In this thesis, the simplified version of the motor and valve control system will be tested in the Simulink simulation model. Implementation of the completed Beckhoff controlling system will be done during future research.

### 3.3 Load system and test bench

The test bench for DDH-system's performance analysis was designed, and the following section will present key aspects of this test system. Generally, hydraulic load actuator's force consists of three components: load resistance, inertia load, and friction. Therefore, the load system should consist of those components. In this test, the system loading scenario is selected to be lifting or lowering load that makes the need for friction load in the loading system minimum. However, friction force still acts against actuator's direction of velocity because the loading system has sliding mechanical connections like loading cylinder's seal friction and linear guide ball bearings. The test system is intended to be able to load the DDH circuit in various loading scenarios to achieve comparative performance data. The data is used to analyse performance and efficiency during every operation quadrant with varying loads. Other aspects that determine the test bench's design choices are related to modular design for different circuit configurations, easily movable structure, compact size, and safety of operation.

The load system consists of two hydraulic cylinders of size 50x30x600 mm, connected to the DDH cylinder through an inertia mass plate and load cell. The system works in vertical direction and thus it can operate against gravity loads without extra loading force produced by the hydraulic cylinders. The minimum loading mass being 87 kg, which consists of the base weight plate of 82 kg, and the mass of other components attached to it of 5 kg. Extra mass for a weight can be added to this base plate in 25 kg increments, increasing the inertia mass up to 345 kg, where 8 kg comes from extra component needed



for fixing these plates. If loading is wanted to be increased, then loading cylinders are pressurized, and the maximum designed loading force is  $\pm 25$  kN, representing a weight produced by approximately 2550 kg. This loading scenario will result in the DDH cylinder's B chamber side pressure to increase close to 200 bar, which is intended to be the highest operation pressure of the DDH circuit. Figure 38 shows different loading force direction and corresponding operation quadrants where the actuator is operating.

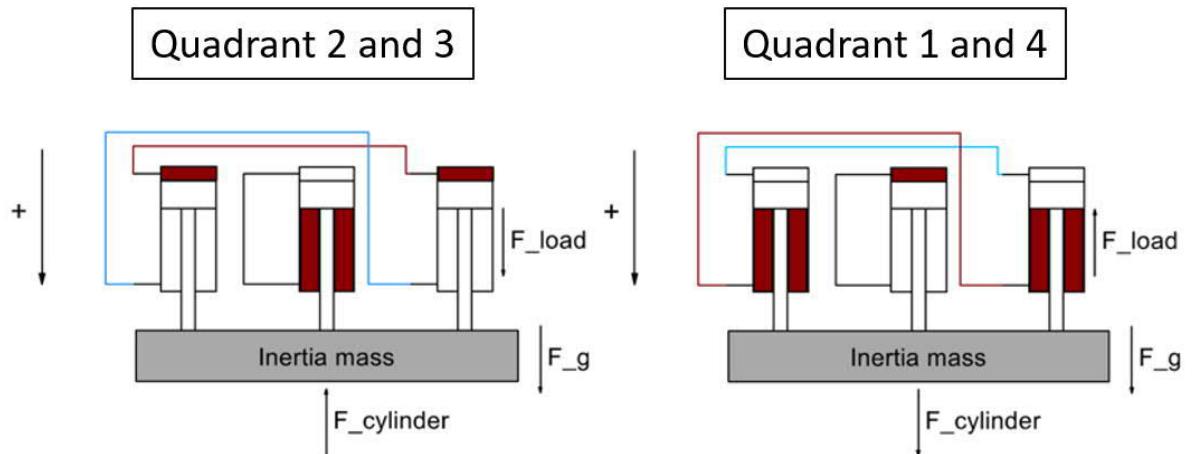


**Figure 38** Different loading scenarios of test bench and corresponding operation quadrants.

When the test setup is functioning in Q2 and Q3, the total load force needs to be in the same direction as the DDH cylinder's positive direction, meaning the same direction as the gravitational force is in this case. Therefore, while the DDH cylinder is intended to be functioning in these quadrants, the load cylinder's A-side is pressurized, and the loading force is working in the same direction as gravitational force. However, when the actuator is wanted to operate in Q1 and Q4, the load force needs to act against the actuator's positive force direction. Therefore, the load cylinder's B side needs to be pressurized. If the same actuator force is wanted to be produced during Q2 and Q3 loading quadrants, the loading cylinder's force needs to be increased. In this case, the load force needs to correspond to the same loading force as in Q2 and Q3 and the gravitational force pull in the opposite direction. The loading force can be determined to be in one direction or multiple directions in cyclic type loading, which will be controlled by Beckhoff's PLC PC and proportional valve.

The load system's 3D model and a hydraulic schematic are shown in Figure 39. The circuit consists of Parker's DFplus 10 4/3 proportional directional control valve regulating the loading force that cylinders produce. This is high performing voice coil driven servo valve capable of functioning up to 350 bar pressure and producing 100 L/min flow rate per control edge. This valve is equipped with an overlapped closed center position to provide the cylinder's rod position hold capabilities. The loading force is controlled with a closed loop pressure control using Trafag NAH 250.0 A pressure sensor data of both loading cylinders. The load circuit has quick couplings that will allow the external power unit to be used as a hydraulic power source. Thus, space otherwise needed for power unit components inside the test bench is saved. This makes the design compact and easily movable if needed. The maximum designed pressure for the load circuit will be 113 bar, which will actualize when the actuator is working in Q1 and Q4 with maximum actuator force. For the case of a system malfunction, while the directional valve is in a closed center position, two pressure relief valves are added between the directional valve and loading

cylinders. These are set to be at 200 bars to provide safety for loading circuit components. When the system is intended to be used without any hydraulic loading force, loading cylinders need to be detached from the main load plate and cylinders are driven to the top position. This will allow the test to be completed with only low inertia loads.

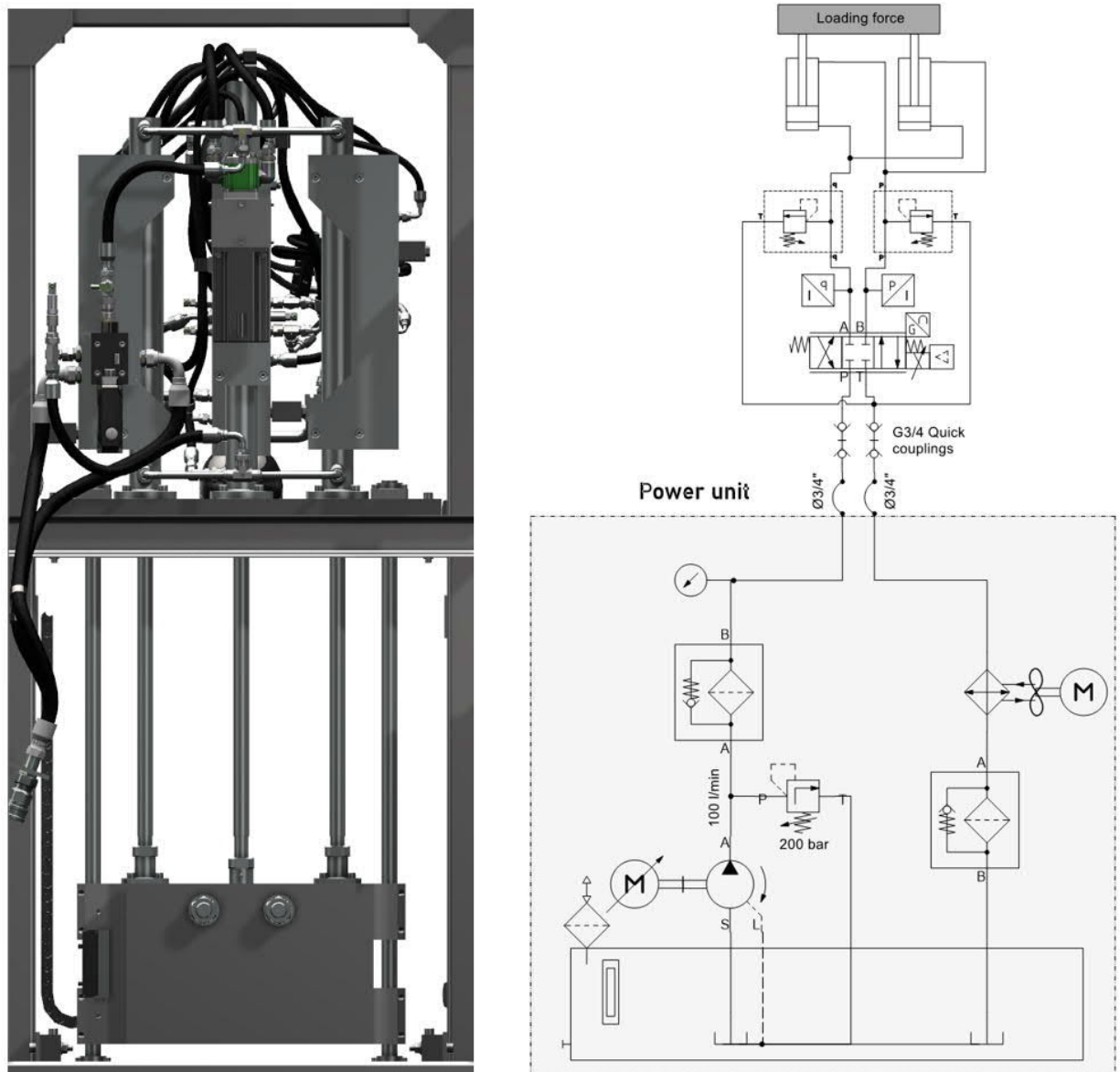


**Figure 39 3D model and hydraulic schematic of the test bench.**

Two linear guides are attached to the main weight plate to limit the system's degree of freedom to only linear vertical motion. This will ensure that there will not be any rotation of weight plates due to the uneven cylinder motion or torque created by inertia mass, which could, in some cases, results in actuator cylinder rod's buckling. Moreover, this allows the DDH cylinder to run without the load cylinder attached to the load system that would otherwise cause a high chance of cylinder's rod to buckle. Also, in this case, the only attachment point between the actuator cylinder and the weight plate is the load cell. The load cell is measuring only the tensile and compressive axial forces. Therefore, any lateral force could affect the results of the load cell and make measurements inaccurate. Additionally, because the load cell is screwed directly to the main load plate without any pivot joints, lateral forces during dynamic loading could damage the transducer if linear guide rails are not used [77].

The safety cage and lifting points are shown in Figure 40 providing better usability and safety for the test bench. The lifting points consist of eyeball bolts on top of the frame and forklift pockets on the frame's bottom. The frame is covered with 6 mm thick acrylic doors, which provide safety in case of system failure. Additionally, the safety frame is built using a BSB aluminum profile, which provides high modularity for future upgrades [77].

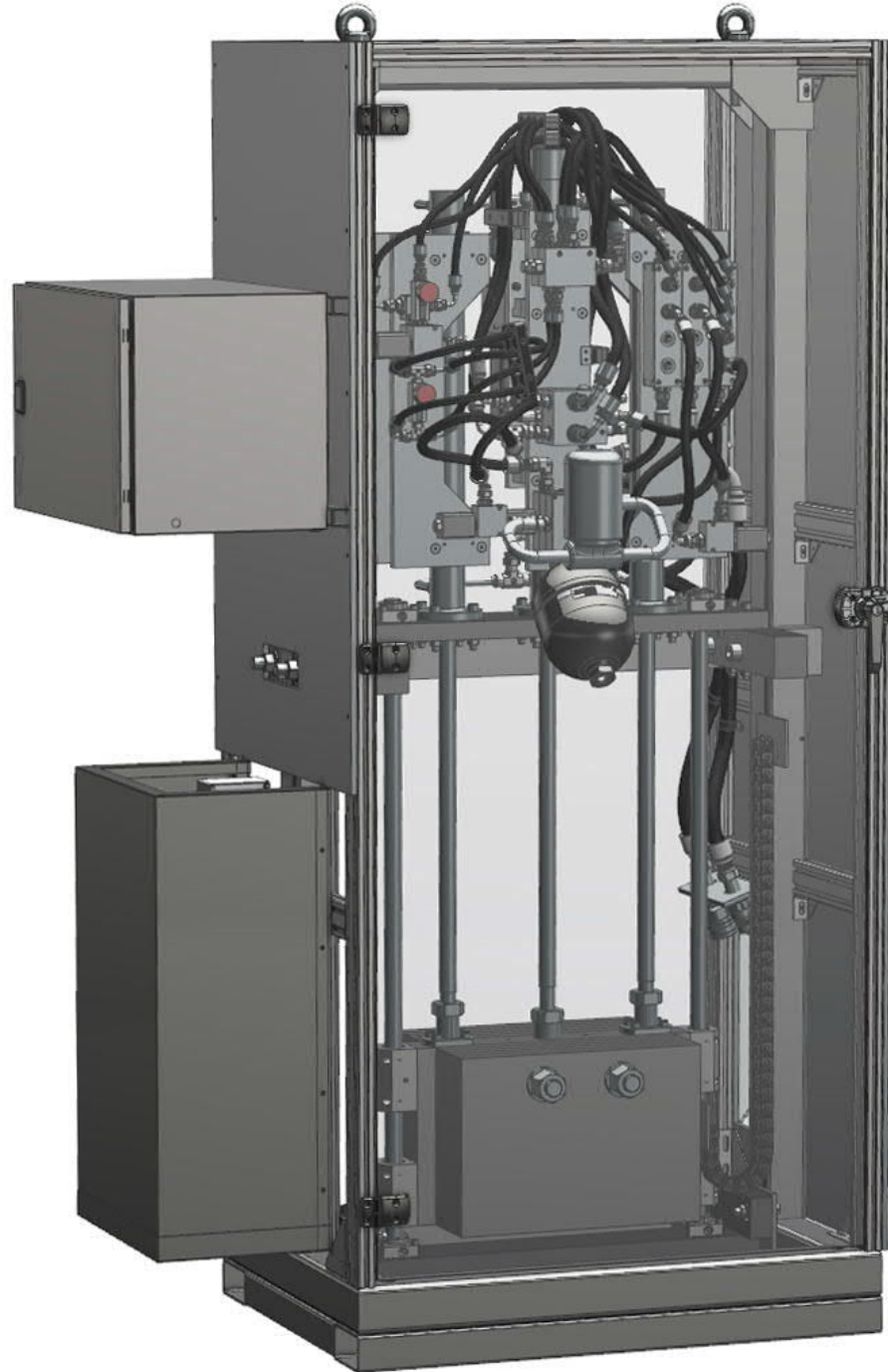


**Figure 40** Test bench safety cage and lifting points.



## 4 Simulation model

The following chapter will introduce the full simulation model that is created in order to test the performance of the proposed DDH circuit and controlling method. This simulation model consists of a model of all the main hydraulic components' sub-models, which are presented in Figure 31. The only thing that is not present is the electrical motor model. Input will be rotational speed generated from a simple motor controlling model, which will drive the hydraulic pump. The DDH circuit model's outputs are variables which are used to analyse the energy efficiency of the system. These are pump's torque, rotational speed, hydraulic cylinder's chamber pressures, actuator force, and load velocity.

The topology of a fluid power system model consists of four different element categories which are connected together [79]. These components are

- Pump, which generates flow rate into a system by using rotational speed from a mechanical power source and pressure difference of volume element as inputs.
- Fluid volumes, which act as fluid transporting and energy storage lines in which pressure is generated as a function of flow rate differences between the connection ports.
- Flow resistors, which control fluid flow rate as a function of pressure differences and flow areas.
- Actuators, which produce force as a function of chamber pressures and load velocity. These components' operation also determines the system's mechanical output power.

All these elements have two-way communication ports between each other. According to the communication's physical properties, this communication is classified into three different types: mechanical, hydraulic, and control communication [79]. Mechanical connections consist of the whole system's inputs and outputs, and these connections exchange dynamic variables between mechanical and hydraulic elements. Hydraulic connections are between fluid power elements and they are exchanging flow rate and pressure variable information. These connections are organized in way that elements like pump, flow resistors, and actuators have pressure as an input variable and flow rate as an output variable. However, volume elements have pressure as output variable and flow rates (in and out) as input variables. In the cases where the fluid volume can be variable, as in the case of cylinders, also the rate of change in fluid volume is one input variable. The last signal type is the controlling signal, such as directional valve's control current, electric or hydraulic pump's displacement command, valve's spring stiffness setting, or another way to have make the system controllable. Figure 41 shows how this topology is implemented into a simple hydraulic circuit.

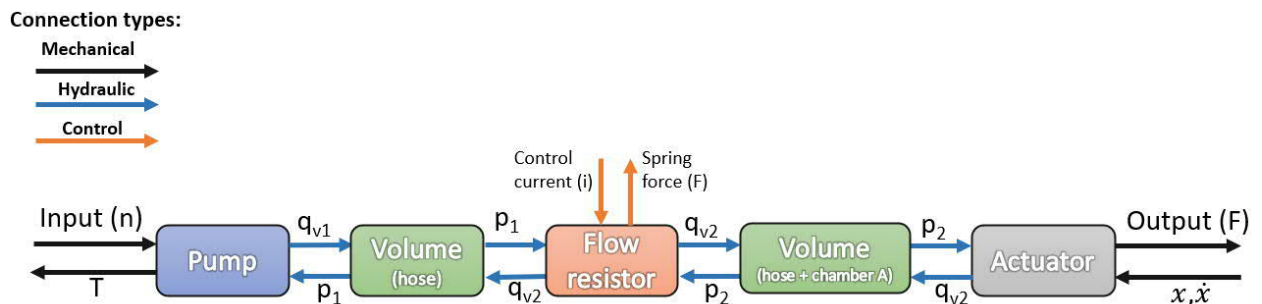


Figure 41 Example of topological presentation of a simplified fluid power system.

The mechanism that generates pressure in the hydraulic system is the change in hydraulic fluid amount and time rate of change of volume that contains hydraulic fluid. This can be expressed as the following equation

$$\frac{dp}{dt} = \frac{K_f}{V_0} \left( \sum q_v - \frac{\partial V}{\partial t} \right) \quad (4.1)$$

where  $K_f$  is bulk modulus of fluid,  $V_0$  is total volume,  $q_v$  is the change in hydraulic fluid amount and  $V$  is element's volume.

#### 4.1 Volume model

Volume elements that are needed to include in simulation model are hoses, fluid cavities, and pipes that connect different hydraulic components. Hose models are used to calculate the pressure generated between hydraulic components as a function of the amount of hydraulic fluid inside the volume element which can be expressed using equation 4.1

$$\frac{dp}{dt} = \frac{K_f}{V_{hose}} (q_{v_{in}} - q_{v_{out}}) \quad (4.2)$$

where  $V_{hose}$  is volume of hose,  $q_{v_{in}}$  is flow rate going into hose and  $q_{v_{out}}$  is flow rate leaving hose.

However, only the hoses included in the simulation model are the one from the pump to the POCVs and hoses of the load-holding system's pilot line. This simplification is made based on the assumption that the flow velocities in fluid cavities and hoses between other hydraulic components are so low that the pressure losses are insignificant. It is also presumed that the volumes are so small that the dynamics of pressure changes are very high and insignificant compared with the other system dynamics. These elements can be connected without volume element between them [80].

#### 4.2 Pump model

The element that often generates the hydrostatic power into a hydraulic system is a pump, which produces positive and negative flow rate in relation to rotational speed and pressure difference over the unit. The required torque to rotate the pump and the produced flow rate can be calculated with Wilson's pump model as a function of the pressure difference over the pump [81]. This model takes into account different losses inside the pump, which decreases its flow rate and increase the torque needed. Inputs for the pump models are the rotation speed of the electrical motor and pump's pressure and suction volume elements', and case drain line's pressures. In this case, the rotational speed is given from a controller block because the electrical motor model is not included in the simulation model. Therefore, the requested torque output is only calculated for energy calculation purposes and will not affect the simulation model's functionality. Another output is the flow rate, which works as input for the chain of other simulation elements.

### 4.2.1 Pump flow

The flow rate of the hydraulic pump depends on the displacement of the pump ( $V_i$ ), rotational velocity ( $n$ ), and in the case of variable displacement pumps also pump's angle setting ( $\epsilon$ ) which will be adjusted with the controller. However, the proposed DDH circuit has a gear pump with fixed displacement and therefore the angle setting is constant 1. These parameters and variables form the pump model's ideal flow rate, which is the maximum possible flow if the pump does not have any leakages. However, all rotating elements need to have clearances between surfaces resulting in leakage ( $q_{v,L,pump}$ ) from the highest-pressure chamber to lower. The flow rate can be expressed as follows

$$q_{v,pump} = \epsilon V_i n - \sum q_{v,L,pump} \quad (4.3)$$

The leakage of the proposed pump is divided into two types: internal and external leakages. Internal leakage results from clearances between the rotating component, depending on pressure difference ( $\Delta p_{AB}$ ) between the pump's inlet and outlet chambers. Additionally, this leakage is needed for providing lubrication for mechanical parts of the pump, for example, bearings. External leakage results from the fluid passing through the pumps shaft seal volume to its case and to the pressure accumulator. This flow rate depends on pressure differences between pump's inlet, outlet, and tank connections. Because these clearances between surfaces need to be small, the leakage can be assumed to be laminar [55]. The following equation contains all pump's leakages

$$q_{v,L,pump} = C_{s,int} \frac{V_i \Delta p_{AB}}{2\pi \nu \rho} + C_{s,ext} \frac{V_i \Delta p_{AT}}{2\pi \nu \rho} + C_{s,ext} \frac{V_i \Delta p_{BT}}{2\pi \nu \rho} \quad (4.4)$$

where  $C_{s,int}$  is internal laminar flow loss coefficient,  $C_{s,ext}$  is external laminar flow loss coefficient,  $\nu$  fluid kinematic viscosity and  $\rho$  is density of a fluid.

### 4.2.2 Pump torque

The needed torque to produce requested pressure difference over the pump with the desired rotational speed can be calculated using the following equation

$$T_p = \epsilon \frac{V_i \Delta p_{AB}}{2\pi} + \sum T_{L,pump} \quad (4.5)$$

where the first part represents the ideal pump's torque and  $T_{L,pump}$  represents torque losses. These include mechanical friction losses, fluid friction losses, and a constant torque loss.

$$T_{L,pump} = \text{sign}(n) C_f \frac{V_i |\Delta p_{AB}|}{2\pi} + C_v V_i n \nu \rho + \text{sign}(n) \frac{V_i}{V_{ref}} T_c \quad (4.6)$$

where  $n$  is rotational velocity,  $C_f$  is Coulomb friction coefficient,  $C_v$  is viscous friction coefficient,  $V_i$  is pump's displacement,  $V_{ref}$  is reference pump's displacement and  $T_c$  is constant torque loss. Signum function of rotation speed is added to the mechanical friction

losses and constant torque loss to make this model function in both rotational directions. This addition is needed because original Wilson's pump model assumed that pump is rotating only in one direction. Additionally, for the constant torque loss a reference pump's previously measured value is used and this is utilized in the calculation by taking into account the pumps' volume ratios. The value will be re-evaluated after the actual tests have been performed and pump's performance is analysed.

### 4.3 Flow resistors

Flow resistor is the element in the system that controls the flow of hydraulic fluid by restricting the flow path and creating a throttling effect. This results in pressure loss across the element, which will dissipate fluid power into heat. The most basic flow resistor model is a turbulent orifice, that is used as a subcomponent for building more complex valve models.

$$q_v = C_q A_0 \sqrt{\frac{2\Delta p}{\rho}} \quad (4.7)$$

where  $q_v$  is the flow through the orifice,  $C_q$  is a discharge coefficient,  $A_0$  is the area of the orifice,  $\Delta p$  is the pressure difference over the orifice and  $\rho$  is the density of the fluid.

#### 4.3.1 Check valve and PRV models

The simplest components of the flow resistors used in the model are CV and PRV, which are spring-loaded seat valves shown in Figure 42. These valves will open according to the pressure difference between poppet's and the mechanical force produced by a pre-tensioned spring. When pressure is higher on port two or spring force is higher than the force produced by pressure in port one, the valve blocks all flow through it. The difference between the CV and PRV is that PRV's spring force can be adjusted with an external knob, and the spring force is usually higher. The pressure when poppet first starts to move is called cracking pressure. Opening of the valve allows the flow to pass through port one to port two. Increasing pressure difference will lift the poppet further off the seat and letting the fluid to flow through it in respect of area between poppet and seat [82].

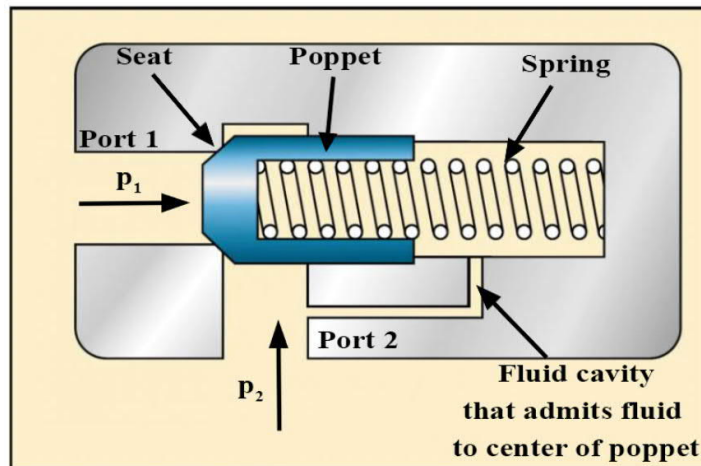


Figure 42 Simplified example of seat valve, picture based on [82].

These components are included in the simulation model using equation 4.7; however, these valves do not have a constant orifice area. The area is depending on spring force and pressure difference over the poppet  $A(p)$  [83]

$$q_v = C_q A(p) \sqrt{\frac{2\Delta p}{\rho}} \quad (4.8)$$

Changing orifice area can be expressed as follow

$$A(p) = \begin{cases} A_{leak} & \text{if } \Delta p \leq p_{crack} \\ A_{leak} + k_L(\Delta p - p_{crack}) & \text{if } p_{crack} < \Delta p < p_{max} \\ A_{max} & \text{if } \Delta p \geq p_{max} \end{cases} \quad (4.9)$$

where  $A_{leak}$  is closed valve leakage area,  $A_{max}$  is fully open valve passage area,  $\Delta p$  is pressure difference over valve,  $p_{crack}$  is cracking pressure,  $p_{max}$  pressure needed to fully open the valve and  $k_L$  is constant defined as

$$k_L = \frac{A_{max} - A_{leak}}{p_{max} - p_{crack}} \quad (4.10)$$

This equation represents linear interpolation of orifice area in respect of pressure difference between minimum and maximum opening. Therefore, this equation assumes that the other forces acting on valves poppet are negligible like inertia load, friction forces, and spring force change [83]. This means also that the valve's response to changes in the pressure difference is instant. Therefore, this will result in unrealistic fast valve operation and the dynamics of the valve opening are added by using the first-order transfer function to provide more realistic operation

$$A(p)_{dynamic}(s) = A(p)(s) \frac{1}{\tau s + 1} \quad (4.11)$$

where  $\tau$  is time constant of the valve dynamics and  $A(p)_{dynamic}(s)$  is a dynamic response of the valve's poppet opening.

These valve models construct Bosch Rexroth's A-VAA-CC-150 valve, which is shown in Figure 43. The assumption made to this model is that pressure and power losses in the CV logic circuit that gives the dominant pressure for PRV are negligible considering the overall efficiency of the DDH system. Therefore, these CVs giving the highest-pressure signal to PRV sub-model are modeled only as Simulink logic and first order dynamics.

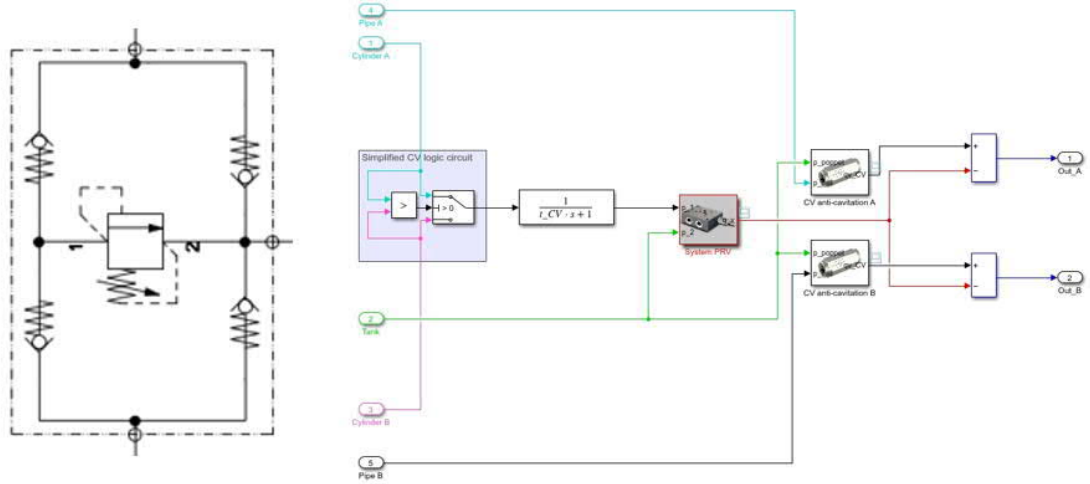


Figure 43 Bosch Rexroth's A-VAA-CC-150 scheme symbol and simulation model.

### 4.3.2 Pilot Operated Check Valve model

For the load holding circuit model the POCV needs to be included. This valve's operation is very similar to CV, but this valve has a pilot piston that holds the poppet open when the pilot line is pressurized, as Figure 23 showed previously. Therefore, the CV model can be used as the base of the model with two exceptions. First is that CV allows flow passing only in one direction, which is often called normal flow. However, POCV has a pilot piston which can hold the poppet open when it is in contact with the poppet's surface and which allows flow to pass from port two to port one, which is called reverse flow. Second is that in the CV model, only pressure difference over the poppet's surface affects valve opening. However, in the POCV valve, also force produced by the pilot piston is affecting orifice's opening area. Hence, orifice opening in POCV is with respect to the force balance of the valve's poppet. Based on these expectations, equation 4.7 is modified, and the following equation is created

$$q_v = \text{sign}(\Delta p) C_q A(F_{POCV}) \sqrt{\frac{2|\Delta p|}{\rho}} \quad (4.12)$$

where signum function of pressure difference allows reverse flow and  $F_{POCV}$  is force balance of the POCV's poppet which is expressed as follow

$$F_{pilot} = \begin{cases} p_x k_3 - p_Y(k_3 - k_4) - p_1 k_4 & \text{if } F_{pilot} \leq 0 \\ p_x k_3 - p_Y(k_3 - k_4) & \text{if } F_{pilot} > 0 \end{cases} \quad (4.13)$$

$$F_{pilot} + p_1 k_{poppet} = F_{spring} + p_1 k_{poppet} \quad (4.14)$$

where  $F_{pilot}$  gives force balance of the pilot piston,  $p_x$  is pilot pressure,  $p_Y$  is drainage pressure,  $p_1$  is valve chamber 1 pressure,  $p_2$  is valve chamber 2 pressure and  $F_{spring}$  is POCV's spring force. Because many valve manufacturers give effective pressure areas as ratios of the actual piston areas as shown in Figure 44. These equations use those ratio parameters instead of areas, like  $A = k$  and therefore  $F = pk$ . Equation 4.14 gives the force balance of the whole valve. Because usually poppet area ratio  $A_1/A_2 = 1$  this relation

can be expressed as  $k_{poppet} = 1$ . However, this pilot piston is not in straight contact with poppet because when pilot line is unpressurized, the POCV needs to operate as a standard CV valve. Therefore, also equation 4.15 needs to be implemented. Additionally, when the pilot piston is in contact with the poppet, the effective area of  $k_4$  is diminished changing the effective chamber one side of the poppet's surface area.

$$F_{POCV} = \begin{cases} k_{poppet} \Delta p & \text{if } F_{pilot} \leq 0 \\ (k_{poppet} - k_4) p_1 - k_{poppet} p_2 + F_{pilot} & \text{if } F_{pilot} > 0 \end{cases} \quad (4.15)$$

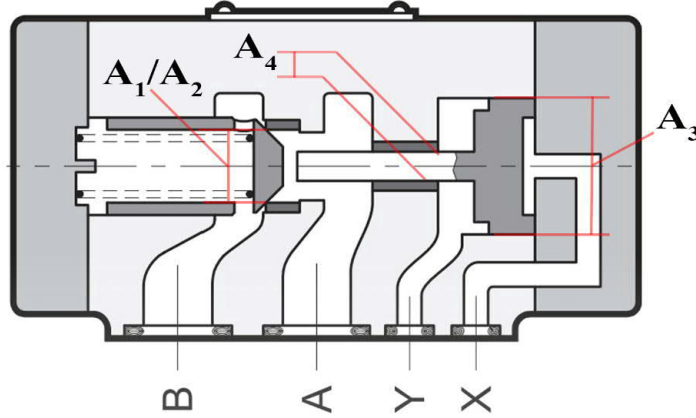


Figure 44 POCV areas [60].

The changing logic related to orifice area can be expressed as follows

$$A(F_{POCV}) = \begin{cases} A_{leak} & \text{if } F_{POCV} \leq F_{crack} \\ A_{leak} + k_L(F_{POCV} - F_{crack}) & \text{if } F_{crack} < F_{POCV} < F_{max} \\ A_{max} & \text{if } F_{POCV} \geq F_{max} \end{cases} \quad (4.16)$$

Where  $F_{crack}$  is cracking pressure force,  $F_{max}$  is force when valve is fully opened.

### 4.3.3 Proportional valve model

Proportional directional control valves are valves which have a spool that is moved by an energizing proportional solenoid's coil. Movement of the spool opens and closes valve's internal flow paths, which provides control over fluid flow direction and rate. These flow paths can be modeled as separate orifices, which are called control edges. Because the manufacturer often does not provide accurate information about the dimensions of the different flow paths inside the directional valve, those are easier to model based on flow rate information given in the valve's datasheet. The control edge equation is expressed as follow

$$q_v = \text{sign}(\Delta p) K(U_c) \sqrt{|\Delta p|} \quad (4.17)$$

where the signum function of pressure difference allows reverse flow  $K(U_c)$  s valve capacity as a function of the control signal,  $U_c$  which is usually DC voltage, or pulse-width modulation (PWM) signal and  $\Delta p$  is pressure difference over valve. Valve capacity is determined as

$$K(U_c) = \begin{cases} K_0 & \text{if } U_c \leq U_{c,min} \\ K_0 + k_L K_{100} & \text{if } U_{c,min} < U_c < U_{c,max} \\ K_{100} & \text{if } U_c \geq U_{c,max} \end{cases} \quad (4.18)$$

where  $U_{c,min}$  is minimum control signal value,  $U_{c,max}$  is maximum control signal value.  $K_0$  is leakage at valve's closed position,  $K_{100}$  is valve flow capacity at valve's fully open position, and  $k_L$  is linear constant which is determined

$$k_L = \frac{K_{100} - K_0}{U_{c,max} - U_{c,min}} \quad (4.19)$$

$$K_{100} = \frac{q_{v,nominal}}{\sqrt{\Delta p_{nominal}}} \quad (4.20)$$

$$K_0 = \frac{q_{v,L,nominal}}{\sqrt{\Delta p_{L,nominal}}} \quad (4.21)$$

where  $q_{v,nominal}$  is nominal flow rate of the valve,  $\Delta p_{nominal}$  is nominal pressure difference of the valve,  $q_{v,L,nominal}$  is nominal leakage flow rate of the valve, and  $\Delta p_{L,nominal}$  is nominal pressure difference of the valve when leakage is measured. If the manufacturer does not provide leakage values, these need to be assumed and later tuned based on measurement data.

Proportional valves used in the DDH circuit are 2/2 directional valves, so those have only one control edge. These valves also have opening and closing time delays caused by the solenoid's dynamics, spool's viscous and mechanical friction, and its mass. An approximation of these effects is implemented by using a first-order transfer function of  $K(U_c)$  similarly as in equation 4.11.

#### 4.3.4 Load holding system

The load holding system is constructed from two POCV and 2/2 proportional flow control valve models. These are implemented into the system, as Figure 45 shows. The actual system has more valves like two needle valves and one shuttle valve. These are assumed to have minimal effect on the DDH system's dynamics and overall efficiency because these are used to control the load holding system's pilot pressure, and flow through this line is assumed to be minimal. Therefore, the needle valve connected between the tank proportional valve and tank line is not included in the model because it is implemented only to limit possible leakage through the proportional valve. The needle valve between proportional valves and POCV is implemented as a first-order transfer function because this valve's primary function is to restrict the pilot pressure dynamics. The load holding circuit also consists of a shuttle valve, which gives dominant chamber pressure for the pilot line. The flow rate through this valve is assumed to be also minimal, also. Therefore, this is modeled as Simulink logic, which gives the highest pressure to the proportional valve with respect to operation dynamics.



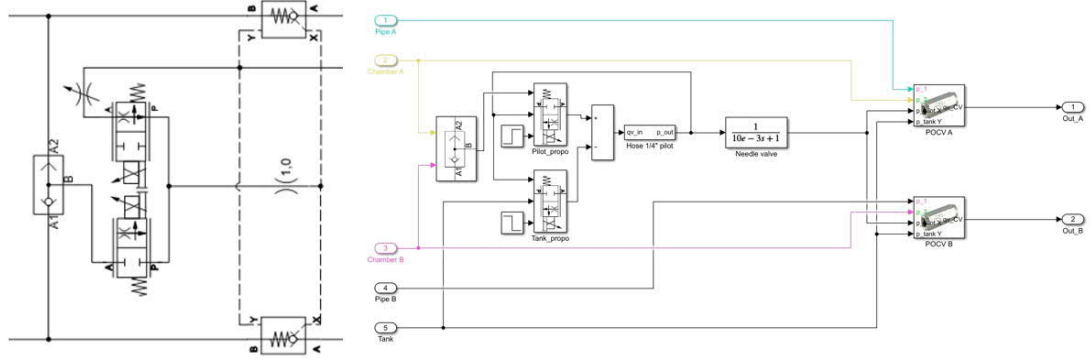


Figure 45 The load holding system's schematic drawing and simulation model.

#### 4.4 Cylinder model

The actuator element of the DDH system is the hydraulic cylinder, which consists of two changing fluid volume elements where pressure difference over the cylinder's piston creates an actuator force that moves the external load attached to the piston rod. The cylinder model has two flow rates, rod end's position and rod end's velocity as input variables. The piston's and rod end's displacements are assumed to be equal. Cylinder chamber pressures  $p_A$  and  $p_B$ , and a cylinder's net force are model's output variables. The pressures that create actuator force can be determined using equation 4.1 and making assumptions:

- There is no external leakages and internal leakage is laminar.
- The pressure inside cylinder chambers is evenly distributed.

Figure 46 illustrates key variables needed for cylinder model.

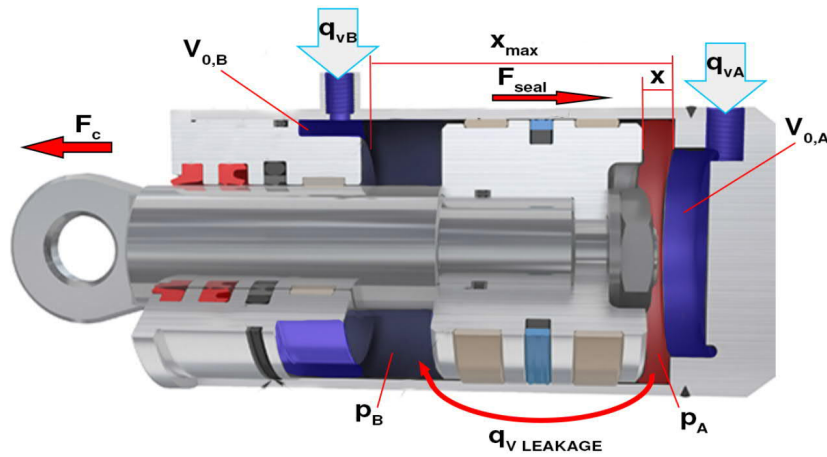


Figure 46 Key variables of a hydraulic cylinder's model, picture based on [84].

Cylinder chamber's volume consisting of dead volume and changing fluid depending on piston area and piston displacement and can be expressed as

$$V_A = V_{A,0} + A_A x \quad (4.22)$$

$$V_B = V_{B,0} + A_B (x_{max} - x) \quad (4.23)$$

where  $V_{A,0}$  and  $V_{B,0}$  are dead volumes consisting of inlet port volume, the volume of the cylinder when the piston is in end position, and fluid volume in cylinder hoses,  $x$  is piston position and  $x_{max}$  is cylinder stroke.

The internal leakage can be expressed [80] as

$$q_{v_{leakage}} = K_L(p_A - p_B) \quad (4.24)$$

where  $K_L$  is internal laminar leakage coefficient. However, in the simulation model these internal leakages are assumed to be irrelevant to the circuit performance and therefore  $K_L$  is assumed to be 0.

Cylinder's pressure equations are obtained combining equations 4.1, 4.22, 4.23 and 4.24

$$\frac{dp_A}{dt} = \frac{K_f}{V_A} (q_{v,A} - q_{v_{leakage}} - A_A \dot{x}) \quad (4.25)$$

$$\frac{dp_B}{dt} = \frac{K_f}{V_B} (q_{v,B} + q_{v_{leakage}} + A_B \dot{x}) \quad (4.26)$$

where  $K_f$  is bulk modulus of fluid.

The pressure force acting on piston surfaces create an actuator force. This force can be calculated using equation 3.1 with few exemptions: the effect of load forces is modeled separately. The end force ( $F_{end}$ ) equation is defined in section 4.4.2. and seal friction force ( $F_{seal}$ ) is explained in section 4.4.1. This net force will act against the load which is mechanically attached to the rod's end. The load model consists of force produced by the load cylinders and the inertia of the load mass ( $F_{load} + m\dot{v}$ ). These factors are explained in section 4.5.

$$F_{net} = p_A A_A - p_B A_B - F_{seal} - F_{end} = F_{load} + m\dot{v} \quad (4.27)$$

#### 4.4.1 Cylinder's seal friction force

The implementation of an accurate friction model to a simulation model is very demanding and involves a lot of measurements. However, it is good to create a rough estimate of the friction's real effect, which can be refined later with the real actuator measurements. The dominating friction mechanism is dependent on the prevailing lubrication regime, such as static friction, mixed friction, or viscous friction [85]. These lubrication regimes are called boundary lubrication, mixed lubrication and elastohydrodynamic lubrication which are shown in Figure 47. The change in lubrication regimes may result in jerky movement of cylinder piston movement, known as stick-flip motion [80]. When actuator velocity is zero, the friction force is dependent on the static friction coefficient. After the actuator force exceeds static friction, the piston starts moving, and a thin film of hydraulic

fluids starts to increase between the seal and chamber surface. This will decrease the friction force relative to actuator velocity until the velocity reaches point specified by parameter  $v_{\mu}^{min}$ . After that point the fluid film is thicker than surface roughness and the viscous friction becomes the dominant friction mechanism [86]. The value of minimum friction force in that point is called the Coulomb friction  $F_c$ . When velocity increases, also the friction coefficient starts increasing relative to  $b_v$  which is the viscous friction coefficient [80]. This phenomenon is often described with a Stribeck curve, which is shown in Figure 47.

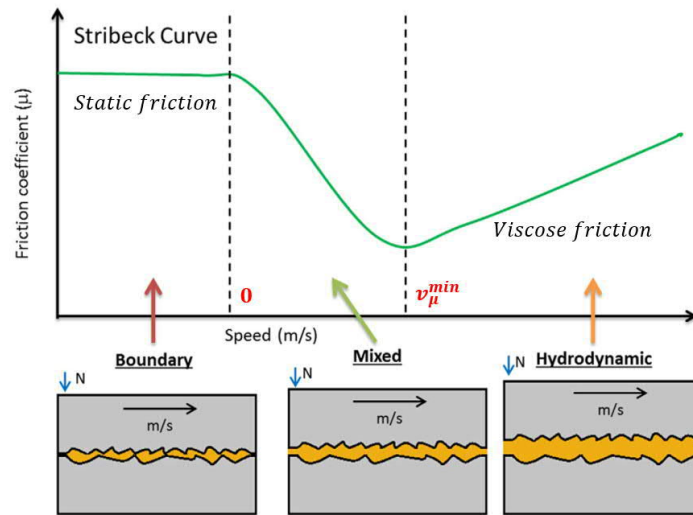


Figure 47 A Stribeck curve and three lubrication regimes and dominating friction mechanics [85]

The seal friction force depends heavily on the pressures applied to the cylinder chambers, causing cylinder seal deformation. Increasing chamber pressures will cause seals to press harder against the chamber surface, increasing the seal force [80]. Additionally, seals are constructed from an elastic material, which will start to yield elastically when force is applied to it. There is small bending of seals before the piston starts sliding, resulting in a small delay in a movement called pre-sliding displacement [87] shown in Figure 48. If actuator force is increased over the static friction force, the seals start sliding while remaining its bent form until the applied force is removed. This will cause seals to straighten to their original form causing small retraction of the cylinder's piston. Therefore, this phenomenon can be modeled as a spring representing the bend of the seal and damper, representing the dissipation which take place when the seal changes its shape [80].

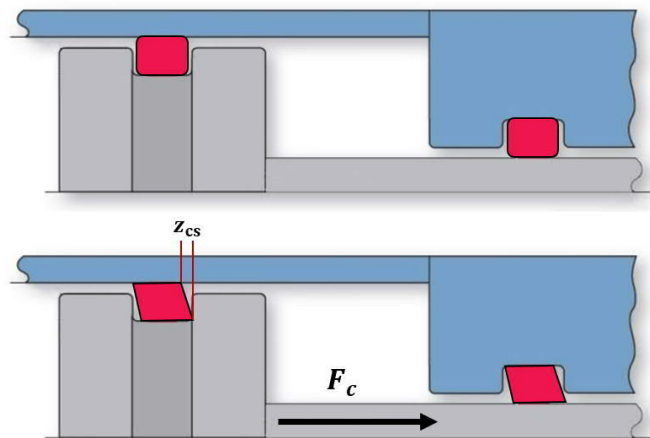


Figure 48 Deformation of the cylinder seals, picture based on [88].

The dynamic friction force is implemented into the cylinder model using the LuGre model [80] that will represent these previously mentioned effects.

$$\dot{z}_{cs} = \dot{x} - \frac{k_{R,cs}|\dot{x}|}{F_{\mu}^*(\dot{x}, p_A, p_B)} z_{cs} \quad (4.28)$$

$$F_{seal} = k_{R,cs} z_{cs} + \zeta_{d,cs} \dot{z}_{cs} + b_v \dot{x} \quad (4.29)$$

where  $z_{cs}$  is bend of the cylinder seal,  $k_{R,cs}$  is spring constant of the cylinder seal,  $\zeta_{d,cs}$  is damping constant of the cylinder seal,  $b_v$  is viscous friction coefficient,  $\dot{x}$  is cylinder velocity and function  $F_{\mu}^*$  is obtained as follow

$$F_{\mu}^*(\dot{x}, p_A, p_B) = \Psi(p_A, p_B) \left( F_{cf} + (F_s - F_{cf}) e^{-\left(\frac{\dot{x}}{v_{\mu}^{min}}\right)} \right) \quad (4.30)$$

where  $F_{cf}$  is the Coulomb friction force,  $F_s$  the static friction force,  $v_{\mu}^{min}$  is the speed indicating when friction reaches its minimum value. In this equation it should be noted that the values are determined such that  $F_{\mu}$  is required to be positive. Additionally, it is very difficult to define exact value for function  $\Psi(p_A, p_B)$  parameters and thus an initial assumption has made that the function value is 1. All other friction parameters are chosen that way that model presents accurately functionality of the DDH cylinder of the system [80].

Spring constant of the cylinder seal is defined by determining maximum possible seal's bend  $z_{cs}^{max}$  using equation

$$k_{R,cs} = \frac{F_s}{z_{cs}^{max}} \quad (4.31)$$

When inertia load is known the appropriate damping constant of the cylinder seal can be defined by using equation

$$\zeta_{d,cs} = d_{adj} \sqrt{(k_{R,cs} m)} \quad (4.32)$$

where  $d_{adj}$  is adjustment constant with values between 0.5-2.0 and  $m$  is inertia load.

These parameters are determined more accurately after the first tests of the proposed DDH circuit.

#### 4.4.2 Cylinder's end force

To limit the cylinder piston's stroke length and to ensure that it remains inside the chamber during simulations, which is its maximum operating region of the piston. The cylinder's end force model needs to be implemented into the model. If these restrictions are not included, the piston can move through the end, resulting in one of the chamber volumes to decrease to zero and causing the simulation to halt [80]. The cylinder end is modeled

as a stiff spring and damper system which calculates counteracting end force proportional to the piston's penetration ( $x$ ) and speed ( $\dot{x}$ )

$$F_{end} = \begin{cases} -K_{end}x - b_{end}\dot{x} & \text{if } x < 0 \\ 0 & \text{if } 0 \leq x \leq x_{max} \\ -K_{end}(x - x_{max}) - b_{end}\dot{x} & \text{if } x > x_{max} \end{cases} \quad (4.33)$$

where  $K_{end}$  is spring constant of cylinder end,  $x_{max}$  is cylinder stroke and  $b_{end}$  is damping coefficient.

This equation allows the piston to travel slightly inside the end because the end is modeled as spring. For making the spring constant value more realistic it can be determined as appropriate deformation caused by the system's maximum pressure

$$K_{end} = \frac{p_{system}A_A}{x_{def}} \quad (4.34)$$

where  $p_{system}$  is the maximum system pressure,  $A_A$  is A chamber area and  $x_{def}$  approximation of the deformation.

Damping coefficient is determined with the following equation

$$b_{end} = \frac{\sqrt{K_{end}m}}{2} \quad (4.35)$$

where  $m$  is the effective inertia load.

These parameters are not required to be fully detailed because in practice piston never should collide the cylinder end, and the most important function of these equations is to prevent the fluid volume in a cylinder chamber from reaching zero, resulting in simulation error [80].

## 4.5 Load model

The load model is used to connect the cylinder rod to the inertia load that affects the displacement and velocity of the cylinder rod. Therefore, the input of this model is the cylinder's net force  $F_{net}$  and outputs are mass velocity and change of mass's position, which are given back to the cylinder as inputs. These are representing the mechanical connection between the mass and cylinder rod. This is expressed with Newton's second law of motion as follow

$$F_{total} = m\dot{v} \quad (4.36)$$

where  $F_{total}$  is force action on the load,  $m$  is inertia load and  $\dot{v}$  is acceleration of the inertia mass.

Because the designed test bench has also loading cylinders, which produce additional loading force to the DDH system, their effect needs to be included in the simulation model. These forces are assumed to be constant forces acting in the same direction or against the cylinder's net force.

$$F_{total} = F_{net} + F_{loading} + F_{load} \quad (4.37)$$

where  $F_{net}$  is net force of the cylinder,  $F_{loading}$  is force of the loading system and  $F_{load}$  is gravity force produced by the load mass.

## 4.6 Motor and valve control system

The system needs to have a simple control system that gives starting input for the pump model and controls the valve models according to logic explained in section 3.2.3. For the motor control model, the closed-loop PI controller is used to control the actuator's movement. The controller adjusts the hydraulic pump's rotation speed according to the load model's position, comparing it to the reference position profile generated by using a trapezoidal velocity input. This profile is later replaced with position data gathered from the test system, and in this way, the simulation model results can be compared with real test setup's results. Because the electrical motor model is not included in this simulation system, the dynamics of the servo motor is added after PI-controller as first-order transfer function to represent the electrical motor's response to rotation speed command coming from PLC PC. Also, speed limits are added to the controller to represent the hydraulic pump's maximum rotation speed.

A valve controller is added to the model to represent the real system's simplified PLC control logic shown in Figure 49. This system controls the opening of the proportional valves according to the acceleration input of the load model and pressure of cylinder chambers. Control logic was shown previously in Figure 37.

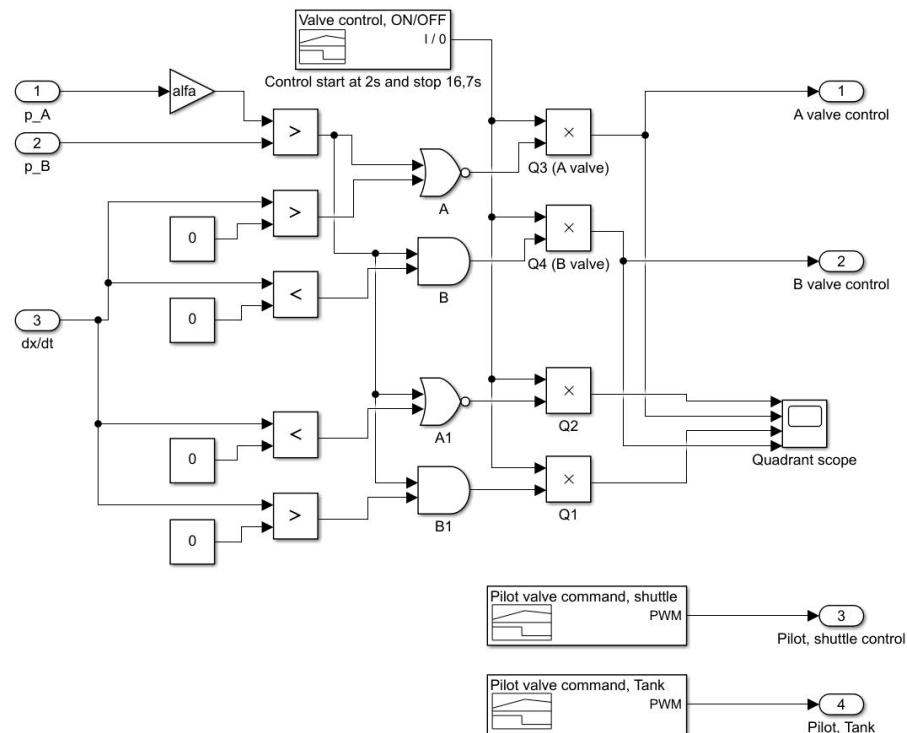


Figure 49 Valve control system.

## 4.7 Simulation model

All previously explained elements are combined to generate a model of proposed DDH system. This model consists of subsystems that are created from parts of mathematical models presented in the previous chapter. The top level of the system is shown in Figure 50. All other parts of the subsystem and the system's parameters are found in Appendix A. However, one more assumption was made for this top-level model. The accumulator pressure is assumed to be constant, and therefore this model assumes that it will not ever be filled in point that it will create higher pressures than nitrogen charge pressure.

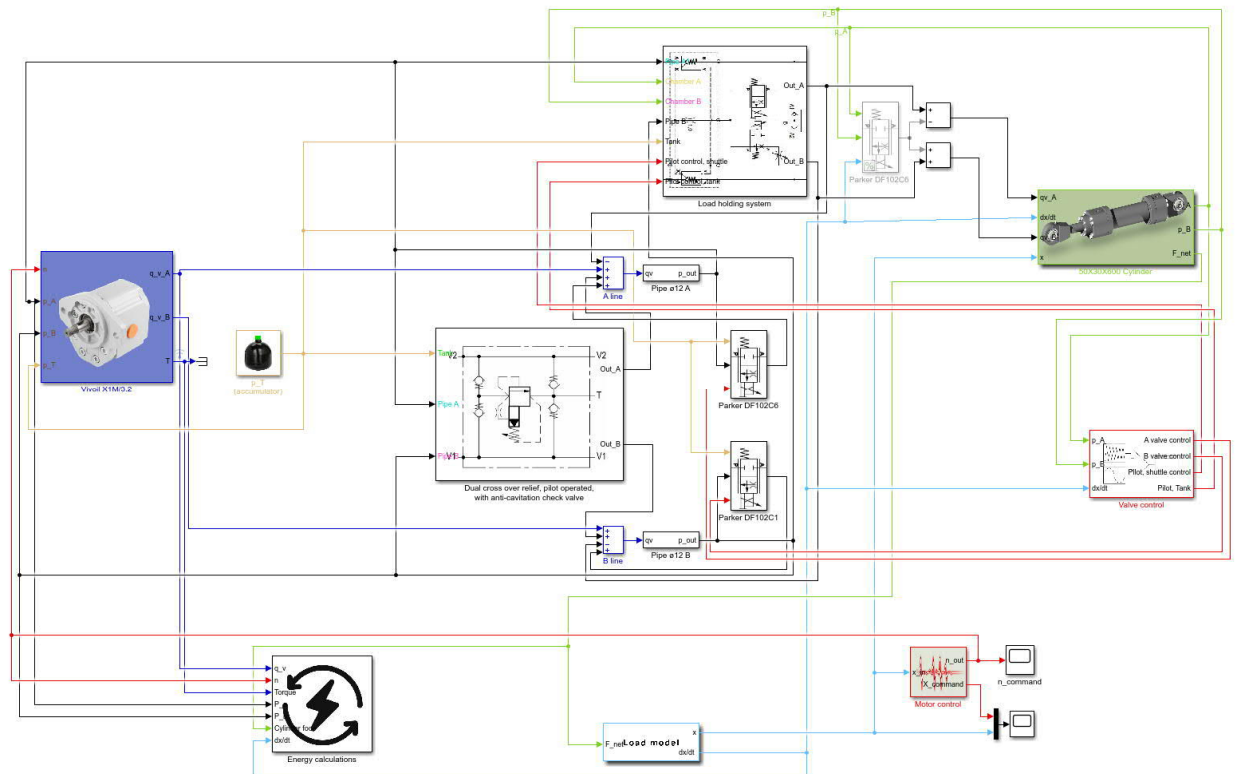
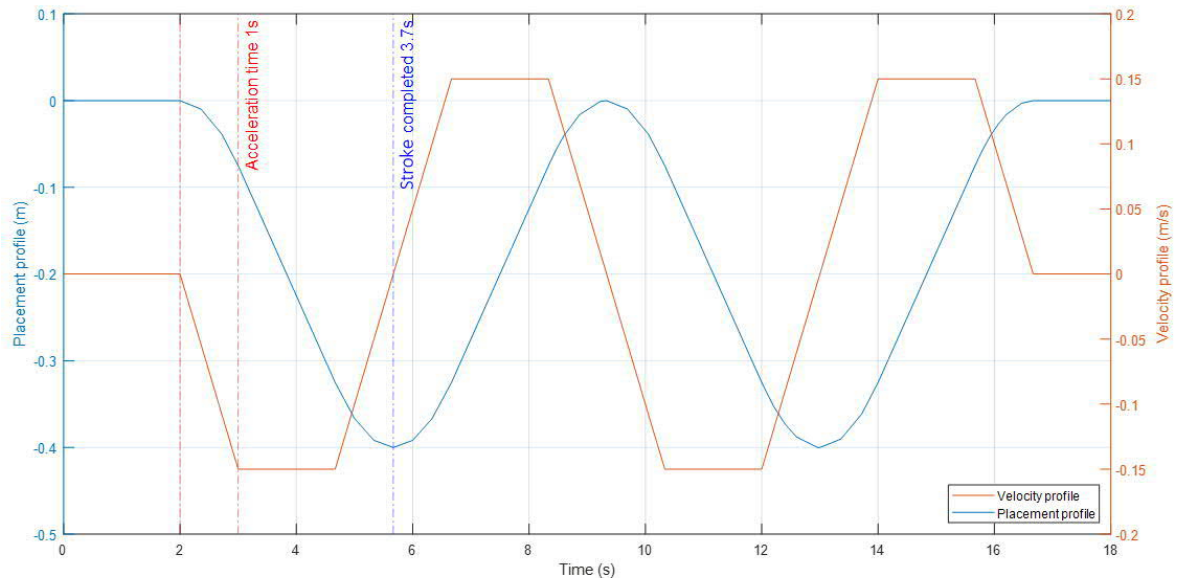


Figure 50 Completed simulation model of the proposed DDH system.

## 5 Results and discussion

The simulation model was tested using a trapezoidal velocity profile shown in Figure 51, which was determined with the following constraints. The stroke that the cylinder needs to move is 400 mm, which is continues two times making cylinder piston to return its original position and this is preferred as one work cycle. During the 18-seconds simulation, the cylinder performs two work cycles. The trapezoidal velocity profile has 1 second acceleration and deceleration time. The maximum velocity is 0.15 m/s and one stroke is completed in 3.7 second. The selected speed is determined by calculating the maximum velocity (0.159 m/s) with the maximum pump flow rate of 18.72 L/min to cylinder's A chamber. However, because the pump has leakages, ideal velocities cannot be achieved in every loading scenario. Therefore, a lower maximum velocity limit was selected, where the hydraulic pump is assumed to maintain at least 94% volumetric efficiency. The work cycle starts with 2 second hold where the load holding system's pilot line is connected to tank pressure, so the system is in a passive load holding position. After work cycles are completed, pilot pressure is again connected to tank pressure, and the system remains in a passive load holding state.



**Figure 51** The work cycles of the simulation model where the orange line is the velocity profile which creates a placement profile shown with the blue line.

The system's performance of is analysed by using different load scenarios. Selected loading cases are 145, 645, and 1145 kg constant loads for testing the performance of Q1/Q4 and Q2/Q3 individually. In these test cases, the maximum inertia mass is 345 kg, which is the maximum mass of the test system's weight plates. These results are intended to show performance that can be achieved with the designed test setup. Therefore, in the loading case 145 kg, inertia mass is lower (145 kg), but in two other cases the inertia mass is maximum 345 kg. Additionally, the system is tested with a steadily changing load cycle. This represents a possible load scenario where the inertia and gravity load is attached to a rod moved from another end, shown in Figure 52. That could be a typical joint assembly, for example, in excavators. This will enable testing system's performance in every operation quadrant where also quadrant changes from Q4 to Q1 and Q2 to Q3 are present, and actuator force is momentarily 0 N. The load cycle uses 345 kg inertia weight combined with loading cycle resulting maximum force of  $\pm 11.232$  kN, corresponding to gravitational force of 1145 kg mass.



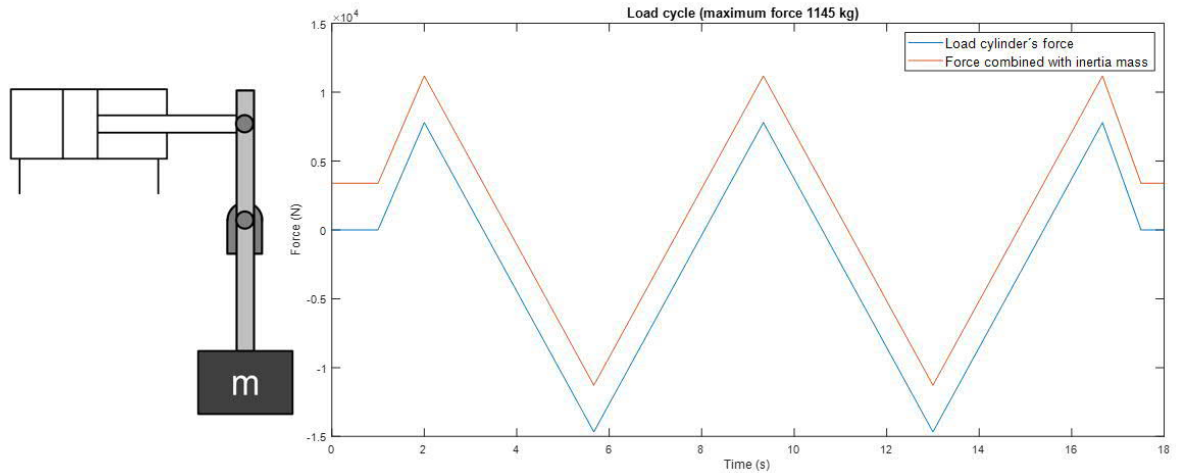


Figure 52 Reference picture represents the load scenario and the load cycle produced by loading cylinders combined with inertia mass.

## 5.1 System performance analysis

The first tests were performed with constant force 145, 645, and 1145 kg demonstrating the system performance during Q1/Q4 in Figure 53 and Q2/Q3 in Figure 54.

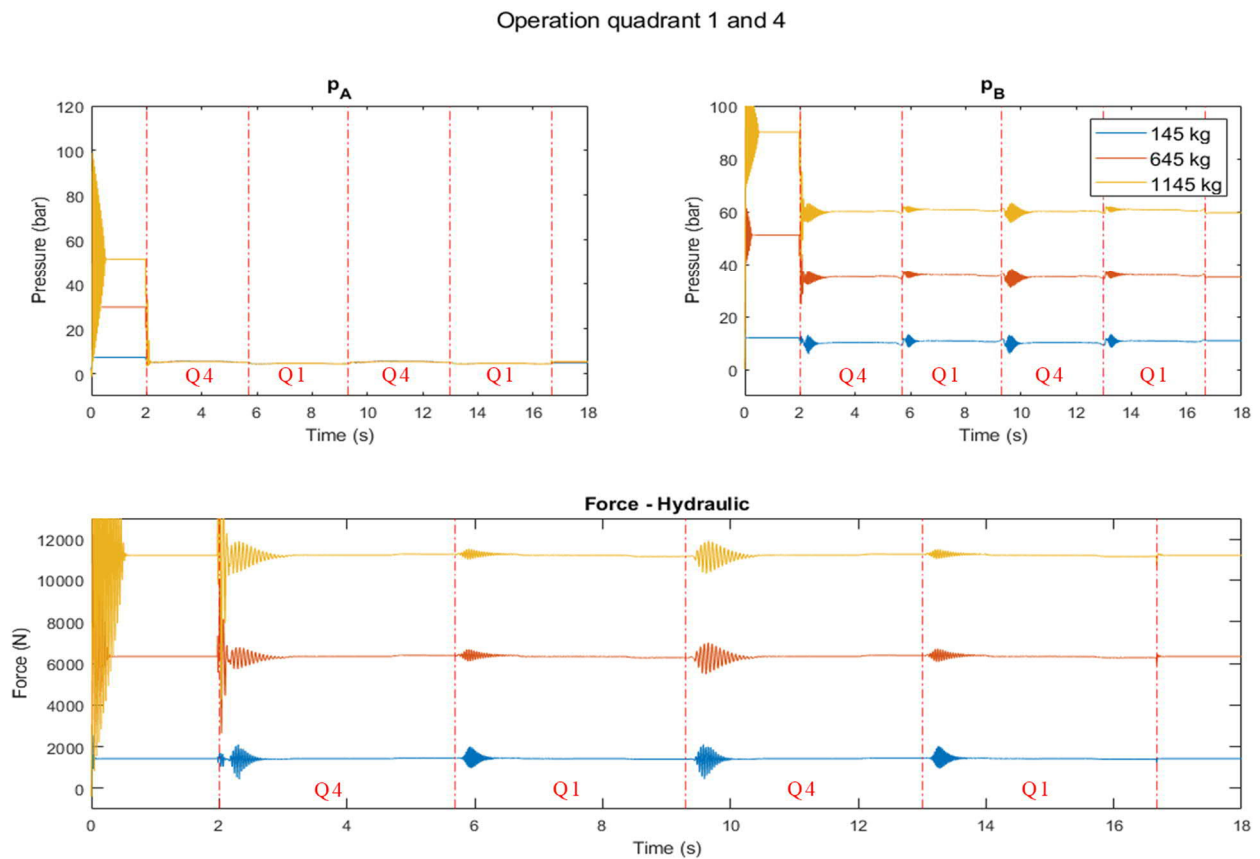


Figure 53 System performance during Q1/Q4, where red line shows quadrant change.

Operation quadrant 2 and 3

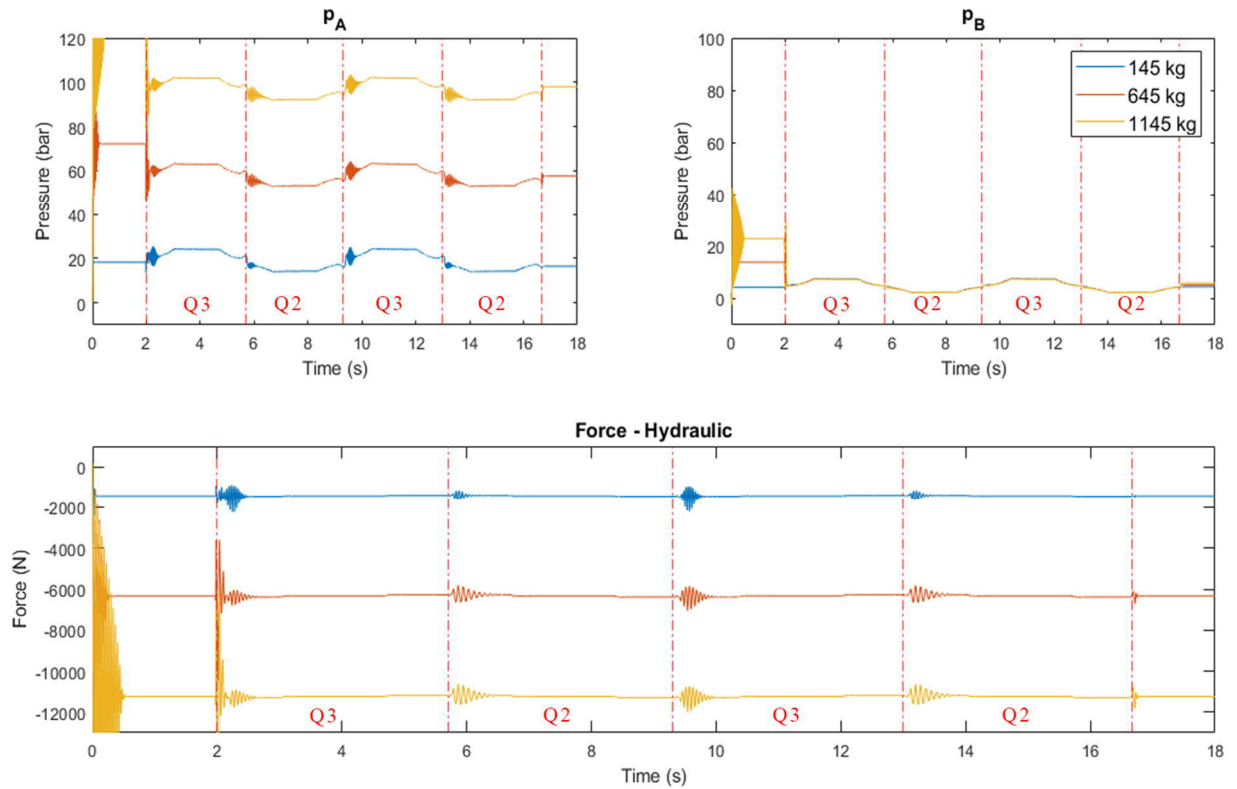


Figure 54 System performance during Q2/Q3, where red line shows quadrant change.

These results showed almost oscillation free performance where the valve controller detected quadrant changes and opened the correct proportional valve according to the logic circuit's output. Small pressure oscillations were observed while actuator was changing operation quadrants, which are shown with red lines. These are caused by seal forces when cylinder direction changes and the piston start to accelerate from zero velocity. However, this did not affect placement tracking, and the tracking performance stayed within  $\pm 11$  mm range in all load scenarios. This is tolerable because in many hydraulic applications, an acceptable cylinder's position error varies from  $\pm 15$  - 20 mm [16], and for this simulation it was selected to be  $\pm 15$  mm. The seal force has more significant impact when inertia mass and load force increase and, therefore load velocity and actuator's seal force results from 1145 kg tests during Q2/Q3 are shown in Figure 55, and placement and position error in Figure 56.

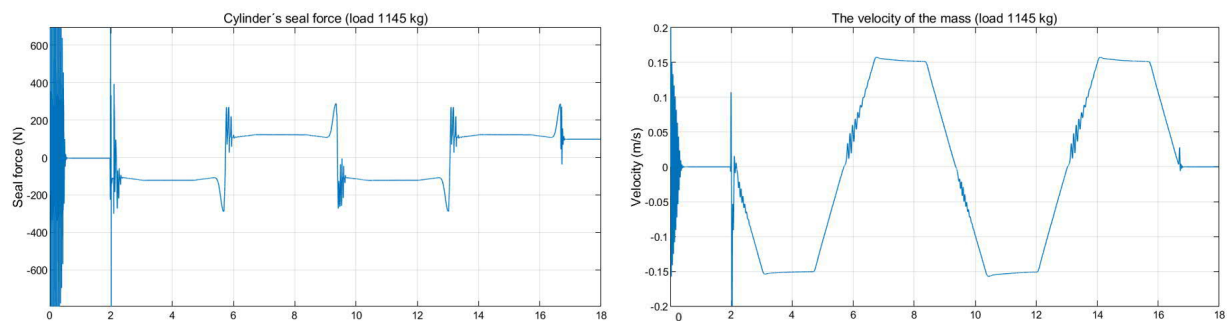
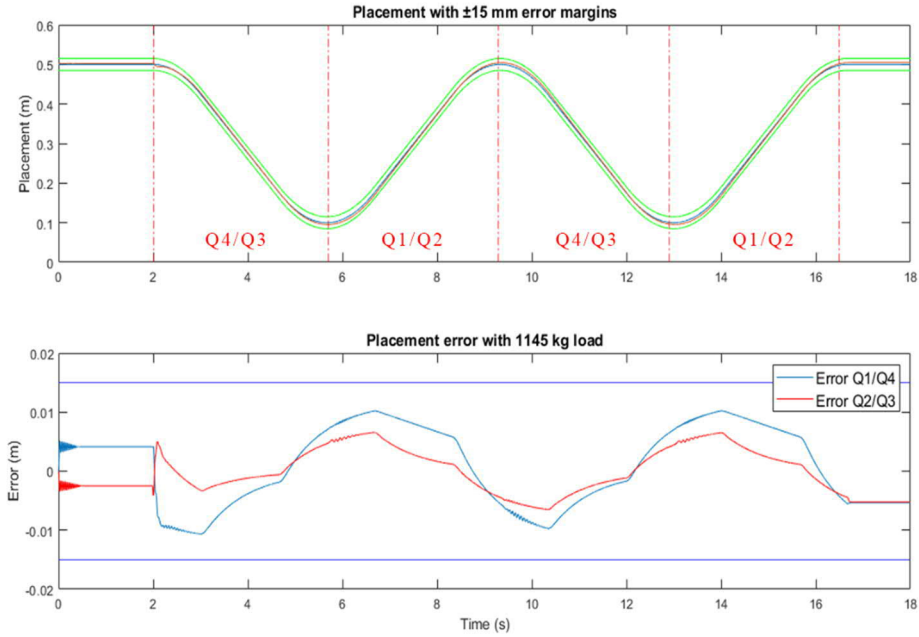
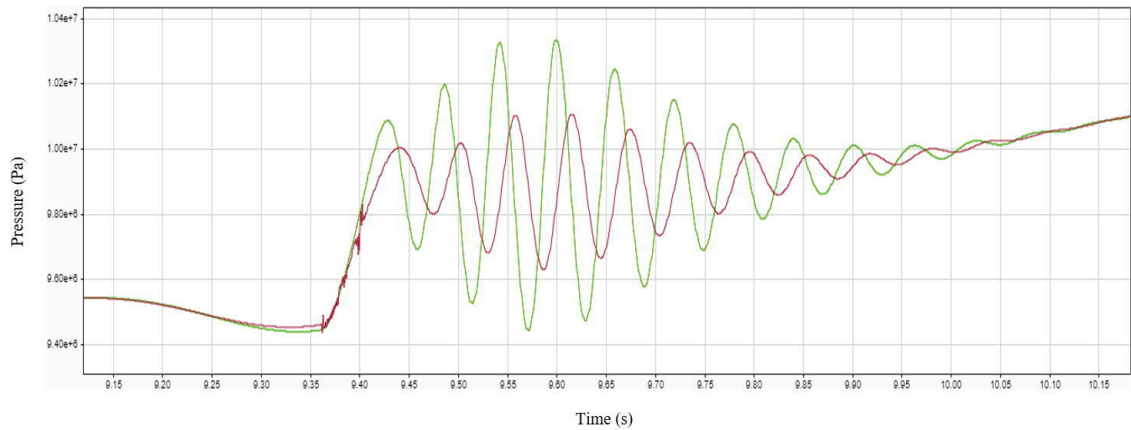


Figure 55 Cylinder's seal force and the velocity of the mass during Q2/Q3.



**Figure 56 Actuator placement and placement error during 1145 kg loading.**

Because seal friction is hard to model without measurement results from the actual hydraulic cylinder, these pressure oscillations may not be present as high in the actual system. For example, if the seal has different flexibility than in the simulation model, this affects the magnitude of pressure oscillations. Figure 57 shows a comparison between the maximum seal bend of 0.1 and 0.3 mm. Therefore, this phenomenon's effect needs to be re-evaluated during tests with the actual DDH system when it performs a similar load and drives cycles presented in this thesis.



**Figure 57 Pressure oscillation comparison during 9.35-10.15 s in Q2/Q3 between maximum seal bends, 0.1 mm shown green and 0.3 mm shown red.**

Otherwise, the mass's velocity followed the input velocity correctly, and no clear sign of mode oscillation was observed. The pump's speed command had variation between load scenarios Q1/Q4 and Q2/Q3. This was caused by a difference in flow rate that the pump needs to produce, which was explained in Figure 18. During Q1/Q4 tests, the speed reached the pump's upper-speed limit 6000 RPM, and the required servo motor torques with the highest load of 1145 kg were 1.676 Nm during Q4 and 3.844 Nm during Q1. During Q2/Q3 tests, rotational speed reached up to 3839 RPM, and required torques with load 1145 kg were 5.77 Nm during Q3 and 3.413 Nm during Q2. This shows that the selected velocity profile is demonstrating a near-maximum dynamic performance of this

DDH system. Also, the torque requirements of the servo motor are close to the rated torque limit. The difference between torque requirement is explained with the cylinder's piston area difference where load's lifting during Q1 requires less torque than lifting during Q3. Therefore, these tests demonstrate well the near maximum performance of the proposed system.

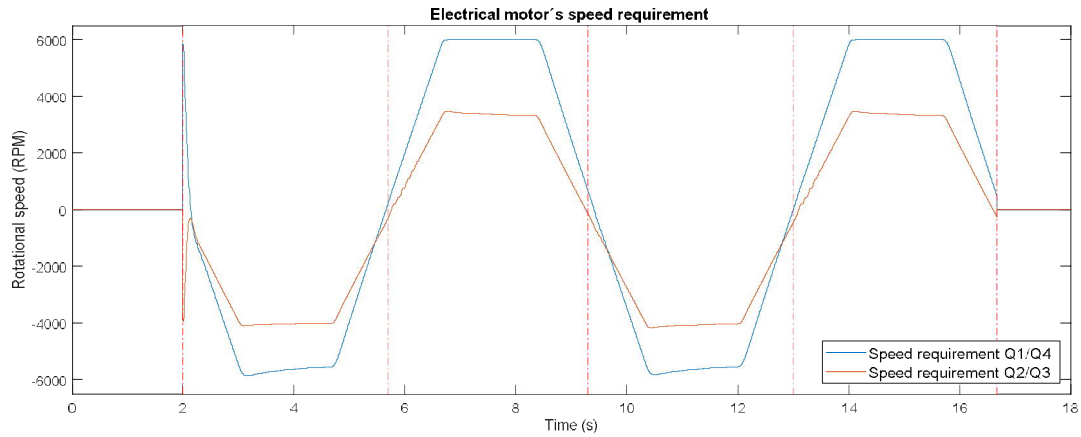


**Figure 58 Electrical motor's speed requirement.**

The load holding system performed well in every load scenario. The POCV's poppet stayed fully open for the whole work cycle and closed at the right moment, providing a passive load holding, which is seen in Figure 59. However, some undesired operation where POCVs close suddenly were observed during extra tests with the lowest 87 kg inertia mass during Q1/Q4. This operation was mainly due to the pressure oscillations generated by the seal force model. These did not greatly affect position tracking, only during the retraction phase error exceeded margins by 27 mm. Additionally, oscillations were mainly caused by seal forces and therefore need to be tested with real system. Also, the seal force parameters must be tuned to represent accurately low load scenarios. Therefore, this result is only included in the annexes section.

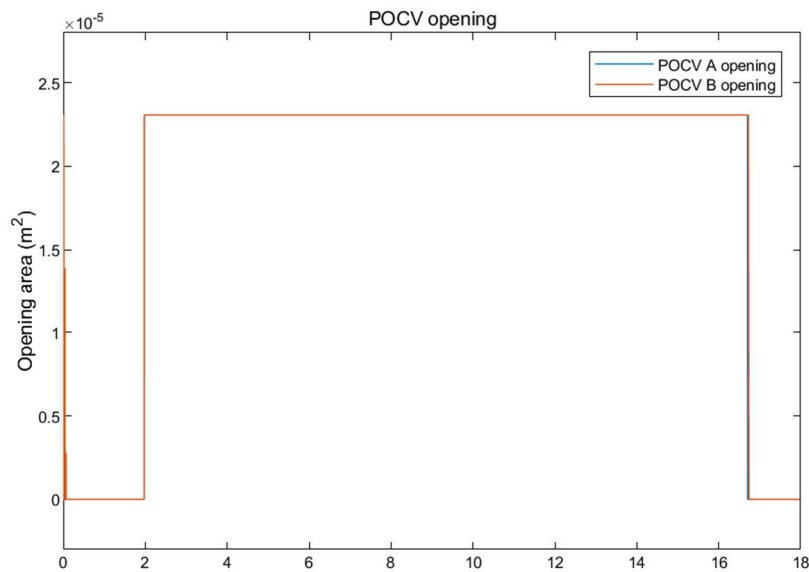


**Figure 59 POCV's poppet opening during Q1/Q4 with 1145 kg load.**

Simulations were also performed for conventional POCV piloting setup, where pilot pressure is taken from opposite pressure lines as present in Figure 21. The test was performed with 1145 kg loading during Q1/Q4. Results show increasing pressure oscillations when the cylinder's rod is retracting. This behaviour is caused by insufficient B-side pilot pressure, which normally stays close to tank pressure during Q1/Q4. When A side POCV suddenly closes because of low pilot pressure, B-side pressure increases, which opens A-side momentarily and then closes when B-side pressure drops back to tank pressure level. This creates oscillation behaviour, which continues throughout the retraction phase, increasing the position error shown in Figure 60. Position error exceeded 63 - 71 mm during retraction, which is not acceptable for many industrial applications. This was also noticed during Q2/Q3. However, with lower load 145 and 645 kg, position error stayed within error margins, but pressure oscillations and jittering movement were still noticeable.

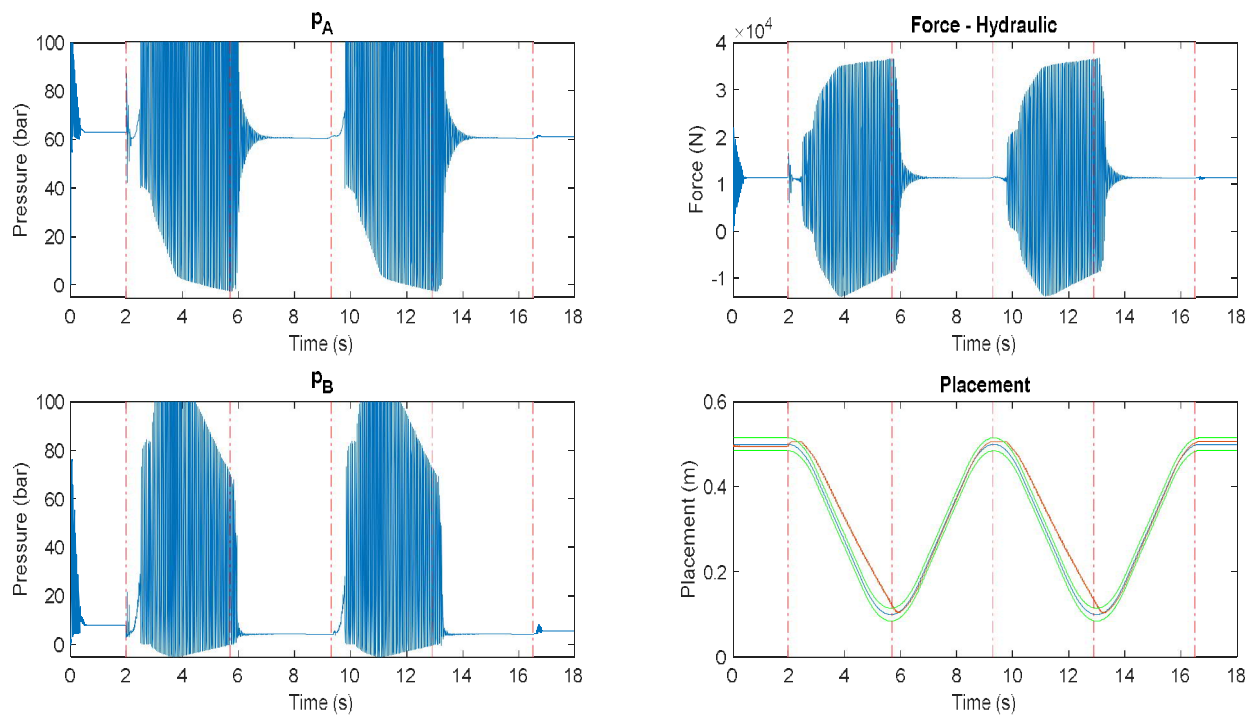


**Figure 60 Performance of circuit during Q1/Q4 which have POCV setup of Figure 21 system.**

Additionally, during the cylinder's extension phase, the A-side POCV did not stay completely open, causing extensive pressure loss over this valve shown in Figure 61. This is caused by insufficient pilot pressure level and high pressure on the spring side of the valve's poppet. Therefore, this POCV setup is not recommended for the DDH system if maximum energy efficiency and operation safety is wanted to be achieved.

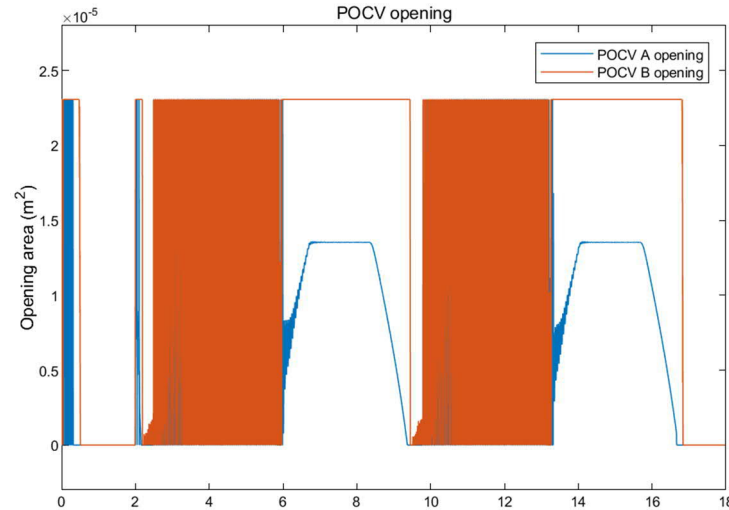


**Figure 61 POCV's poppet opening during Q1/Q4 with 1145 kg load and conventional POCV pilot line setup.**

The test was performed with the presented load cycle, which shows the additional unwanted performance when the system shifts operational quadrants from Q1 to Q2 and Q3 to Q4. These shifts may create noticeable mode oscillations. The pressure, actuator force, and placement result of this test are presented in Figure 62.

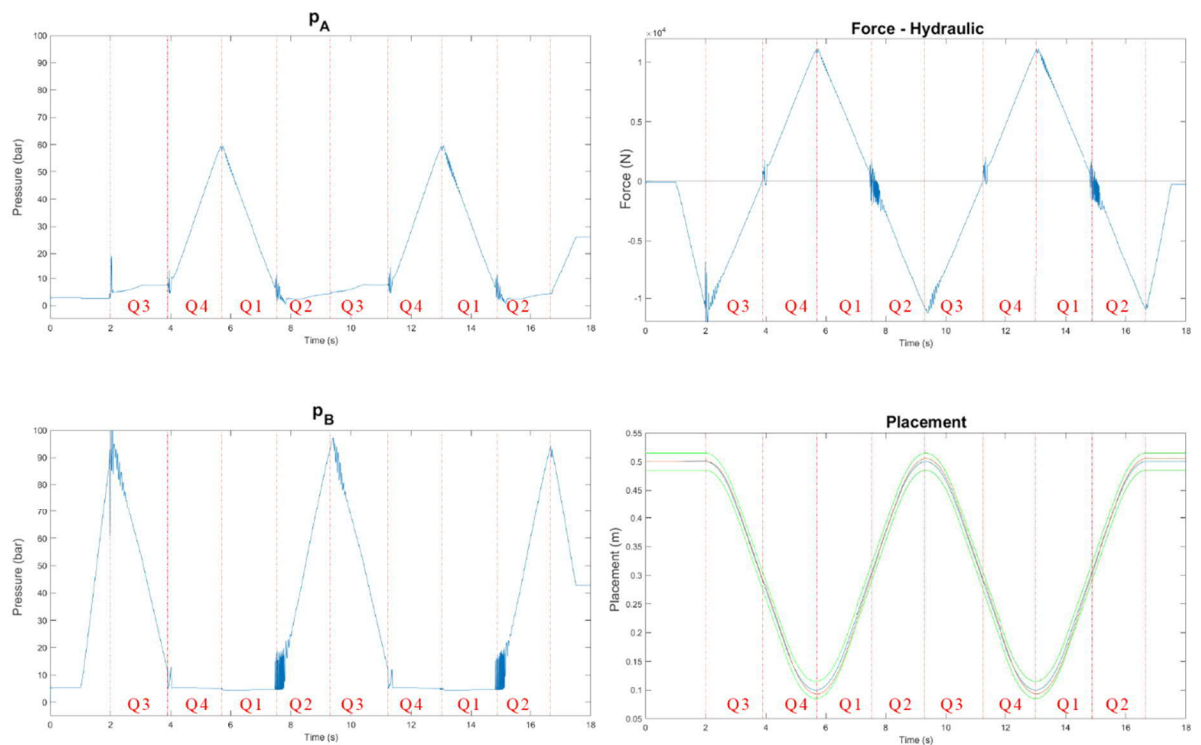


**Figure 62 Test results of load cycle.**

Results show otherwise similar oscillation free performance with good position tracking. However, during the transition from Q3 to Q4 small mode oscillations can be observed. Furthermore, the transition from Q1 to Q2 generates an even greater mode oscillation phenomenon, which can be seen from B side pressure and actuator force results. These mode oscillations can be observed better from results from operation quadrant detection logic shown in Figure 63.



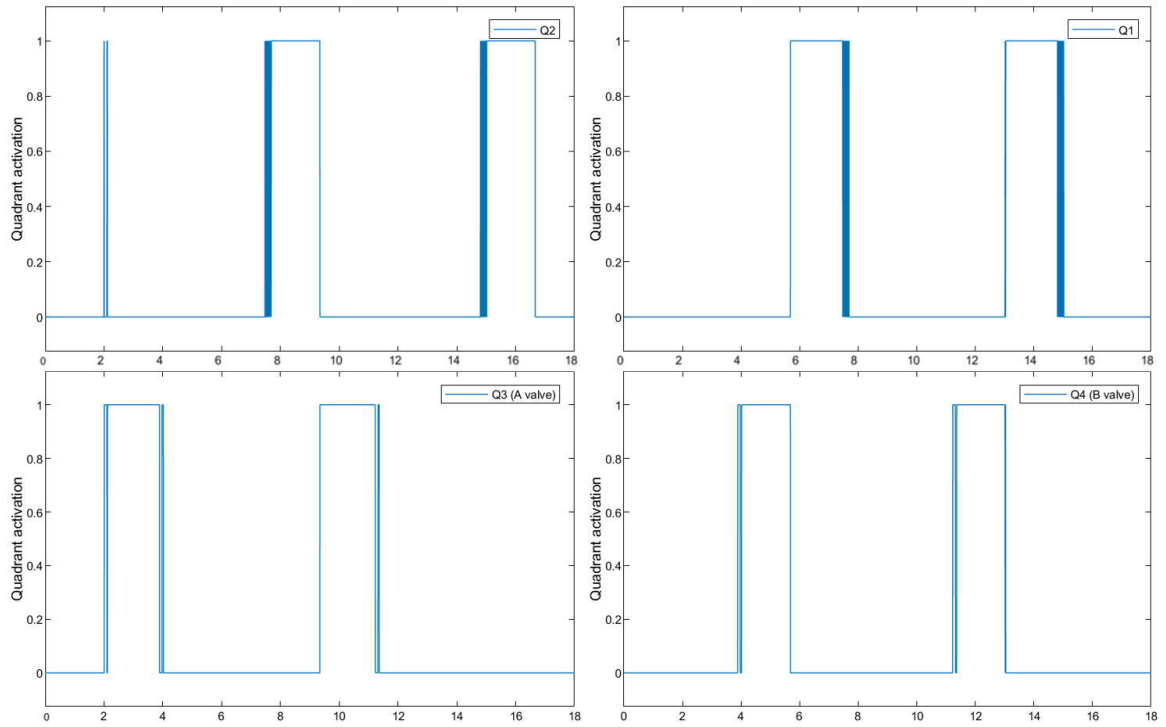


**Figure 63 Mode oscillation during load cycle.**

These results show that the mode oscillation between Q1 and Q2 generates more mode switching than the transition between Q3 and Q4. These switches happen because when the system makes the transition from Q3 to Q4, it also makes the A side proportional flow compensation valve to close suddenly, which stops the flow compensation of A chamber. At this point, seal forces are higher than the actuator force, which makes the system switch back to Q3 that closes the B side compensated valve. Because excess flow is not properly compensated for a moment, B side pressure increases, and velocity will decrease with factor of  $\alpha$ , which means that in a case of 0.15 m/s, the velocity should decrease to 0.0657 m/s. In the case of transition between Q1 and Q2 the flow compensation valve is an anti-cavitation valve. When the transition takes place, B side CV closes, and A side valve opens, leading excess flow to A chamber. Because of seal forces A side pressure increases, and the mode is switched back to Q1 which opens B side CV, causing an excess flow to A chamber. This will increase the velocity with a factor of  $\alpha$ , which means that velocity should increase to 0.2344 m/s. Because the CVs have higher response time than coil operated proportional flow control valves, this phenomenon is stronger between Q1 and Q2. The actuator velocity result is inspected in Figure 64 where this phenomenon can be clearly seen. The actuator velocities increase and decrease close to theoretical values, which confirms that these are mode oscillations. The electrical motor's rotational speed requirement is compared with actuator velocity, which shows that these changes in velocities are quickly damped with motor control. Figure 65 shows the load cycle's position error, which stays within set error margins and confirms that the proposed circuit can be operated accurately, even if the mode oscillation phenomenon is present with 1145 kg loads.



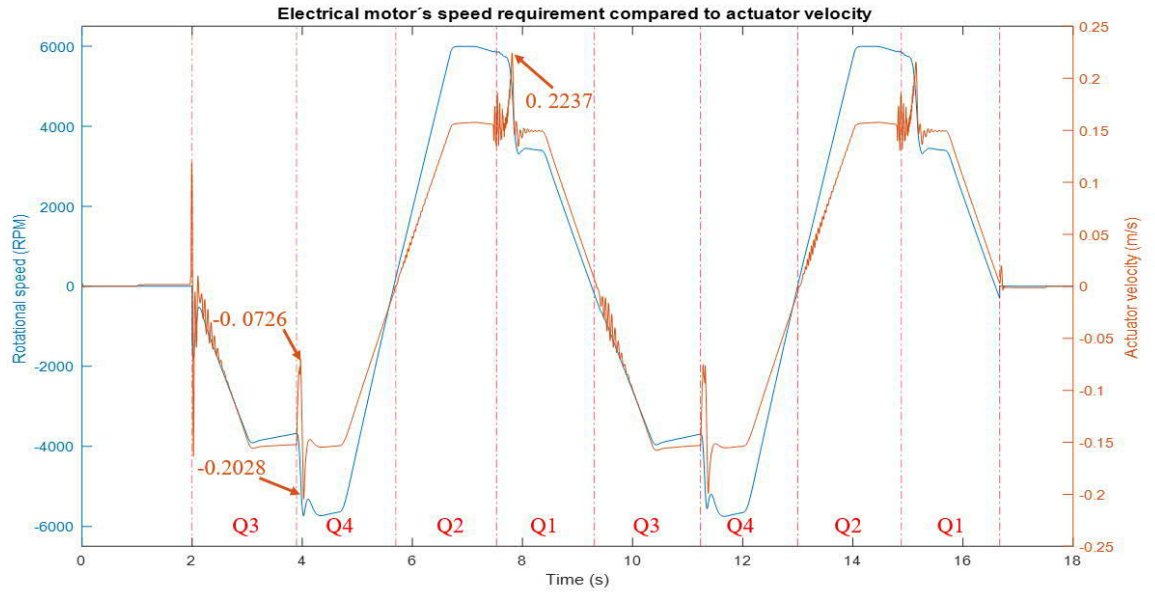


Figure 64 Electrical motor speed (blue) and actuator velocity during load cycle (orange).

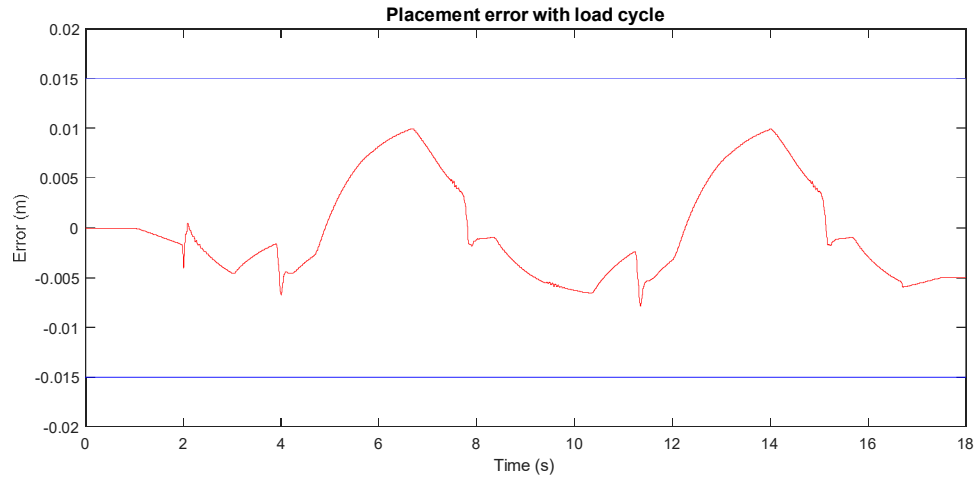


Figure 65 Position error during load cycle.

## 5.2 Energy efficiency analysis

In order to determine the proposed system's energy efficiency following equations were used with various loading cycles.

The overall power need is calculated using mechanical power which is a product of torque output and rotation speed command input of the hydraulic pump model which is combined with the energy efficiency of the servo motor system.

$$P_{e.motor} = T_p \omega / \eta_{servo} \text{ if } (T_p \omega > 0, \text{energy consumed}) \quad (5.1)$$

$$P_{e.motor.reg} = T_p \omega \eta_{servo} \text{ if } (T_p \omega < 0, \text{energy regenerated}) \quad (5.2)$$

where  $T_p$  is needed torque of the pump,  $\omega$  is the angular velocity of the pump and  $\eta_{servo}$  is the servo system's energy efficiency. The mechanical energy is consumed when the mechanical power product is positive and regenerated when the product is negative. Therefore, when mechanical energy is consumed, the servo system's efficiency increases overall energy consumption, and when the servo motor acts as a generator, the efficiency

decreases regenerated energy. Because the required torque is close to the Beckhoff servo motor's rated torque level, the efficiency is assumed to be constant 88%. Generally, servo motor's efficiency remains close to 88% when the motor is exposed to 38% of standstill torque, and the efficiency will decrease slightly to 87.6% when exposed to 90% of standstill torque [89]. However, most of the servo motors' efficiency remains always over 85%. Additionally, the servo drive also dissipates energy, but the power losses are generally low, and therefore efficiency is assumed to be 99% [90]. When these are combined servo system's efficiency is assumed to be 87.12%

The hydraulic power output produced by the hydraulic pump is a product of pressure difference over pump  $\Delta p_{pump}$  and flow rate produced by the pump  $q_{v,pump}$ . It is lower than the mechanical power input according to the overall efficiency of the hydraulic pump.

$$P_{hydraulic} = \Delta p_{pump} q_{v,pump} \quad (5.3)$$

The power of cylinder is calculated from actuator force  $F_c$  and velocity  $v$ .

$$P_{c.lift} = F_c v \quad \text{if } (F_c v > 0, \text{lifting}) \quad (5.4)$$

$$P_{c.lower} = F_c v \quad \text{if } (F_c v < 0, \text{lowering}) \quad (5.5)$$

When the cylinder power product is positive, the system consumes energy and when negative the system receives mechanical power from lowering a gravity load or decelerating a moving mass. Therefore, power is not typically consumed in the lowering phase. However, either the braking power needs to be converted into heat or stored for later use.

The cumulative lifting and lowering energies are calculated by integrating the power as shown in the following equations:

$$E_{lift} = \int_{t_1}^{t_2} P_{c.lift} dt \quad (5.6)$$

$$E_{lower} = \int_{t_1}^{t_2} P_{c.lower} dt \quad (5.7)$$

where  $t_1$  is start and  $t_2$  is the end of the loading cycle. The  $E_{lift}$  is often called the ideal lifting energy consumption of a system that cannot regenerate energy. The  $E_{lower}$  is the potential energy of load mass which is the maximum possible energy that can be regenerated from the system. These are used for determining the overall efficiencies of the DDH system.

The cumulative energy consumption and regeneration of DDH system is calculated by integrating the electrical powers from equation 5.1 and 5.2 as follows:

$$E_{DDH} = \int_{t_1}^{t_2} P_{e.motor} dt \quad (5.8)$$

$$E_{Reg} = - \int_{t_1}^{t_2} P_{e.motor.reg} dt \quad (5.9)$$

where  $t_1$  is start and  $t_2$  is end of the loading cycle.

The overall efficiency of the DDH system  $\eta_{DDH}$  is described as the ratio of input and output energies which are lifting energy consumption  $E_{lift}$  and energy consumption of the electrical motor  $E_{DDH}$ .

$$\eta_{DDH} = \frac{E_{lift}}{E_{DDH}} \quad (5.10)$$

The efficiency does not take into account the regeneration of energy and describes the system's capabilities to pass energy through it.

The regeneration efficiency is described as the ratio of regenerated energy from the electrical motor  $E_{Reg}$  (acting as a generator) and the potential energy from lowering the load  $E_{lower}$ .

$$\eta_{Reg} = \frac{E_{Reg}}{E_{lower}} \quad (5.11)$$

To achieve the best efficiency that the DDH system could produce, the regenerated energy needs to be reused. This energy will reduce the cumulative energy consumption of the DDH system, where energy can be either fed to the electrical grid to reduce overall energy cost or stored in the battery to be used for rotating the electrical motor. Because a conventional hydraulic system cannot regenerate energy while lowering a load, traditional efficiency assumes that the ideal system consumes the same amount of energy that is used during lifting. Therefore, when calculating the efficiency, which is comparable to the traditional system, the reduced energy input may result in an efficiency greater than 100%. The DDH system efficiency with energy reuse is calculated as follows:

$$\eta_{DDH.w.reuse} = \frac{E_{lift}}{E_{DDH} - E_{Reg}\eta_{reuse}} \quad (5.12)$$

where  $E_{lift}$  is lifting energy,  $E_{DDH}$  is the energy consumption of the electrical motor system,  $E_{Reg}$  is regenerated energy from the hydraulic pump and  $\eta_{reuse}$  is reuse efficiency. Reuse efficiency is determined by how much energy can be reused after storage. If storage is chosen to be an electrical grid, this is determined by the ratio of buying and selling price. This ratio is usually 17 – 35% where the selling price is lowered by fixed cost for grid fees and taxes [91]. In this thesis, 35% efficiency is used. Another solution would be using electrical batteries, which could be in this case Li-ion battery to achieve a compact design. The batteries have charge and discharge efficiency, where some of the store energy is turned into heat. For Li-ion batteries, this is 80 – 90%, and because reused energy is stored and later discharged from the battery, reuse efficiency is 64 – 81% for battery storage [92].

Energy analysis was performed for all load scenarios, and results are shown in Table 1. The power distribution analysis was also performed and showed below, where different system energy losses are represented as colors. In these figures, when the value is positive, the system is lifting the load, and power is consumed. Useful power is used for lifting and different losses increase the required power need. These are hydraulic losses of valves and other components shown as blue, mechanical losses of the hydraulic pump shown as red and electrical losses of the servo motor and servo drive shown as yellow. When power is a negative the system is regenerating energy and, in these figures, negative useful power indicates regenerated power from load-mass lowering.

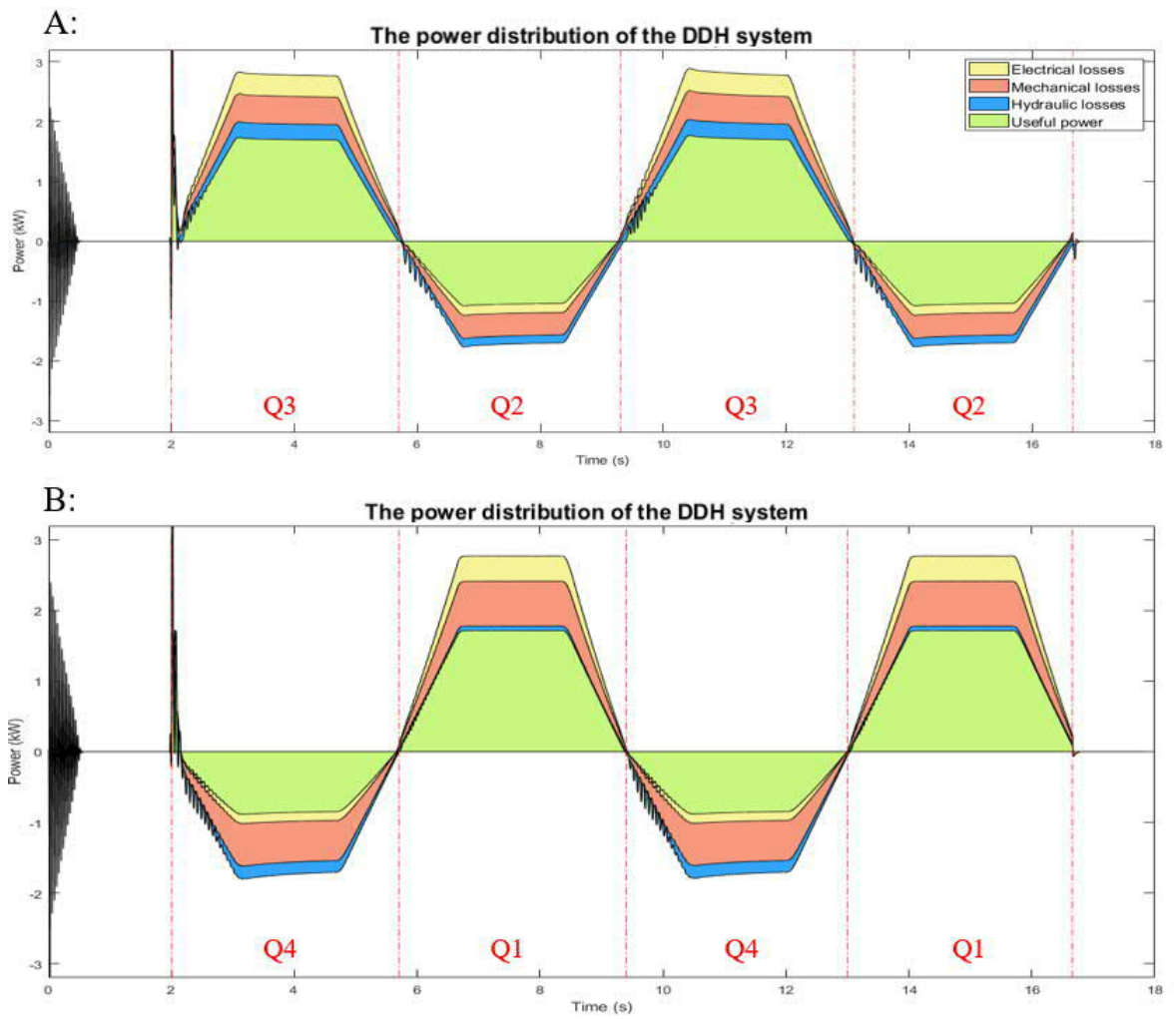


Figure 66 A: The power distribution during Q2/Q3, B: The power distribution during Q1/Q4 with 1145 kg load.

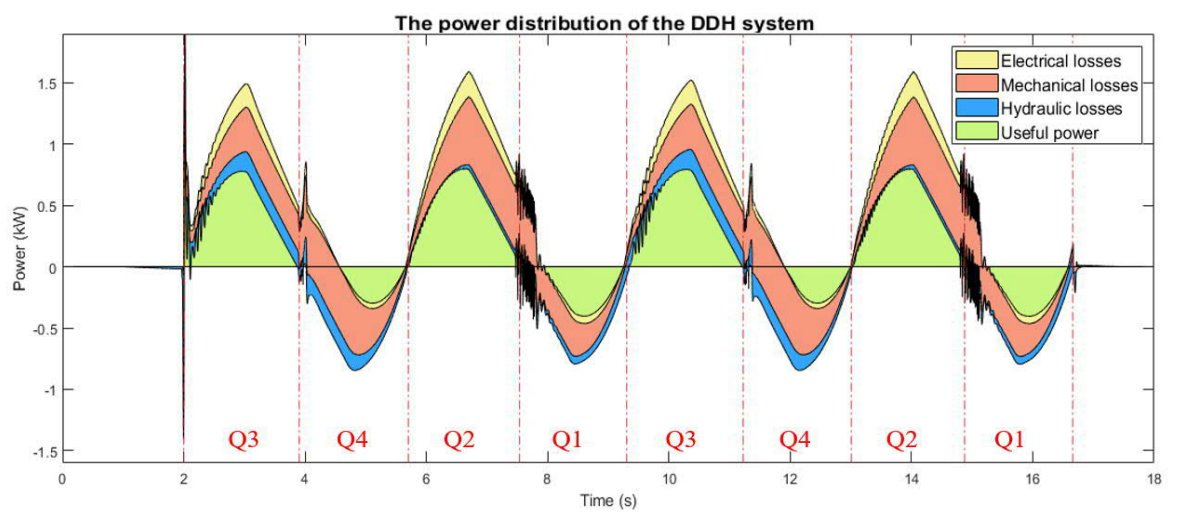


Figure 67 The power distribution during the load cycle.

**Table 1** Energy and efficiency results.

Load scenario	Parameter	Loading quadrants	
		Q1/Q4	Q2/Q3
<b>Constant load 145 kg</b>	DDH system efficiency (%)	16.38	23.99
	Energy consumed (kJ)	7.204	4.826
	Regeneration efficiency (%)	0	0
	Energy regenerated (kJ)	0	0
	Efficiency with reuse, grid (%)	16.38	23.99
	Efficiency with reuse, battery (%)	16.38	23.99
<b>Constant load 645 kg</b>	DDH system efficiency (%)	53.75	54.29
	Energy consumed (kJ)	9.886	9.544
	Regeneration efficiency (%)	27.07	50.6
	Energy regenerated (kJ)	1.424	2.640
	Efficiency with reuse, grid (%)	56.61	60.1
	Efficiency with reuse, battery (%)	59.22 - 60.86	65.95 - 69.94
<b>Constant load 1145 kg</b>	DDH system efficiency (%)	62.86	60.73
	Energy consumed (kJ)	15.23	15.38
	Regeneration efficiency (%)	48.71	58.4
	Energy regenerated (kJ)	4.635	5.490
	Efficiency with reuse, grid (%)	70.36	69.39
	Efficiency with reuse, battery (%)	78.07 - 83.43	78.70 - 85.42
<b>Load cycle with 1145 kg (all quadrant active)</b>	DDH system efficiency (%)	42.48	
	Energy consumed (kJ)	8.507	
	Regeneration efficiency (%)	30.92	
	Energy regenerated (kJ)	1.105	
	Efficiency with reuse, grid (%)	44.5	
	Efficiency with reuse, battery (%)	46.33 - 47.47	

The results show that energy efficiency is good at higher loads, and the system can regenerate energy during Q3 and Q4. However, at low loads, the DDH system energy efficiency is lower, between 16.4 – 24.0%, and the system cannot regenerate any energy. This happens because the pump's pressure difference remains low and therefore, the pump's overall efficiency is during pumping at Q1/Q4 is 32.7% and at Q2/Q3 is 52.7%. Furthermore, this will also result that mechanical losses during lowering are higher than regenerated power and pump needs to use energy to provide the desired flow rate. However, with higher load cases, the system's overall efficiency is better, and energy regeneration is possible.

The fluctuation between efficiency results is also caused by the pump's overall efficiency, proportional to pressure difference over the pump. During Q1/Q4, the pressure levels remain lower than during Q2/Q3 because the control volume remains on the A-chamber's larger surface. Therefore, this results in more mechanical losses in the pump with lighter loads. However, when loads get higher, the pressure difference increases during Q1/Q4 to the point where the overall difference reaches near maximum value of 82%. Because of this fact that during Q1/Q4 the cylinder requires less torque than in Q2/Q3, the overall system efficiency is higher with the high load during Q1/Q4. In other words, the overall efficiency is lower with Q1/Q4 because of low-pressure difference, which makes the pump operate in an inefficient area. This transition can be seen in the Table 1 between load case 645 and 1145 kg.

Pump's low efficiency is also the reason why efficiency is relatively low if load cycle case is compared with the other loading scenarios. During the load cycle, the pressure difference over the pump stays between 0 – 50 bar, which leads to that pump operates in an inefficient area. Additionally, the energy regeneration during the load cycle was lower than with other load cycles because the time when regeneration was possible was shorter. The system cannot regenerate energy when the loading force is low, as shown in the 145 kg loading case results and this can be observed from Figure 67.

However, the energy efficiency of the DDH system is good with higher loads. With 1145 kg load case, the overall system's efficiency without regeneration was 60.7 – 62.9%. This is excellent if compared to a conventional valve-controlled system which efficiency is ranging from 6% to 40% varying in terms of load scenarios [93]. Additionally, when the system utilizes regenerated energy, the system's efficiency increases to 69.4 – 70.4% with grid reuse. This shows that if the facility where the system is operating enables a supply of electricity back to the electric grid, it will allow a cost-efficient way of increasing efficiency. This solution would be cheaper than battery use because the price of battery systems with limited life cycle can be deducted from the system's total cost. However, when high taxes and fixed electricity grid costs lower the grid reuse solution's efficiency, the separate battery storage system offers better efficiency levels. Li-ion battery-based system's efficiency level varies from 78.1% to 85.4% with the highest load case. In other words, with a battery reuse solution, the proposed system can achieve over two times better efficiency than the most efficient conventional valve-controlled system. Therefore, this new system design is a genuinely potential solution in the future to replace traditional hydraulic systems that require high energy efficiency. This is as well a promising unit because of the additional power and compact size provided by a differential cylinder offers greater industrial application possibilities than a symmetric cylinder driven EHA systems.

## 6 Conclusion

In this thesis it was investigated which features are required to have a high-performance DDH system with good energy efficiency. This investigation provided a good understanding of the problems that the DDH system faces, which enabled the proposed circuit to be designed. The circuit consisted of an active flow compensation circuit and load holding circuit which uses POCVs. The test setup and simulation model were designed to determine the performance of the proposed circuit. The obtained simulation results showed that the system operated as desired and fully filled all set requirements for the system. The flow compensation valves opened correctly according to the proposed logic circuit's output, which recognizes which operation quadrant is currently active. The position tracking remained within set error margins during all tests, being less than  $\pm 11$  mm in most of the load scenarios. The results also indicated that there could be small pressure oscillations due to the seal forces. However, because seals' effect is challenging to model, this phenomenon needs to be re-evaluated in the with the actual test rig. Furthermore, some mode oscillation behaviour was observed during cyclic loading. However, this also heavily depends on the magnitude of seal forces, and it did not affect the displacement tracking of the simulation model. Therefore, there is small uncertainty about this phenomenon's true effect on the system, but if the actual circuit behaves almost like the simulation model, the system can be suitable for industrial load lifting application.

The energy analysis was also performed based on the obtained simulation results, which showed that the proposed circuit could fully fill the energy regeneration capability in every motoring quadrants. Additionally, the energy efficiency was very good with heavier loads where overall systems efficiency without regeneration was 60.7 – 62.9%. Energy efficiency with the reuse of regenerated energy reached up to 85.4%, which shows excellent performance compared to conventional systems. The most significant factor affecting the energy efficiency was the hydraulic pump, whose overall efficiency remained between 50 – 75% in low-pressure operation. Although this was the case with the simulation model, the actual pump could perform better because accurate efficiency measurement data of the pump's performance was not available. The inefficient area can be located differently as is in the pump model used in the simulations, which can increase efficiencies of the actual test system. However, generally, this low-pressure operation was found to be a problem to the DDH system. With light load scenarios, the system may maintain pressure difference over pump between 0 – 50 bar, which can be for the most commercial pumps an inefficient operation area.

These simulation results gave an optimistic picture that the proposed circuit can fill all set requirements of basic functionalities and provide safe and energy-efficient operation for industrial load-lifting applications. Therefore, the system's building process should be continued and the found problems can be re-evaluated based on the actual system's measurement data.



## 6.1 Future work

This thesis has been covering the design process of the proposed DDH system and the simulation model. After this thesis, the designed test bench is assembled, and Beckhoff measuring and controlling system is implemented. This thesis's conclusions are based on theories, simulation models, and other research. However, actual tests and analyses are essential to ensure the proposed circuit's functionality. This section contains research questions that have emerged as the investigation of the proposed circuit has been in progress. Answers to these questions can be given after the test system is built and test results are analysed.

A most important aspect of the DDH is the flow compensation system, and therefore functionality of the proposed active system and its controlling algorithm needs to be tested. The simulation results presented small oscillation behaviour due to the seal forces. If these are also present in the actual system, it must be determined whether these are such large oscillations that they need to be dampened in order to achieve better operational safety and quality. In this thesis, it was proposed that the leakage between the cylinder's piston chambers could dampen the oscillation. However, these could also be dampened by adding the throttling function to flow compensation valves like the limited throttling valves system presented in Figure 14 d had. Additionally, the DDH system could have a controlling system that uses the mathematical model to predict its functions. This could be added to the system by utilizing the model presented in this thesis and adding it to Beckhoff's controlling algorithm. Moreover, the controlling logic used in the simulation model is the most basic PI controller that could be further developed to be more sophisticated. In this way, better position tracking capabilities can be achieved during work cycles with changing dynamic and loading conditions. Above all, effects of seal forces need to be specified because these are found to be the main cause of undesired oscillations. The effect of different material and geometrical choices for cylinder seals could be researched.

A big part of the system's functionality is also the load holding system and how well it can react to different loading conditions and keeping load holdings valves open. Therefore, it also needs to be tested with a real circuit. Additionally, the simulation model is based on Sun Hydraulic's POCV model, which does not have pre-opening functionality. The system needs to be studied with these valves, and if there are pressure oscillation problems, then try if high-end Duplomatic POCV with pre-opening could solve these. Additionally, the simulation model was found to have some oscillation behaviour while operating in Q1/Q4 with light loads. The main reason causing this behaviour was the effect of seal forces and therefore the existence of this phenomenon needs to be re-evaluated during the actual tests.

The filtration system needs to be tested, and measurements of the system contamination levels carried out. In this thesis filtering solution, the return filter for flow compensation line and pump's case drain filtering was proposed. This solution has the least effect on system's driving stiffness. However, the flow rate through these lines is limited, and the filtering effectiveness needs to be tested. If the proposed filtering circuit proves insufficient, additions like pressure filters or separate filtering circuits need to be tested. Additionally, the elevated pressure level of the case drain line due to the drain filter needs to be investigated. If the filter has an effect on case pressures, it needs to be removed to ensure the durability of the pump's shaft seals. Also, the heat generated during the long work cycles could be an issue, and therefore the temperature levels of the system's oil

need to be monitored. The need for the oil cooler addition to the proposed circuit needs to be evaluated. If the oil cooler is required, a compact design needs to be chosen, which can be easily added to the circuit. Additionally, deaeration process has been found to be problematic and therefore, separated oil circulation system could be tested while the test system is assembled.

During low-pressure operations, the hydraulic pump's energy efficiency was found to be inefficient therefore lowering the system's overall efficiency levels. The operation of the proposed Vivoil pump needs to be analysed, and if the pumps operation range is inefficient, a replacement for this pump must be considered. Additionally, the effect and space requirement for regenerated energy storage solutions must be considered in the future. If this is chosen to be battery storage, an energy-efficient and lightweight solution needs to be chosen to maintain the system's compact size.

## References

- [1] N. Manring. Hydraulic Control Systems. John Wiley & Sons, New Jersey, 2005. ISBN 0-471-69311-1.
- [2] J. E. Johnson. Hydraulics for Engineering Technology. New Jersey: Prentice Hall, 1996. 79 p. ISBN 0-13-232513-6.
- [3] H. Kauranne, J. Kajaste, M. Vilenius. Hydrauliteknikka. 2nd ed. Helsinki: Sanoma Pro, 2013. 496 p. ISBN 978-952-63-0707-7
- [4] B. Eriksson. Mobile Fluid Power Systems Design with a Focus on Energy Efficiency. Ph.D. Thesis, Linköping University, Linköping, Sweden, 2010.
- [5] J. Zimmerman, M. Pelosi, C. Williamson, M. Ivantysynova. Energy Consumption of an LS Excavator Hydraulic System. In Proceedings of the 2007 ASME International Mechanical Engineering Congress and Exposition, Seattle, WA, USA, 11–15 November 2007.
- [6] Z. Quan, L. Quan, and J. Zhang. Review of energy efficient direct pump controlled cylinder electro-hydraulic technology. Renewable and Sustainable Energy Reviews, 35:336–346, 2014. doi: 10.1016/j.rser.2014. 04.036.
- [7] D. Hagen, W. Pawlus, M.K. Ebbesen, T.O. Andersen. Feasibility Study of Electromechanical Cylinder Drivetrain for Offshore Mechatronic Systems. Modeling, Identification and Control, Vol. 38, No. 2, 2017, pp. 59–77.
- [8] Firgelli Automations Team. Five Benefits of Electromechanical Actuators, 2015. URL: <https://www.firgelliauto.com/blogs/news/five-benefits-of-electromechanical-actuators>
- [9] Sun Hydraulics. Protect Hydrostatic Transmission Circuits with Sun’s Delayed Shift Hot Oil Shuttle. URL: <https://www.sunhydraulics.com/es/node/37094>
- [10] W. Ur Rehman, W. Shaoping, W. Xingjian, F. Lei, K. Ali Shah. Motion synchronization in a dual redundant HA/EHA system by using a hybrid integrated intelligent control design. Chinese Journal of Aeronautics, 2016, 29(3): 789-798.
- [11] M. Chiang. A novel pitch control system for a wind turbine driven by a variable-speed pump-controlled hydraulic servo system. Mechatronics, Volume 21, Issue 4, June 2011, Pages 753-761
- [12] M. Chiang, C-C. Chen, and C-F. Kuo. The high response and high efficiency velocity control of a hydraulic injection molding machine using a variable rotational speed electro-hydraulic pump-controlled system. The International Journal of Advanced Manufacturing Technology, 43 (9-10):841–851, 2009. ISSN 0268-3768. doi: 10.1007/s00170-008-1759-z

- [13] Kyntronics Innovation in Motion. Product / Application Overview. Rev 4.22. URL: [https://www.kyntronics.com/images/info-and-specs/Kyntronics\\_Product\\_Overview\\_4\\_22.pdf](https://www.kyntronics.com/images/info-and-specs/Kyntronics_Product_Overview_4_22.pdf)
- [14] Kyntronics Innovation in Motion. SMART Hydraulic Actuator for Wire Forming Machine upgrade. URL: <https://www.kyntronics.com/docman/33-wire-forming-press-upgrade-app-success-story/file>
- [15] T. Koitto, H. Kauranen, O. Calonius, T. Minav, M. Pietola. Experimental Study on Fast and Energy-Efficient Direct Driven Hydraulic Actuator Unit. *Energies* 2019, 12, 1538; doi:10.3390/en12081538
- [16] D. Padovani, S. Ketelsen, D. Hagen, L. Schmidt. A Self-Contained Electro-Hydraulic Cylinder with Passive Load-Holding Capability. *Energies* 2019, 12, 292; doi:10.3390/en12020292.
- [17] A. Imam, M. Rafiq, E- Jalayeri, N. Sepehri. Design, Implementation and Evaluation of a Pump-Controlled Circuit for Single Rod Actuators. *Actuators* 2017, 6, 10; doi:10.3390/act6010010
- [18] R. M. Livesey, M. Hi. Ettinger. Separator deaerates oil, stops shimmy on F-104 nose wheel. OCT 05, 1967. *Hydraulics & Pneumatics*. URL: <https://www.hydraulicspneumatics.com/technologies/hydraulic-fluids/article/21883214/separator-deaerates-oil-stops-shimmy-on-f104-nose-wheel>
- [19] G. K. Costa, N. Sepehri. A Critical Analysis of Valve-Compensated Hydrostatic Actuators: Qualitative Investigation. *Actuators* 2019, 8, 59; doi:10.3390/act8030059.
- [20] S. Ketelsen, D. Padovani, T. O. Andersen, M. K. Ebbesen, L. Schmidt. Classification and Review of Pump-Controlled Differential Cylinder Drives. *Energies* 2019, 12, 1293; doi:10.3390/en12071293
- [21] J. Huang, H. Zhao, L. Quan, X. Zhang. Development of an asymmetric axial piston pump for displacement-controlled system. *Proc. Inst. Mech. Eng. Part C* 2013, 228, 1418–1430.
- [22] Kenyon, R.L.; Scanderberg, D.; Wilkerson, W.D. Electro-Hydraulic Actuator. European Patent 90304554.0, 26 April 1990.
- [23] J. Huang, Y. Gao, L. Quan, J. Cheng. Simulation Analysis and Experiment of Variable-Displacement Asymmetric Axial Piston Pump. *Appl. Sci.* 2017, 7, 328; doi:10.3390/app7040328
- [24] A. Järf, T. Minav, M. Pietola. Nonsymmetrical Flow Compensation Using Hydraulic Accumulator. In *Proceedings of the 9th FPNI Ph.D. Symposium on Fluid Power*, Florianopolis, Brazil, 26–28 October 2016; pp. 1–6.
- [25] H.C. Pedersen, L. Schmidt, T.O. Andersen, ; H. Brask, M. Investigation of New Servo Drive Concept Utilizing Two Fixed Displacement Units. *JFPS Int. J. Fluid Power Syst.* 2014, 8, 1–9.

- [26] G. E. M. Vael, P. A. J. Achten and Z. FuThe. Innas Hydraulic Transformer The Key to the Hydrostatic Common Pressure Rail. SAE Transactions Vol. 109, Section 2: JOURNAL OF COMMERCIAL VEHICLES (2000), pp. 109-124.
- [27] INNAS BV. POWER TRANSFORMATION. URL: <https://www.innas.com/hydraulic-transformer.html>
- [28] G. K. Costa, N. Sepehri. Four-Quadrant Analysis and System Design for Single-Rod Hydrostatic Actuators. Journal of Dynamic Systems, Measurement, and Control. 2019, Vol. 141.
- [29] P. H.Gøytil, D. Padovani, M. R. Hansen. A Novel Solution for the Elimination of Mode Switching in Pump-Controlled Single-Rod Cylinders. Actuators 2020, 9, 20; doi:10.3390/act9010020
- [30] J. Johnson. Case Drain Issues with Pumps and Motors. 2017. Hydraulics and Pneumatics. URL: <https://www.hydraulicspneumatics.com/technologies/hydraulic-pumps-motors/article/21887505/case-drain-issues-with-pumps-and-motors>.
- [31] Vivolo, Domenico 40065 Pianoro (IT), Detachable heads for hydraulic pumps and motors, 2003, Patent 03012289.9.
- [32] JBL Techniques Limited. A special radial sealing system driven by customer demand. URL: <https://www.jbj.co.uk/marzocchiteflonseal.html>
- [33] B. Casey. When Hydraulic Motor Case-Drains Are Optional—Unless You Want Reliability! 2015. Hydraulics and Pneumatics. URL: <https://www.hydraulicspneumatics.com/hydraulics-at-work/article/21886556/when-hydraulic-motor-casedrains-are-optionalunless-you-want-reliability>
- [34] Fluid Power Journal. Energy-Efficient Hydraulics: Variable Frequency Drives as Pump Prime Movers. 06.28.2013. Fluid Power Journal.
- [35] INNAS. Floating cup. URL: <https://www.innas.com/floating-cup.html>
- [36] Bucher Hydraulics GmbH. Axial Piston Pumps AX. URL: <https://www.bucherhydraulics.com/ax>
- [37] Parker Hannifin Corp. Ten Dos and Don'ts of Applying Variable Speed Drives to Hydraulic Pumps. URL: <http://blog.parker.com/ten-dos-and-donts-of-applying-variable-speed-drives-to-hydraulic-pumps>
- [38] Viking Pumps, Inc. External gear pumps. Pump school. URL: <http://pump-school.com/principles/external.php>
- [39] Vivolo. Vivolo reversible motors, 2009. URL: [http://www.vivoil.com/files/vivoil\\_m\\_en.pdf](http://www.vivoil.com/files/vivoil_m_en.pdf).

- [40] Hydraulics & Pneumatics. How To Size A Hydraulic Tank. URL: <https://www.hydraulicspneumatics.com/hydraulics-at-work/article/21884901/how-to-size-a-hydraulic-tank>
- [41] Hiab. Hiab Cyclone tanks. URL: <https://webshop.hiab.com/en/loader-crane-accessories/cyclone-tanks/>
- [42] B. Casey. The Pressure-Flow Conundrum And What It Means For Hydraulic Machine Reliability. 2014. Hydraulics and Pneumatics. URL: <https://www.hydraulicspneumatics.com/hydraulics-at-work/article/21886511/the-pressureflow-conundrum-and-what-it-means-for-hydraulic-machine-reliability>
- [43] Hawe Hydraulik. Hydraulic spring constant. URL: <https://www.hawe.com/fluid-lexicon/hydraulic-spring-constant/>
- [44] Hydraulics & Pneumatics. Bud Trinkel. CHAPTER 16: Accumulators. 2007. URL: <https://www.hydraulicspneumatics.com/technologies/other-technologies/article/21884186/chapter-16-accumulators>
- [45] Hydraulics & Pneumatics. Accumulators. 2012. URL: <https://www.hydraulicspneumatics.com/technologies/accumulators/article/21883829/accumulators#:~:text=Horizontally%20mounted%20accumulator%20can%20cause,the%20fluid%20can%20shorten%20life.>
- [46] C. Williamson, M. Ivantysynova. Pump mode prediction for four-quadrant velocity control of valveless hydraulic actuators. In Proceedings of the 7th JFPS International Symposium on Fluid Power, TOYAMA 2008. 15–18 September 2008; pp. 323–328. ISBN 4-931070-07-X.
- [47] H. Çalıskan, T.Balkan, B.E. Platin. A Complete Analysis for Pump Controlled Single Rod Actuators. In Proceedings of the 10th International Fluid Power Conference, Dresden, Germany, 8–10 March 2016; pp. 119–132.
- [48] R. Rahmfeld, M. Ivantysynova. Energy saving hydraulic actuators for mobile machines. In Proceedings of the 1st Bratislavian Fluid Power Symposium, Casta Pila, Slovakia, 2–3 June 1998; pp. 47–57.
- [49] Parker Hannifin. Compact EHA—Electro-Hydraulic Actuators for high power density applications, 2011. URL: <http://www.parker.com/Literature/Hydraulic%20Pump%20Division/Oildyne%20EHA/Compact-EHA-Catalog-HY22-3101E-7-13.pdf>
- [50] A. Imam, M. Rafiq, E. Jalayeri, N. Sepehri. A Pump-Controlled Circuit for Single-Rod Cylinders that Incorporates Limited Throttling Compensating Valves. Actuators 2018, 7, 13; doi:10.3390/act7020013
- [51] E. Jalayeri. Design and Experimental Evaluations of a Pump-Controlled Hydraulic Circuit. Ph.D. Thesis, University of Manitoba, Winnipeg, MB, Canada, 2016

- [52] E. Jalayeri, A. Imam, Z. Tomas and N. Sepehri. A throttle-less single-rod hydraulic cylinder positioning system: Design and experimental evaluation. *Advances in Mechanical Engineering* 2015, Vol. 7(5) 1–14 DOI: 10.1177/1687814015583249
- [53] P. H. Gøystil, D. Padovani, and M. R. Hansen. A Novel Solution for the Elimination of Mode Switching in Pump-Controlled Single-Rod Cylinders. *Actuators* 2020, 9, 20; doi:10.3390/act9010020.
- [54] M. Gannon. Load-holding valves made simple. *Fluid Power World*. 2017 URL: <https://www.fluidpowerworld.com/load-holding-valves-made-simple/>
- [55] A. Akers, M. Gassman, R. Smith. *Hydraulic Power System Analysis*. 2006. Taylor & Francis Group. 195-197 p. FL 33487-2742. p 195-197. P 221-223.
- [56] G. Altare, A. Vacca. A Design Solution for Efficient and Compact Electro-hydraulic Actuators. *Procedia Eng.* 2015, 106, 8–16.
- [57] G. Altare, A. Vacca, C. Richter. A Novel Pump Design for an Efficient and Compact Electro-Hydraulic Actuator. In *Proceedings of the 2014 IEEE Aerospace Conference*, Big Sky, MT, USA, 2014.
- [58] Counterbalance valves. Bosch Rexroth Oil Control S.p.A. URL: <https://apps.boschrexroth.com/products/compact-hydraulics/ch-catalog/pdf/Counterbalance.pdf>
- [59] Bosch Rexroth AG. Advantages of Electrification and Digitalization Technology For Hydraulics. 2018. URL: <https://www.boschrexroth.com/en/xc/products/product-groups/industrial-hydraulics/the-fitness-program-for-hydraulics>
- [60] Duplomatic motion solutions. Hydro-pilot operated check valves. URL: <https://www.duplomatic.com//assets/SchedeTecniche/GB/46300.pdf>
- [61] HYDAC Fluidtechnik GmbH. 2/2 Solenoid Directional Valve Poppet Type, Pilot Operated Normally Open (Reverse Flow) Metric Cartridge - 350 bar. WSM06020YR-01. E 5.948.3/09.13.
- [62] Parker Hannifin Corporation. Bi-Directional Poppet Type, 2-Way Valve. Catalog HY15-3502/US.
- [63] Parker Hannifin Corporation. Pilot Operated Check Valve. Catalog HY15-3502/US.
- [64] Bucher hydraulic. Double Pilot Operated Cartridge Check Valve, Size 8. 300-P-9050061-EN-01/08.2018. Series DERV 8.
- [65] Sun Hydraulics LLC. Vented pilot-to-open check valve. URL: <https://www.sunhydraulics.com/model/CVCV>
- [66] S. Michel, J. Weber. Investigation of Self-Contamination of Electrohydraulic Compact Drives. In *Proceedings of the 10th JFPS International Symposium on Fluid Power*, Fukuoka, Japan, 24–27 October 2017.



- [67] B. Casey. Hydraulic Pump and Motor Case Drains: Should You Filter? Machinery Lubrication 5/2005. URL: <https://www.machinerylubrication.com/Read/748/hydraulic-pump-motor-case-drains#:~:text=Due%20to%20the%20rea-sons%20above,other%20condition%2Dbased%20maintenance%20techniques>.
- [68] V. G. Magorien. What is Bulk Modulus, and When is it Important? Hydraulics & Pneumatics.01, 2000. URL: <https://www.hydraulicspneumatics.com/technologies/hydraulic-fluids/article/21885309/what-is-bulk-modulus-and-when-is-it-important#:~:text=Temperature%20and%20Bulk%20Modulus&text=com-press%20the%20fluid%20very%20slowly,with%20tempera-ture%20and%20air%20content>.
- [69] Hydac. Vacuum-packed: The cutting-edge, patented solution for hydraulic systems OXiStop OXS. E 7.660.1/10.15
- [70] Peninsular Cylinder CO. Model HP - NFPA High Pressure Hydraulic Cylinders "Air Bleed: /C". URL: [https://www.peninsularcylinders.com/HH\\_Links/HH\\_HP\\_NFPA\\_Cylinders/x\\_HH\\_HP\\_NFPA\\_Air%20Bleed.htm](https://www.peninsularcylinders.com/HH_Links/HH_HP_NFPA_Cylinders/x_HH_HP_NFPA_Air%20Bleed.htm)
- [71] Beckhoff. CX51x0 Embedded-PC. URL: [https://download.beckhoff.com/download/document/ipc/embedded-pc/embedded-pc-cx/cx5100\\_en.pdf](https://download.beckhoff.com/download/document/ipc/embedded-pc/embedded-pc-cx/cx5100_en.pdf)
- [72] Oriental motor. Brushless DC Motors vs. Servo Motors vs. Inverters. URL: <https://www.orientalmotor.com/brushless-dc-motors-gear-motors/technology/brushless-dc-motors-servo-motors-inverter.html>
- [73] H. Zhang, L. Ren, Y. Gao and B. Jin. A Comprehensive Study of Energy Conservation in Electric-Hydraulic Injection-Molding Equipment. Energies 2017, 10, 1768; doi:10.3390/en10111768
- [74] V. Koivusaari, P. Westberg, M. Smolander. Development of motor efficiency test setup for direct driven hydraulic actuator. Tallinn, 2019. Proceedings of the 4th Baltic Mechatronics Symposium
- [75] Beckhoff. AM8000 + AM8500 Synchronous-servomotor. URL: [https://download.beckhoff.com/download/document/motion/am8000\\_am8500\\_ba\\_en.pdf](https://download.beckhoff.com/download/document/motion/am8000_am8500_ba_en.pdf)
- [76] Beckhoff. EL3174 | 4-channel analog input, -10/0...+10 V, -20/0/+4...+20 mA, 16 bit. URL: <https://www.beckhoff.com/EL3174/>
- [77] HBM. Operating manual Force transducer with strain gauge measuring system U9B. B 20. U9B.40 en.
- [78] Easy-systems Oy. BSB ALUMIINIPROFIILIT. URL: [https://easy-systems.fi/tuote-osasto/alumiiniprofiilit/bsb\\_alumiiniprofiilit/](https://easy-systems.fi/tuote-osasto/alumiiniprofiilit/bsb_alumiiniprofiilit/)
- [79] S. Esqu'e. A New Approach for Numerical Simulation of Fluid Power Circuits Using Rosenbrock Methods A New Approach for Numerical Simulation of Fluid

Power Circuits Using Rosenbrock Methods. Phd thesis, Tampere University of Technology, 2008.

- [80] A. Ellman, M. Linjama. Modeling and Simulating Fluid Power Systems. Document. Tampere University of Technology, 2002. ISSN 1098-6596.
- [81] A. Ellman, H. Kauranne, J. Kajaste, M. Pietola. Effect of parameter uncertainty on reliability of hydraulic transmission system simulation. Proceedings of IMECE2005 2005 ASME International Mechanical Engineering Congress and Exposition November 5-11, 2005, Orlando, Florida USA.
- [82] Hydraulics & Pneumatics. Engineering Essentials: Pressure-Control Valves. URL: <https://www.hydraulicspneumatics.com/technologies/hydraulic-valves/article/21884995/engineering-essentials-pressurecontrol-valves>
- [83] MathWorks. Check Valve. URL: <https://www.mathworks.com/help/physmod/hydro/ref/checkvalve.html>
- [84] American High Performance Seals. Hydraulic & Fluid Seals. URL: <https://www.ahpseals.com/hydraulic-fluid-seals/>.
- [85] J. W. Robinson, Y. Zhou, P. Bhattacharya<sup>1</sup>, R Erck, J. Qu, J. T. Bays and L. Cosimbescu. Probing the molecular design of hyper-branched aryl polyesters towards lubricant applications. 2016. Scientific Reports DOI: 10.1038/srep18624.
- [86] Q. Liu. Friction in Mixed and Elastohydrodynamic Lubricated Contacts Including Thermal Effects. FEBO druk B.V., Enschede. ISBN:90-365-1796-6
- [87] J. Swevers, F. Al-Bencer, C.G. Ganseman, T. Prajogo An integrated friction model structure with improved presliding behavior for accurate friction compensation IEEE Trans Automatic Control, 45 (4) (2000), pp. 675-686
- [88] Apple Rubber. What you Need to Know About Dynamic Seal Applications. URL: <https://www.applerrubber.com/hot-topics-for-engineers/what-you-need-to-know-about-dynamic-seal-applications/>.
- [89] J. Mazurkiewicz. Servomotor Efficiency. Baldor Electric. URL: [http://www.baldormotion.com/support/SupportMe/Documents/white\\_papers/servo\\_eff.pdf](http://www.baldormotion.com/support/SupportMe/Documents/white_papers/servo_eff.pdf)
- [90] Elmo Motion Control. Servo System Efficiency. URL: <https://www.elmomc.com/wp-content/uploads/2018/07/1-Servo-System-Efficiency.pdf>
- [91] J. Widén, J. Munkhammar. Evaluating the benefits of a solar home energy management system: impacts on photovoltaic power production value and grid interaction. 2013. Conference: ECEEE 2013 Summer Study, Presqu'île de Giens, France.
- [92] J Sun. Car Battery Efficiencies. 2010. Submitted as coursework for Physics 240, Stanford University, Fall 2010. URL: <http://large.stanford.edu/courses/2010/ph240/sun1/>

- [93] K. A. Stelson. Saving the World's Energy With Fluid Power, 2011, Eighth JFPS International Symposium on Fluid Power, Okinawa, Japan, pp. 1–7.

## List of Annexes

### A. Simulink model

This section contains all the parameters used to create the Simulink model presented in this thesis. The section also includes all those parts of the Simulink model that had not yet been presented. These are presented in the order of the simulation chapter heading.

Thesis notation	Matlab notation	Value
<b>Hydraulic fluid parameters</b>		
$K_f$	K_f	1.3e9
$C_q$	C_q	0.7
$\rho$	ro	870
<b>Loading system parameters</b>		
$g$	g	9.81
$m$	m_inertia	82 - 345
$F_{load}$	F_load	< 25000
<b>Hydraulic pump parameters</b>		
$p_{system}$	p_system	210e5
$V_i$	Vi	3.12e-6
	Cs	65.5e-9
$C_f$	Cf	0.0376
$C_v$	Cv	16.893e3
$T_c$	Tc_0	10
$K_L$	K_laminar	1.33e-12
$\nu$	nu	32e-6
$C_{s,int}$	Cs_i	3.275e-09
$C_{s,ext}$	Cs_e	3.275e-09
<b>Pipe/hose parameters</b>		
	A_pipe	1.2668e-04
$V_{hose}$	V_pipe	1.9002e-04
<b>Hydraulic cylinder parameters</b>		
$x_{max}$	x_max	0.6
$V_{A,0}$	V_0A	1.091e-04
$V_{B,0}$	V_0B	1.091e-04
	x_0	0.5
$A_A$	A_A	0.00196
$A_B$	A_B	0.00125
$\alpha$	alfa	1.5625
<b>Cylinder seal parameters</b>		
$F_s$	F_S	300
$F_{cf}$	F_C	100
$b_v$	b_v	140
$v_{\mu}^{min}$	v_s	0.02
$z_{cs}^{max}$	z_max	0.1e-3

$k_{R,cs}$	$k_R$	3000000
<b>Cylinder end parameters</b>		
$x_{def}$	$x_{def}$	0.2e-3
$K_{end}$	$K_{end}$	2.061e+08
<b>Check valve parameters</b>		
$\tau$	$t_{CV}$	0.5e-3
$\tau$	$t_{POCV}$	2e-3
$A_0$	$A_{CV}$	4.5442e-5
$A_0$	$A_{POCV}$	2.3075e-5
$p_{crack}$	-	0.5e5
<b>Parker DF102 valve's parameters</b>		
$q_{v,nominal}$	$q_{v\_orifice}$	3.750e-04
$\Delta p_{nominal}$	$\Delta p_{orifice}$	13.8e5
$K_{100}$	$K_{10V}$	3.1922e-07
$q_{v,L,nominal}$	$q_{v\_leakage}$	2.0833e-06
	$\Delta p_{leakage}$	210e5
$K_0$	$K_{0V}$	4.5462e-10

Table A. 1 Simulation parameters

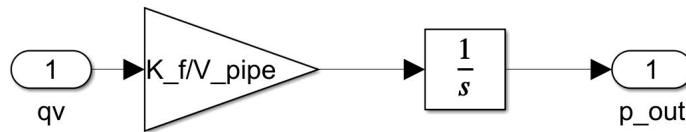


Figure A. 1 Hose model.

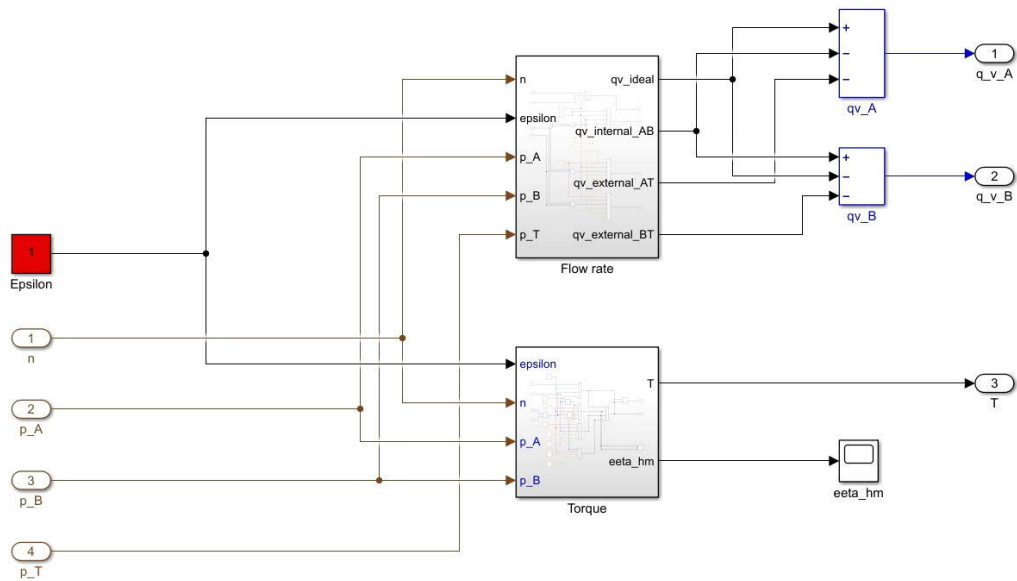


Figure A. 2 Pump model.

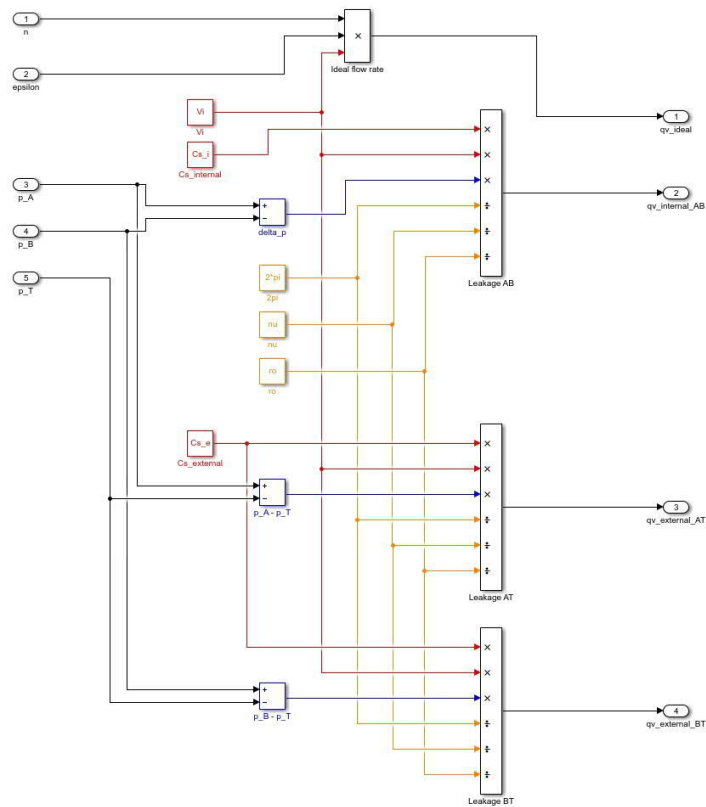


Figure A. 3 Pump model, flow rate.

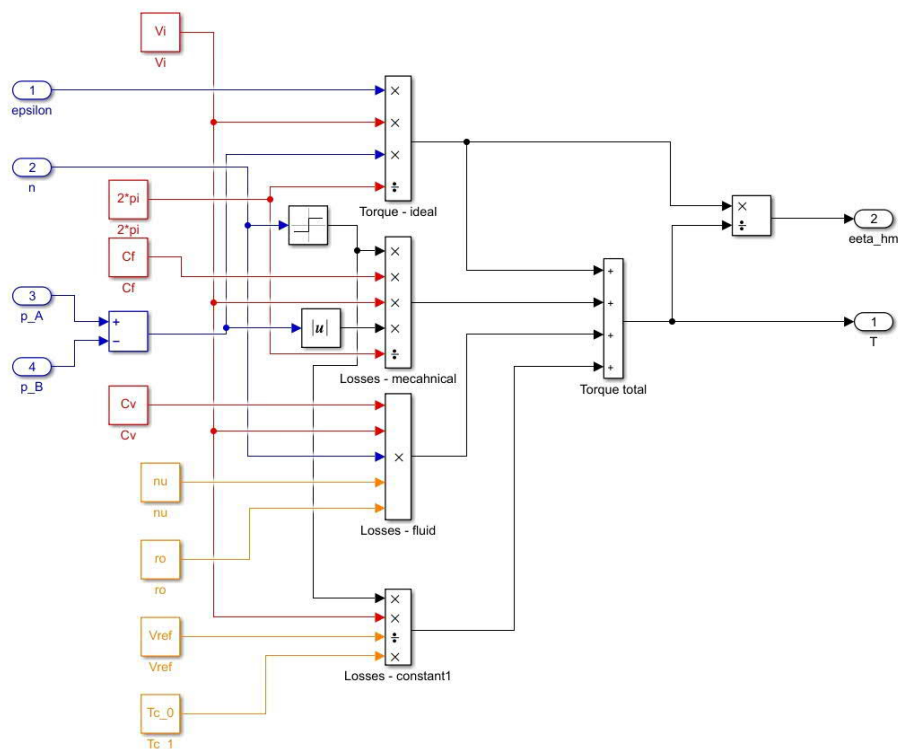


Figure A. 4 Pump model, torque.

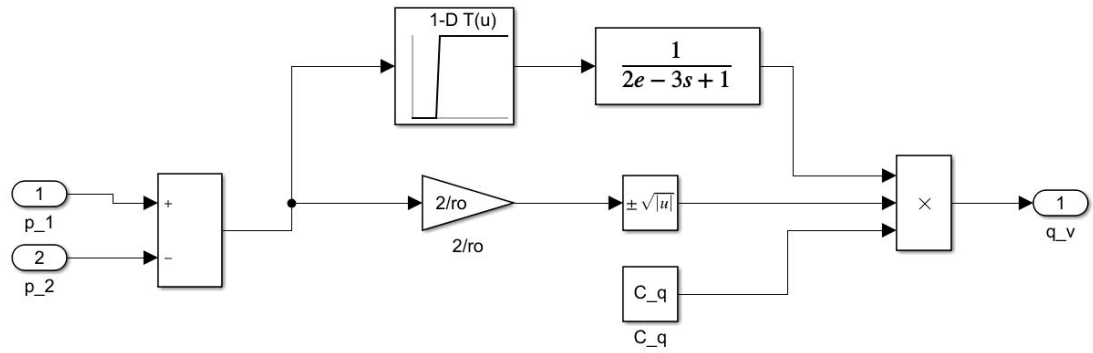


Figure A. 5 Bosch Rexroth's A-VAA-CC-150, PRV model.

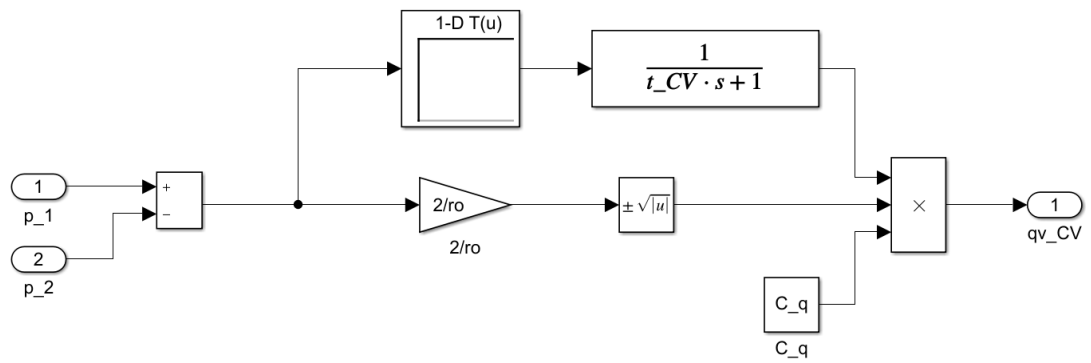


Figure A. 6 Bosch Rexroth's A-VAA-CC-150, CV model.

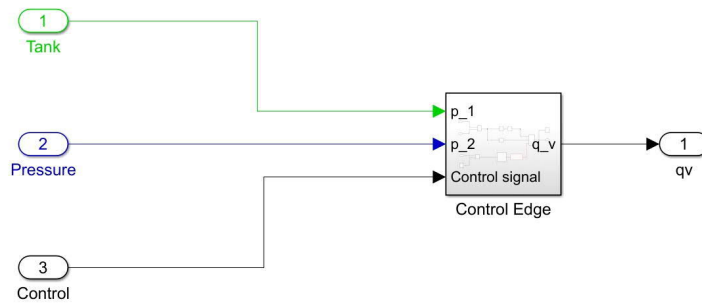


Figure A. 7 Proportional valve model.

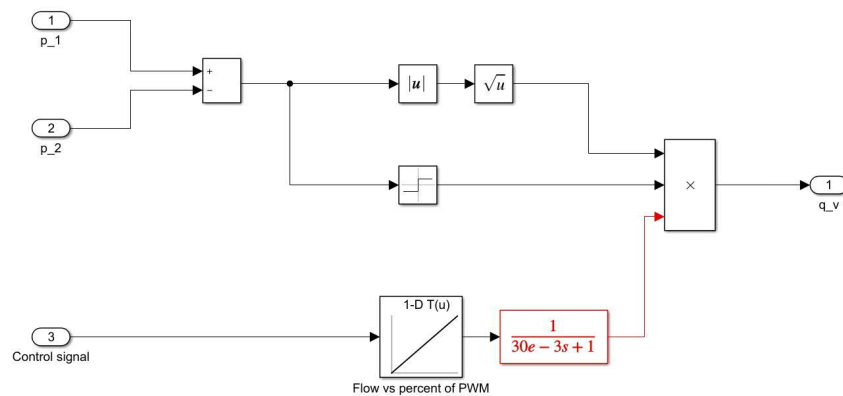


Figure A. 8 Proportional valve model, control edge.



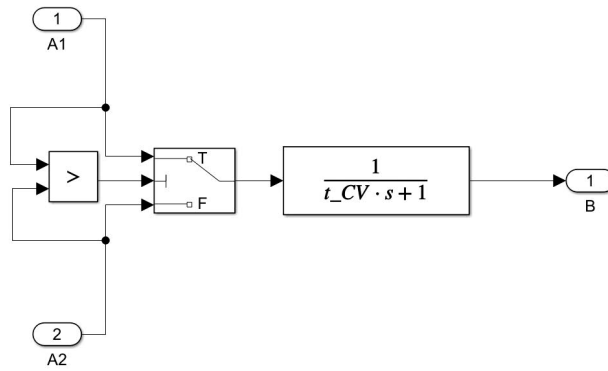


Figure A. 9 Load holding system, shuttle valve.

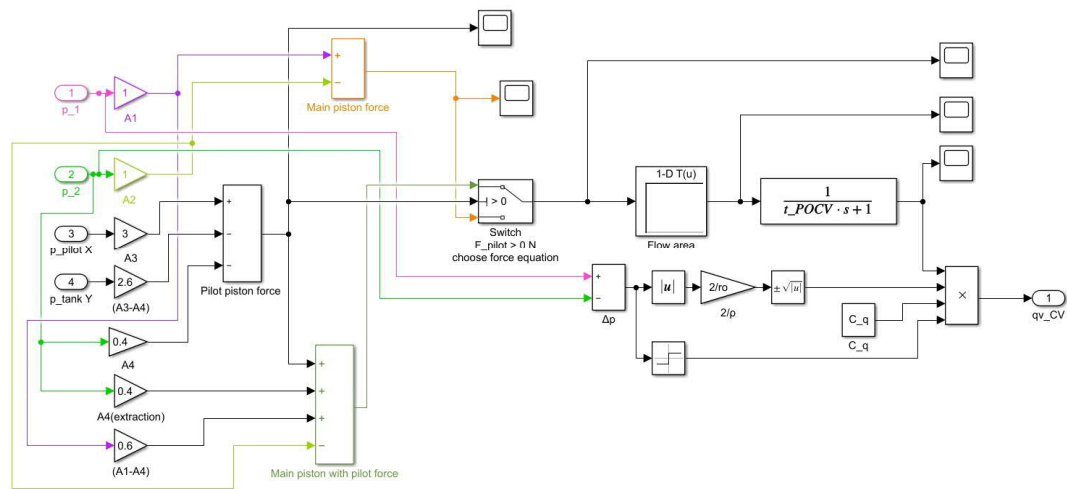


Figure A. 10 Load holding system, POCV model.

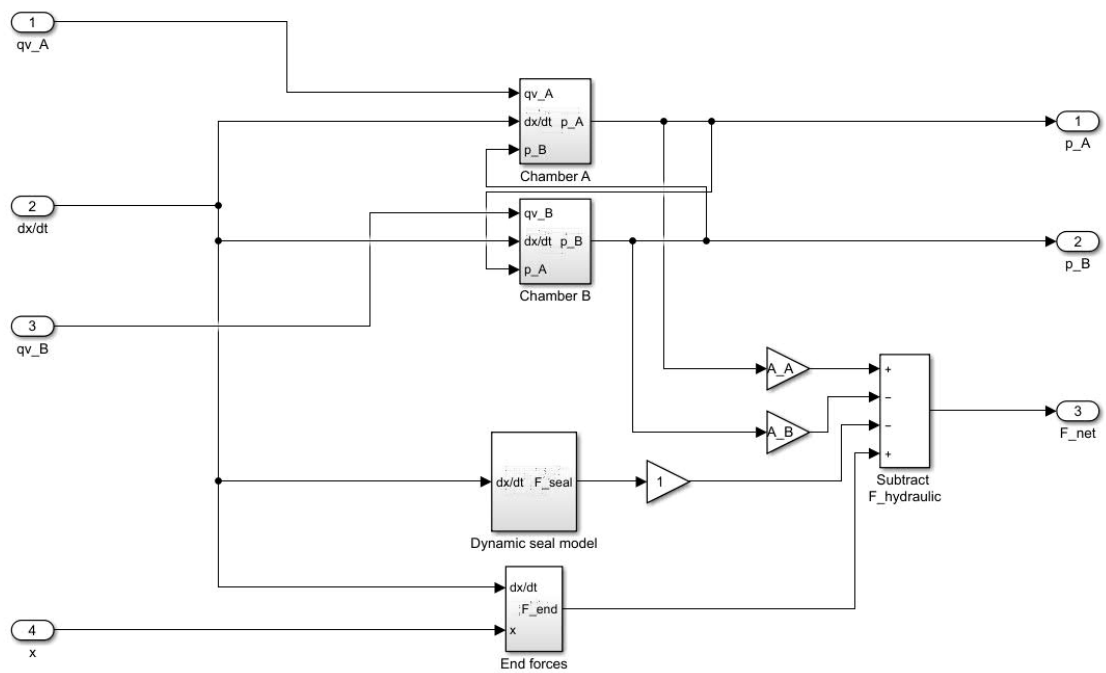


Figure A. 11 Cylinder model.

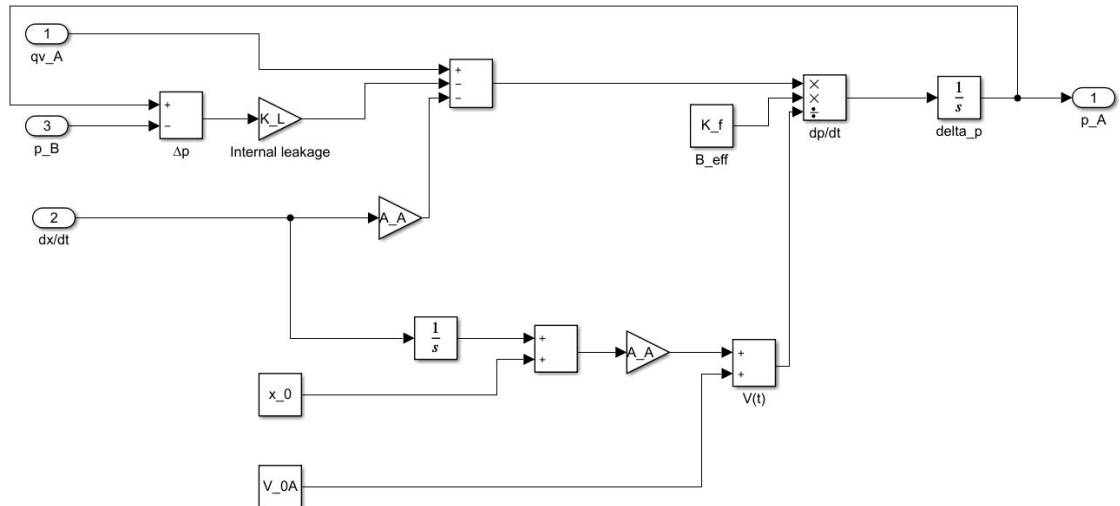


Figure A. 12 Cylinder model, chamber A.

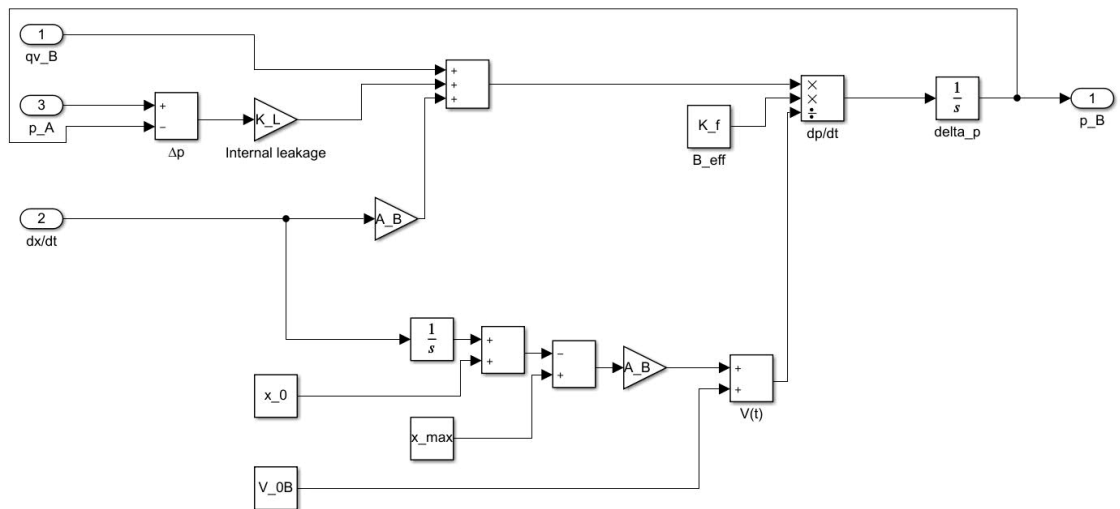


Figure A. 13 Cylinder model, chamber B.

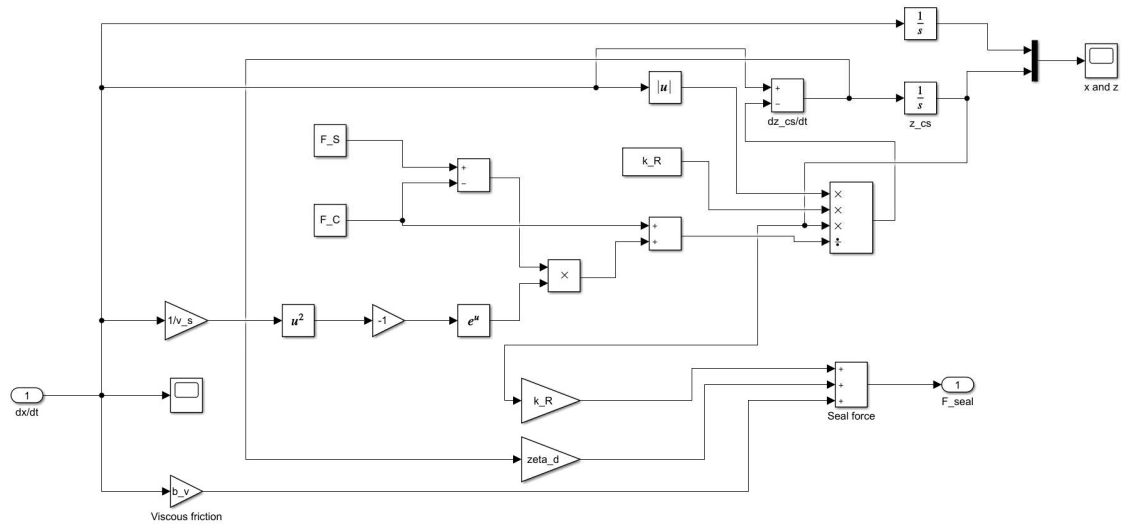


Figure A. 14 Cylinder model, chamber seal force model.

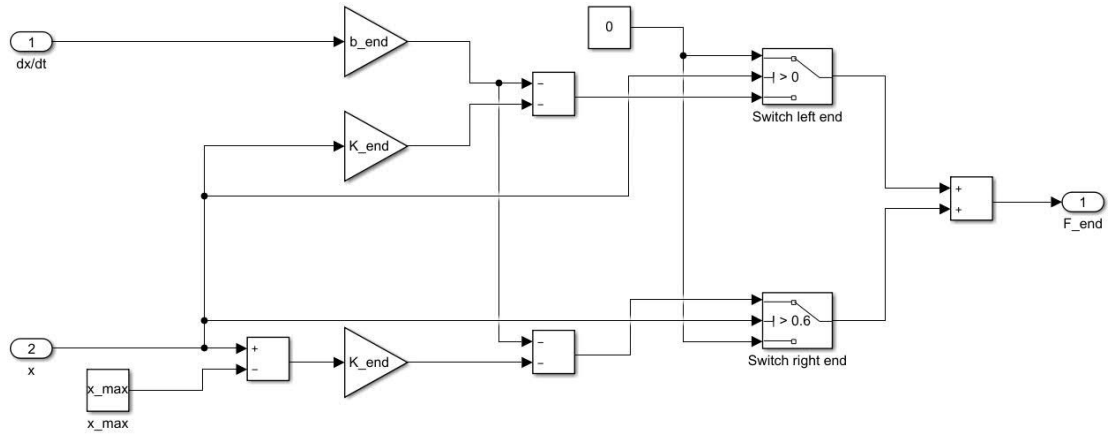


Figure A. 15 Cylinder model, end force model.

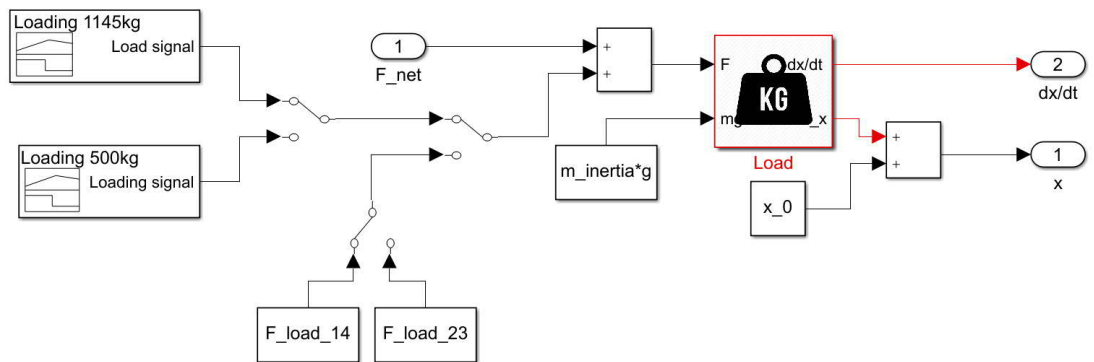


Figure A. 16 Load model.

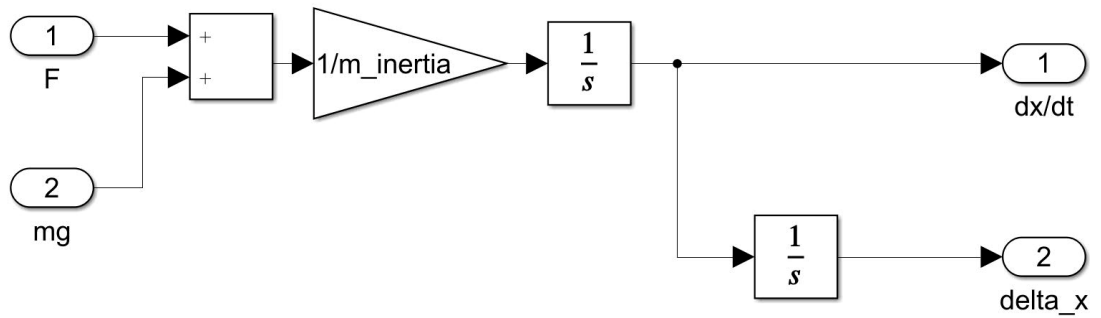


Figure A. 17 Load model, inertia force.

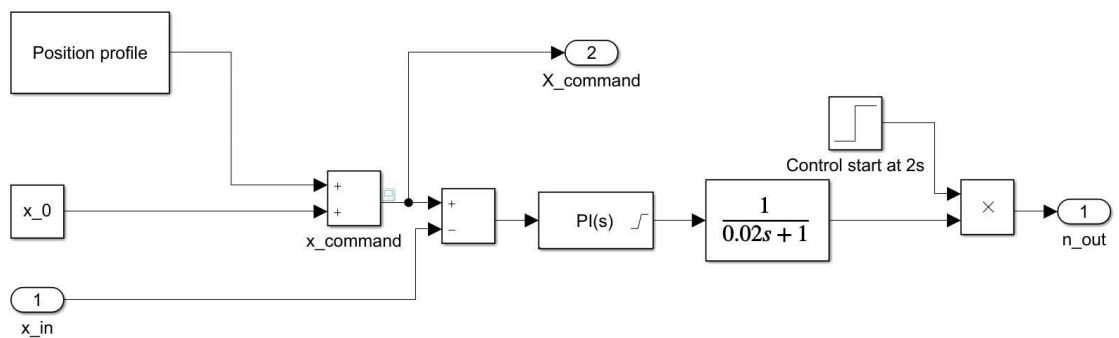


Figure A. 18 Control system model.

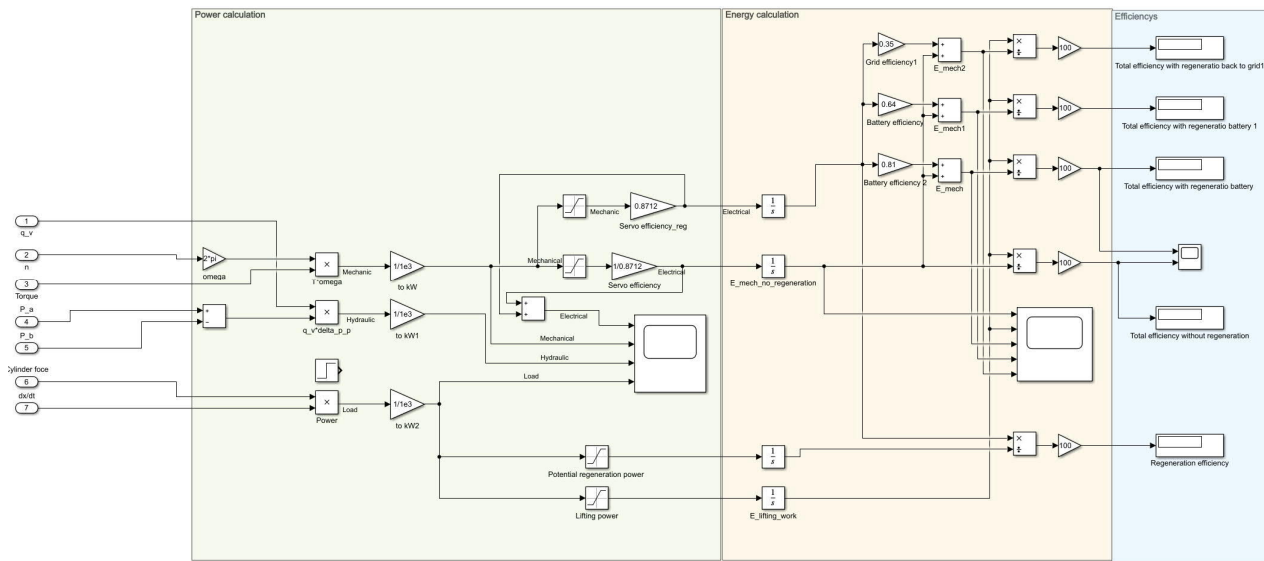


Figure A. 19 Energy calculations.

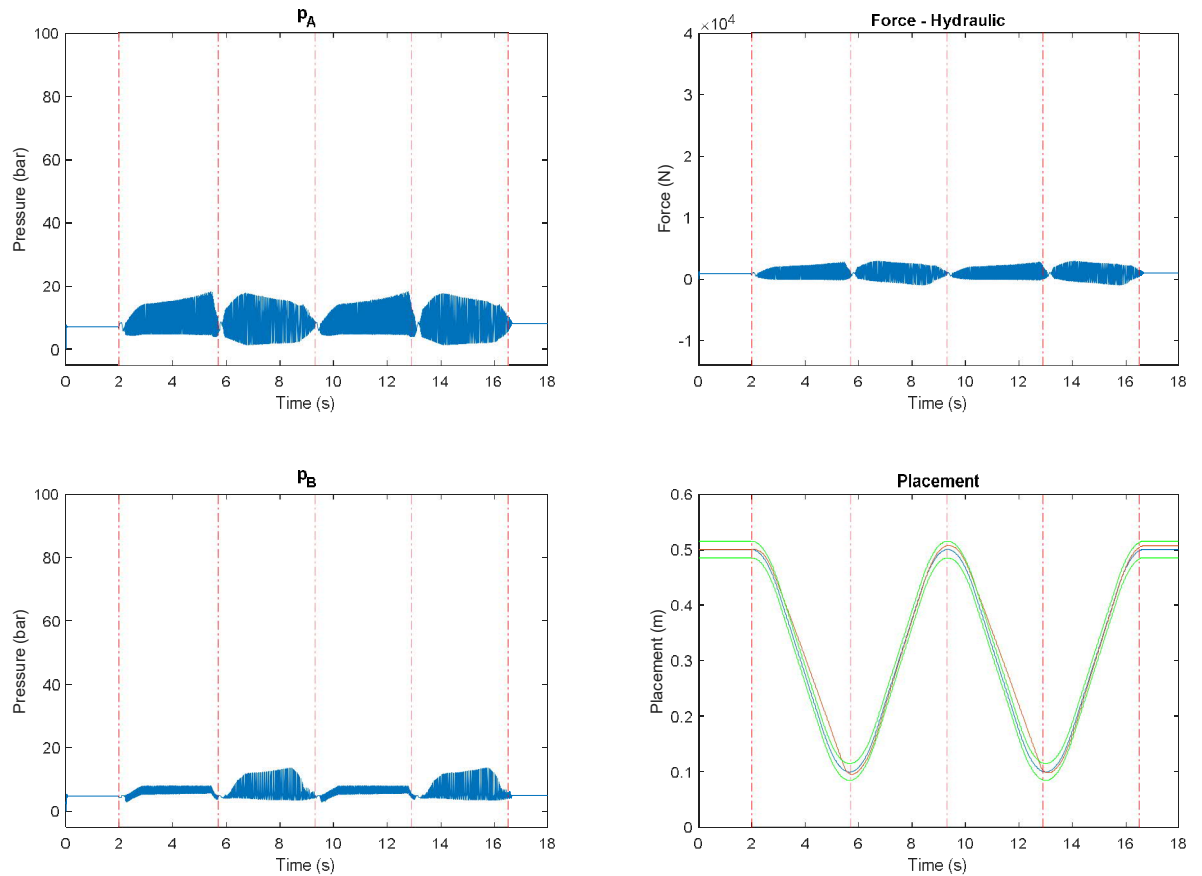


Figure A. 20 POCV results Q1/Q4 with 87 kg load.